NATIONAL CENTER FOR EARTHQUAKE ENGINEERING RESEARCH

State University of New York at Buffalo

Seismic Behavior and Design Guidelines for Steel Frame Structures with Added Viscoelastic Dampers

by

K.C. Chang, M.L. Lai, T.T. Soong, D.S. Hao and Y.C. Yeh
State University of New York at Buffalo
Department of Civil Engineering
Buffalo, New York 14260

Technical Report NCEER-93-0009

May 1, 1993

NOTICE

Seismic Behavior and Design Guidelines for Steel Frame Structures with Added Viscoelastic Dampers

by

K.C. Chang[1], M.L. Lai[2], T.T. Soong[3], S-T. Oh[4], D.S. Hao[4] and Y.C. Yeh[5]

May 1, 1993

Technical Report NCEER-93-0009

1   Professor, Department of Civil Engineering, National Taiwan University
2   R&D Specialist, The 3M Company
3   Samuel P. Capen Professor, Department of Civil Engineering, State University of New York at Buffalo
4   Assistant Professor, Department of Structural Engineering, National Seoul Polytechnic University
5   Professor, Department of Civil Engineering, Beijing Polytechnic University

NATIONAL CENTER FOR EARTHQUAKE ENGINEERING RESEARCH
State University of New York at Buffalo
Red Jacket Quadrangle, Buffalo, NY 14261
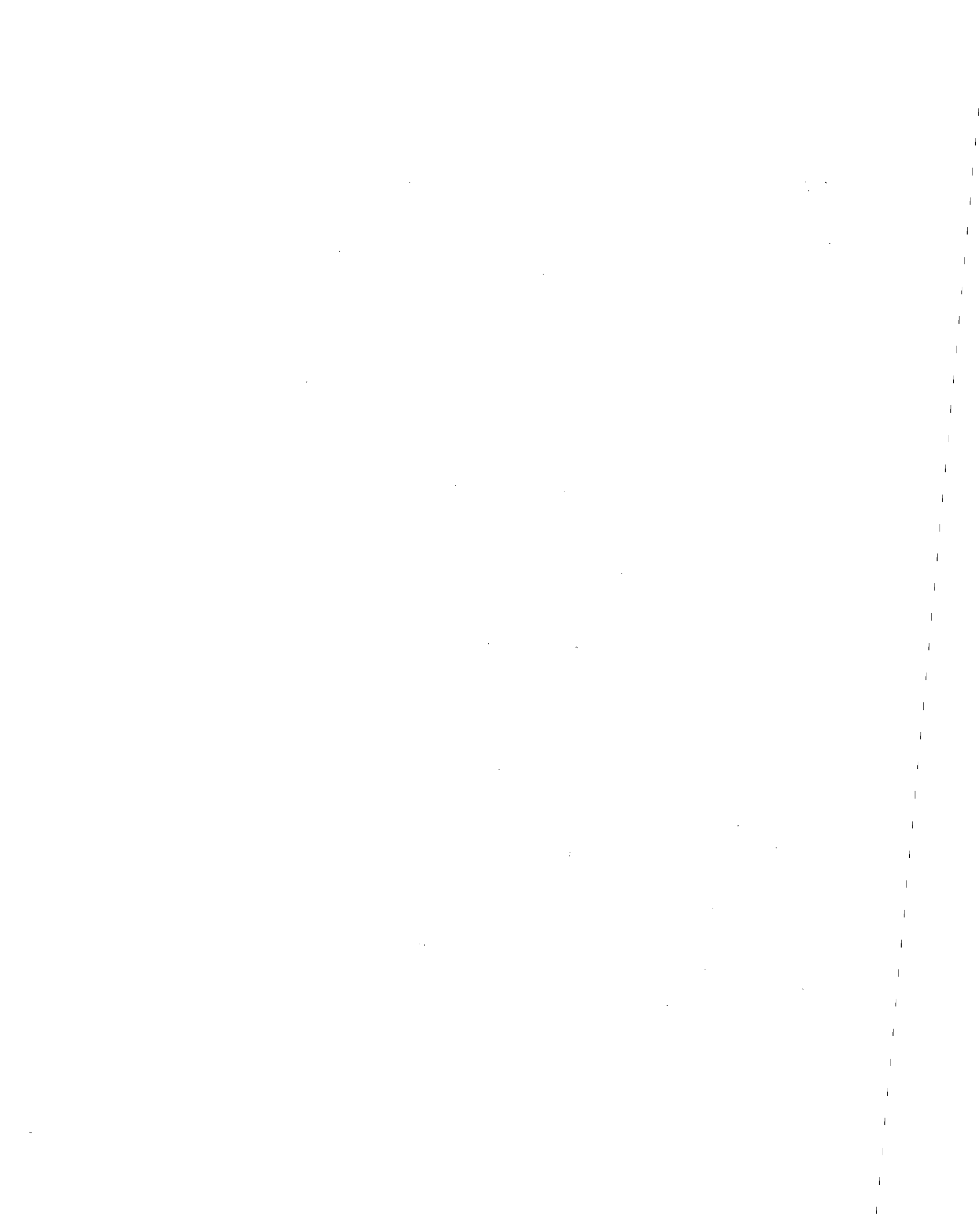
PREFACE

The National Center for Earthquake Engineering Research (NCEER) was established to expand and disseminate knowledge about earthquakes, improve earthquake-resistant design, and implement seismic hazard mitigation procedures to minimize loss of lives and property. The emphasis is on structures in the eastern and central United States and lifelines throughout the country that are found in zones of low, moderate, and high seismicity.

NCEER's research and implementation plan in years six through ten (1991-1996) comprises four interlocked elements, as shown in the figure below. Element I, Basic Research, is carried out to support projects in the Applied Research area. Element II, Applied Research, is the major focus of work for years six through ten. Element III, Demonstration Projects, have been planned to support Applied Research projects, and will be either case studies or regional studies. Element IV, Implementation, will result from activity in the four Applied Research projects, and from Demonstration Projects.

ELEMENT I BASIC RESEARCH	ELEMENT II APPLIED RESEARCH	ELEMENT III DEMONSTRATION PROJECTS
• Seismic hazard and ground motion • Soils and geotechnical engineering • Structures and systems • Risk and reliability • Protective and intelligent systems • Societal and economic studies	• The Building Project • The Nonstructural Components Project • The Lifelines Project • The Highway Project	Case Studies • Active and hybrid control • Hospital and data processing facilities • Short and medium span bridges • Water supply systems in Memphis and San Francisco Regional Studies • New York City • Mississippi Valley • San Francisco Bay Area

ELEMENT IV
IMPLEMENTATION

• Conferences/Workshops
• Education/Training courses
• Publications
• Public Awareness

Research in the **Building Project** focuses on the evaluation and retrofit of buildings in regions of moderate seismicity. Emphasis is on lightly reinforced concrete buildings, steel semi-rigid frames, and masonry walls or infills. The research involves small- and medium-scale shake table tests and full-scale component tests at several institutions. In a parallel effort, analytical models and computer programs are being developed to aid in the prediction of the response of these buildings to various types of ground motion.

iii

Two of the short-term products of the **Building Project** will be a monograph on the evaluation of lightly reinforced concrete buildings and a state-of-the-art report on unreinforced masonry.

The **protective and intelligent systems program** constitutes one of the important areas of research in the **Building Project**. Current tasks include the following:

1. Evaluate the performance of full-scale active bracing and active mass dampers already in place in terms of performance, power requirements, maintenance, reliability and cost.
2. Compare passive and active control strategies in terms of structural type, degree of effectiveness, cost and long-term reliability.
3. Perform fundamental studies of hybrid control.
4. Develop and test hybrid control systems.

NCEER's activities in viscoelastic dampers research for seismic applications began in 1987 with analytical and experimental work carried out at the State University of New York at Buffalo and at the University of California at Berkeley. The ultimate aim is to determine their effectiveness when incorporated into a structure under seismic loads, and to develop a rational design procedure for such structures. This report summarizes results of a comprehensive analytical and experimental program for steel frame structures. The experimental program was first conducted on a 2/5-scale steel frame in the laboratory, followed by verification tests conducted on a full-scale prototype structure. A rational seismic design procedure for viscoelastically damped steel frame structures is developed based on these results.

ABSTRACT

In order to determine the effectiveness of adding viscoelastic dampers to structures on the reduction of their seismic response, a comprehensive analytical and experimental program was carried out. The experimental program was first conducted on a 2/5-scale five-story steel frame under precisely controlled ambient temperatures and subject to simulated ground motions with peak accelerations ranging from 0.12g to 0.60g. Results show that viscoelastic dampers are very effective in attenuating seismic structural response at all levels of earthquake ground motions, and that their energy dissipation capacity decreases as ambient temperature increases. However, they are effective at all temperatures tested in the research program. A rational seismic design procedure for viscoelastically damped structure is developed based on these results.

Further tests using a full-scale prototype structure confirm that damping in the full-scale structure can be significantly increased by adding relatively small viscoelastic dampers. The damper design procedure developed based on the scaled model can also be applied to the full-scale structure. This full-scale analytical and experimental study provides an important base for applying the extensive data generated from the scaled model testing to the full-scale structures.

ACKNOWLEDGEMENT

Preceding page blank

TABLE OF CONTENTS

Preceding page blank

TABLE OF CONTENTS (continued)

LIST OF FIGURES

LIST OF FIGURES (continued)

LIST OF TABLES

Preceding page blank

SECTION 1

INTRODUCTION

Viscoelastic (VE) dampers have been successfully applied to tall buildings to reduce wind-induced vibrations for over twenty years. The application of VE dampers to reduce seismic response of buildings, however, has been investigated only in the last few years. Analytical investigations on the use of VE dampers in civil engineering structures have been carried out at the University of Michigan, Ann Arbor, and at the State University of New York at Buffalo. Results from these studies showed that the response of buildings due to strong earthquakes can be reduced significantly. Experimental studies using shaking tables have also been conducted on a three-story and a nine-story steel frames at Buffalo and Berkeley, respectively. These results showed notable increases in measured structural damping. The corresponding structural responses due to seismic loading also decreased accordingly. However, test results also showed that, while they can be effective in attenuating seismic response of the structure, their proper design for maximum efficiency must take into account important factors such as excitation frequencies and environmental temperature within which they operate. In addition, reliable analytical models which can accurately predict the equivalent structural damping due to the addition of VE dampers were not available. Therefore, a rational design procedure for viscoelastically damped structures could not be established.

Recently, further analytical and experimental studies on dynamic response of VE dampers and on seismic response of viscoelastically damped structures have been carried out. The experimental program was conducted on a 2/5-scale five-story steel model under a variety of precisely controlled ambient temperatures and recorded ground motions. Results from that study showed that the viscoelastic dampers are very effective in reducing seismic structural response at all levels of earthquake ground motions, and that their energy dissipation capacity decreases as temperature increases. However, they were effective in reducing excessive vibrations of the test structure at all temperatures tested in the research program. More importantly, based on the test results, it appears that the dynamic characteristics of viscoelastically damped structures can simply and accurately be predicted by using the modal strain energy method and that conventional dynamic linear analysis routines can be used to predict the seismic response at all levels of ambient temperatures and earthquake ground motions. Based on these studies, a rational design procedure has been developed.

Preceding page blank

In order to verify the test results obtained and the damper design procedure developed from the 2/5-scale structural model, an experimental program using a full-scale prototype structure was carried out at the Beijing Polytechnic University. The modal strain energy method used for the reduced scaled model was employed to design the dampers and to predice the added damping to the structure with added dampers. Two eccentric mass vibration generators were used to sinusoidally excite the structure.

This report summarizes the aforementioned experimental and analytical studies on the model structure and the prototype structure, and proposes a procedure for design and retrofit of structures with added viscoelastic dampers.

SECTION 2

DYNAMIC CHARACTERISTICS OF VISCOELASTIC DAMPERS

2.1 Basic Equations of VE Dampers

The behavior of a single-degree-of-freedom (SDOF) system consisting of a mass m and a viscoelastic element subject to a simple harmonic excitation with amplitude P_o and frequency ω is governed by

$$m\ddot{u} + g(u, \dot{u}) = P_o \sin \omega t \qquad (2.1)$$

where $g(u, \dot{u})$ is a function of the displacement and velocity. For steady-state harmonic motion, $g(u, \dot{u})$ can be expressed as the sum of a spring force $f_s = k'u$, where k' is the damper storage stiffness, and a damping force f_d given by

$$f_d = \frac{\eta k'}{\omega} \dot{u} \qquad (2.2)$$

in which η is a constant (loss factor of the damper). The total force f is then given by

$$f = k'u + \frac{\eta k'}{\omega} \dot{u} \qquad (2.3)$$

In order to plot the relationship between the total force f and the damper displacement u, $\dot{u} = u_o \omega \cos \omega t$ is substituted into Eq. (2.3), giving

$$\frac{f - k'u}{\eta k' u_o} = \cos \omega t \qquad (2.4)$$

Since $u = u_o \sin \omega t$, Eq. (2.4) becomes

$$\left(\frac{f - k'u}{\eta k' u_o} \right)^2 + \left(\frac{u}{u_o} \right)^2 = 1 \qquad (2.5)$$

The plot of the above relationship is shown in Fig. 2.1, where

f_o = maximum damper force
f' = damper force at maximum displacement
f'' = damper force at zero displacement $(= \eta k' u_o)$
u_o = maximum damper displacement
k' = damper storage stiffness $(= f'/u_o)$

If the hysteretic behavior of the damper under harmonic motion is linear, the strain alternates sinusoidally but is out of phase with the stress (Fig. 2.2). Thus, the strain and the stress can be expressed by

$$\gamma = \gamma_o \sin \omega t \tag{2.6a}$$

$$\sigma = \sigma_o \sin(\omega t + \delta) \tag{2.6b}$$

where δ is the phase angle. The relationship between the stress and the strain is

$$\sigma = G^* \gamma_o \sin(\omega t + \delta)$$

$$= \gamma_o (G' \sin \omega t + G'' \cos \omega t) \tag{2.7}$$

where

G^* = complex shear modulus

G' = shear storage modulus

G'' = shear loss modulus

From Eq. (2.7), the phase angle δ can be expressed by

$$\delta = \tan^{-1} \frac{G''}{G'} = \tan^{-1} \eta \tag{2.8}$$

and the energy dissipated per cycle due to the hysteretic damping, E_d, is given by [4]

$$E_d = \int_0^{\frac{2\pi}{\omega}} \sigma (d\gamma/dt) dt \tag{2.9}$$

Using the relationships in Eqs. (2.6) and (2.7),

$$E_d = \int_0^{\frac{2\pi}{\omega}} \gamma_o^2 \omega (G' \sin \omega t + G'' \cos \omega t) \cos \omega t dt$$

$$= \pi \gamma_o^2 G'' \tag{2.10}$$

Now, the stress-strain relationship of the hysteretic behavior of the damper can be expressed by using the force-displacement relationship [Eq. (2.5)]. Let $\sigma = f/A$ and $\gamma = u/h$, where A and h are the damper area and thickness, respectively, one has

$$\left(\frac{\sigma - \frac{\sigma'}{\gamma_o} \gamma}{\sigma''} \right)^2 + \left(\frac{\gamma}{\gamma_o} \right)^2 = 1 \tag{2.11}$$

2-2

$$\sigma = \gamma \frac{\sigma'}{\gamma_o} \pm \frac{\sigma''}{\gamma_o} \sqrt{\gamma_o^2 - \gamma^2} \tag{2.12}$$

The plot of the $\sigma - \gamma$ relationship is shown in Fig. 2.3, where

σ_o = maximum damper stress

σ' = damper stress at maximum damper strain

σ'' = damper stress at zero damper strain

γ_o = maximum damper strain

Equation (2.12) can also be expressed in terms of the shear moduli as

$$\sigma = \gamma G' \pm G'' \sqrt{\gamma_o^2 - \gamma^2} \tag{2.13}$$

where, from Eqs. (2.6a) and (2.7),

$$G' = \frac{\sigma'}{\gamma_o}, \quad \text{when } \gamma = \gamma_o \tag{2.14}$$

$$G'' = \frac{\sigma''}{\gamma_o}, \quad \text{when } \gamma = 0 \tag{2.15}$$

One also has

$$(G')^2 + (G'')^2 = (G^*)^2 = \left(\frac{\sigma_o}{\gamma_o}\right)^2 \tag{2.16}$$

Since $k' = f'/u_o$, from Eq. (2.6),

$$k' = \frac{f'}{u_o} = \frac{\sigma' A}{\gamma_o h} = \frac{G' A}{h} \tag{2.17}$$

The dynamic properties of the viscoelastic damper are characterized by: (a) the shear loss modulus G'', (b) the shear storage modulus G', and (c) the loss factor $\eta = G''/G'$. The shear loss modulus controls the specific energy dissipation capacity of the damper. High values of G'' indicate high energy dissipation capacity of the damper. The shear storage modulus affects the change in stiffness of the structural system to which the damper is added. The loss factor η is a measure of the suitability of the damper as a damping medium.

2.2 VE Damper Test Program

The VE damper properties described above are, however, dependent on temperature, frequency, and, to a certain degree, the damper strain. They can be characterized through damper tests.

Three types of viscoelastic dampers distinguished by dimensions and types of the viscoelastic material are used in this study. They are designated as Type A, B and C, respectively. Types A and B dampers are made of similar VE materials but different in damper dimensions. Type C damper is made from a different VE material. Table 2.1 lists the area, thickness and volume of each type of the dampers. A typical sketch of the damper used in the test is shown in Fig. 2.4. At least three dampers from each group were studied experimentally. The test set-ups are the same as those reported earlier [7].

Type A dampers were first tested under six different ambient temperatures (21°C, 24°C, 28°C, 32°C, 36°C and 40°C). At each temperature, six tests were conducted at frequencies of 0.1 Hz, 1.0 Hz, 2.0 Hz, 3.0 Hz, 3.5 Hz and 4.0 Hz, respectively, for up to fifty cycles of deformation in three different strain ranges (5%, 20% and 50%). Detailed test results of Type A dampers have been reported in [7]. Next, Type B and Type C dampers were tested at constant 5% strain for frequencies of 3.0 Hz, 3.5 Hz and 4.0 Hz under five different ambient temperatures (25°C, 30°C, 34°C 38°C and 42°C). Finally, Type B dampers were tested at three more strains (15%, 25% and 50%) at 24°C to simulate the effect of damper strain on the energy dissipation capacity of the VE dampers under medium to strong earthquake ground motions. A list of the damper test program is summarized in Table 2.2.

2.3 Test Results

The force-deformation curves of the three types of dampers subjected to sinusoidal excitations with frequency 3.5 Hz and 5% damper strain at two ambient temperatures are shown in Figs. 2.5a-2.5f. All the loops are fairly rounded in shape, indicating that the dampers can effectively dissipate energy. It is seen from these figures that the damper stiffness and the amount of energy dissipation in one cycle decrease for all types of dampers with increasing ambient temperature. This is consistent with that reported earlier [7] on Type A dampers. The loss factors, however, remain more or less constant for each type of dampers regardless of the change in ambient temperature. Comparisons of damper properties among the three types of dampers are listed in Table 2.3.

From Table 2.3, it may be concluded that the Type C damper is less sensitive to the change of ambient temperature. The percent reductions in energy dissipation capacity due to the change of ambient temperature from 24°C to 42°C are 73%, 71% and 60%, respectively, for Types A, B and C dampers. The lower temperature sensitivity of the Type C damper can also be observed in the reduction rates of the damper stiffness, which are

70%, 68% and 34%, respectively, for Types A, B and C dampers. These results suggest that the temperature-dependent property of the VE dampers can be improved by further research in viscoelastic materials.

2.4 Damper Properties for Practical Applications

From the above descriptions, it is clear that one has to take into account the effect of ambient temperature and excitation frequency for an effective design of viscoelastic dampers in seismic applications. The damper properties are also, to a certain degree, dependent on the number of loading cycles and the range of deformation, especially under large strain due to temperature increase within the damper material. However, these effects have been shown to be less significant in seismic applications because peak accelerations typically occur in only a few cycles of excitation. The average excitation is normally far less severe than the peaks. Tests results of typical Type B dampers under the excitation frequencies of 1 Hz and 3 Hz, ambient temperatures of 24°C and 36°C and damper strains of 5% and 20% are listed in Table 2.4. It can be seen that the damper properties remain somewhat constant and independent of strain (below 20%) for each temperature and frequency. Therefore, it is possible to analyze the seismic response of viscoelastically damped structures with sufficient accuracy based on the properties of the VE dampers corresponding to 20% strain.

In general, constitutive relationships of viscoelastic dampers can be derived based on the theory of viscoelasticity [12,13]. For practical design purposes, the damper loss factor can be considered as a constant but different for each viscoelastic material. In order to include the effect of ambient temperature and vibration frequency in the estimation of damper stiffness, empirical formulae can be derived based on linear regression analysis using the data obtained from damper component tests. The empirical formulae for the three types of dampers used in this study are obtained as follows:

(1) Type A Damper:

$$K_d = e^{14.78}(\omega)^{0.69}(T)^{-2.26} \tag{2.18}$$

(2) Type B Damper:

$$K_d = e^{15.68}(\omega)^{0.50}(T)^{-2.25}(\gamma)^{-0.28} \tag{2.19}$$

(3) Type C Damper:

$$K_d = e^{11.87}(\omega)^{0.43}(T)^{-0.69} \tag{2.20}$$

where

K_d = stiffness of the damper (lb/in)

ω = vibration frequency (Hz)

T = ambient temperature (°C)

γ = shear strain of the damper (%)

The above formulae for Type A and Type C dampers were derived based on the average of first twenty cycles of damper deformation with an average strain of 5%, which is considered to be reasonable under a typical moderate earthquake excitation. For Type B dampers, the damper strain γ was included in the equation to account for the various ranges of damper strain due to strong earthquake ground motions.

Table 2.1   Viscoelastic Damper Dimensions

Type	Area (in^2)	Thickness (in)	Volume (in^3)
'A'	1.0 x 1.5 = 1.50	0.20	0.30
'B'	2.0 x 1.5 = 2.00	0.30	0.90
'C'	6.0 x 3.0 = 18.0	0.15	2.70

Table 2.2   Damper Test Program

	Type 'A'	Type 'B' & 'C'	Type 'B'
Freq. (Hz)	0.1, 1.0, 2.0, 3.0, 3.5, 4.0	3.0, 3.5, 4.0	3.0, 3.5, 4.0
Strain (%)	5, 20, 50	5	5, 15, 25, 50
Temp.(°C)	21, 24, 28, 32, 36, 40	25, 30, 34, 38, 42	24

Table 2.3   VE Damper Properties at 3.5 Hz and 5% Strain

Damper Type	Temp. (°C)	W (lb.in)	K_d (lb/in)	G' (psi)	G" (psi)	η
'A'	21	2058	6135	402.8	436.7	1.08
	24	1623	4506	305.0	344.5	1.13
	28	1296	3562	228.4	275.1	1.20
	32	934	2636	169.0	198.2	1.17
	36	619	1871	120.7	130.7	1.08
	40	434	1353	91.4	92.0	1.01
'B'	25	4196	5142	251.1	301.3	1.20
	30	3023	3751	187.8	223.5	1.19
	34	2146	2740	136.9	161.5	1.18
	38	1590	2126	110.9	122.0	1.1
	42	1236	1647	89.8	94.3	1.05
'C'	25	925	6965	28.2	24.6	0.87
	30	680	5589	23.1	18.1	0.78
	34	562	5021	21.0	15.0	0.71
	38	438	4414	17.6	11.6	0.65
	42	370	3899	15.6	9.8	0.62

Table 2.4   Typical Damper Properties

Temp.(°C)	Freq.(Hz)	Strain(%)	K'(lb/in)	G'(psi)	G"(psi)	η
24	1.0	5	2124	142	170	1.2
24	1.0	20	2082	139	167	1.2
24	3.0	5	4084	272	324	1.19
24	3.0	20	3840	256	306	1.2
36	1.0	5	880	59	67	1.13
36	1.0	20	873	58	65	1.12
36	3.0	5	1626	108	119	1.1
36	3.0	20	1542	103	112	1.09
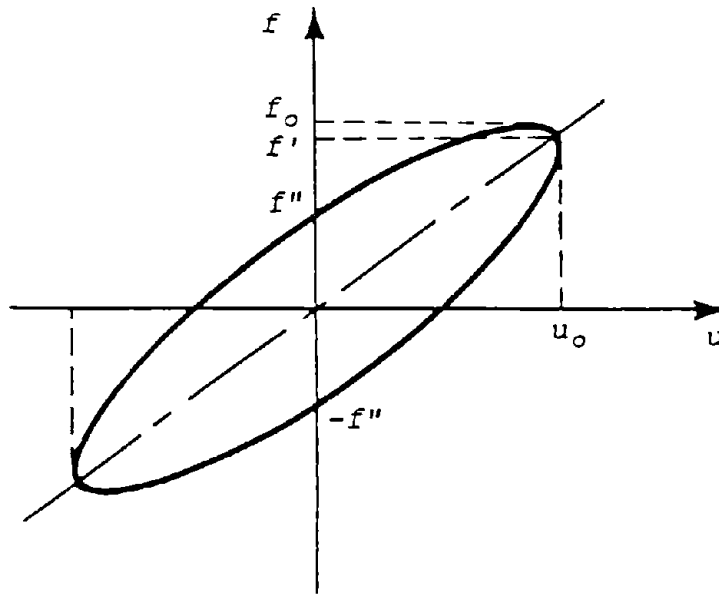
Fig. 2.1   Plot of Force Versus Displacement
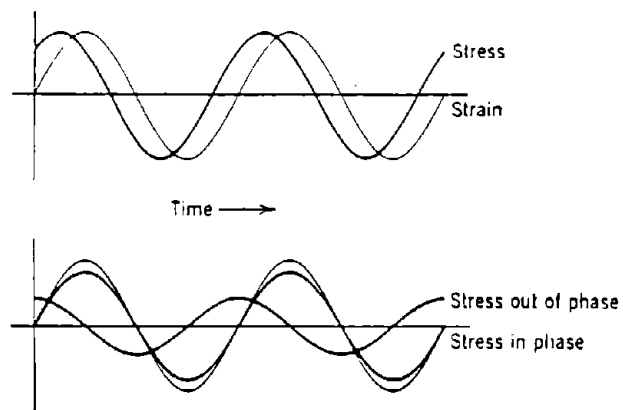
Fig. 2.2   Stress and Strain under Steady-State Periodic Deformations

2-9
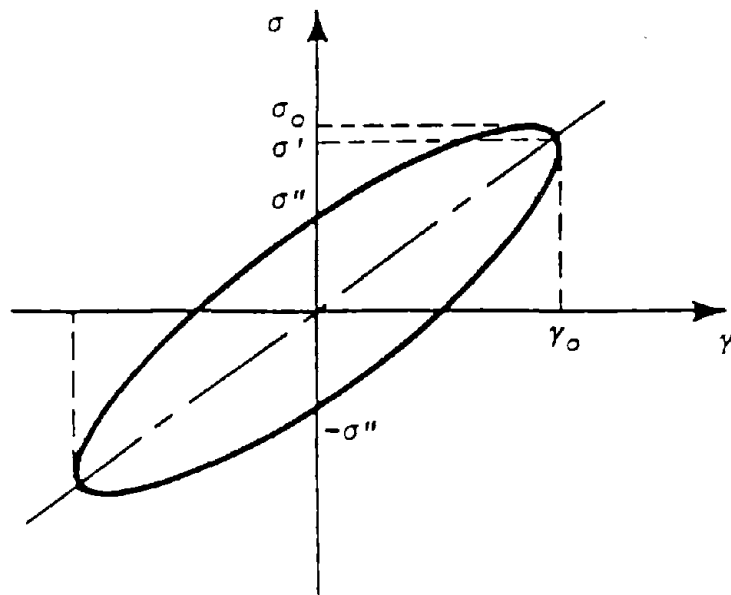
Fig. 2.3   Plot of Stress versus Strain
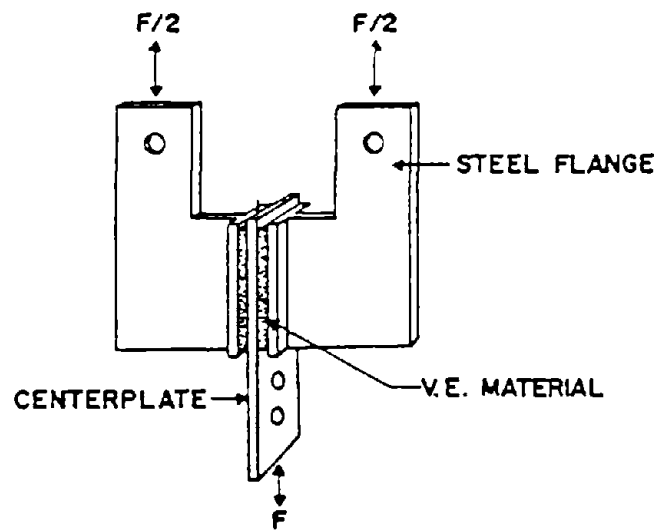
Fig. 2.4   Damper used in Test Program
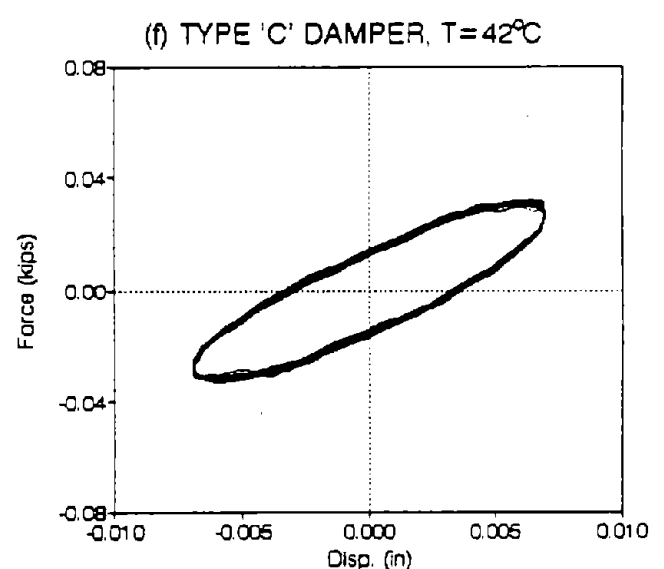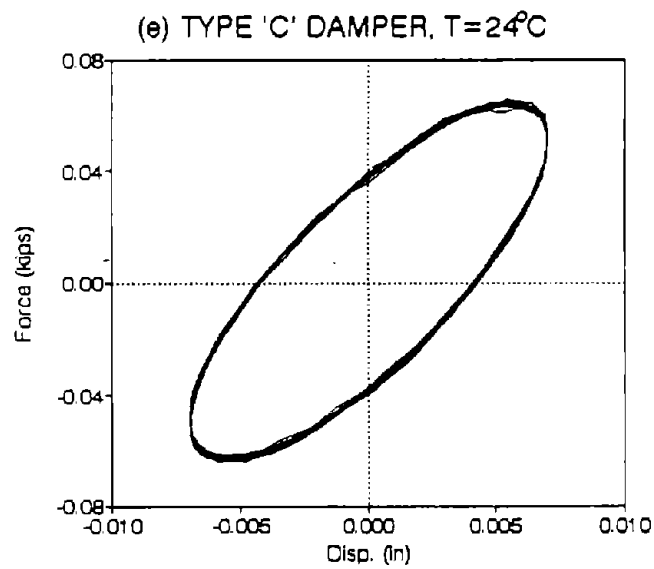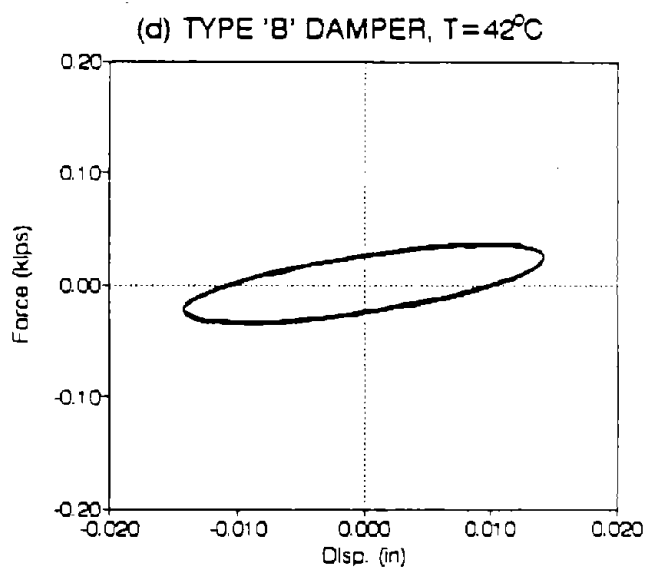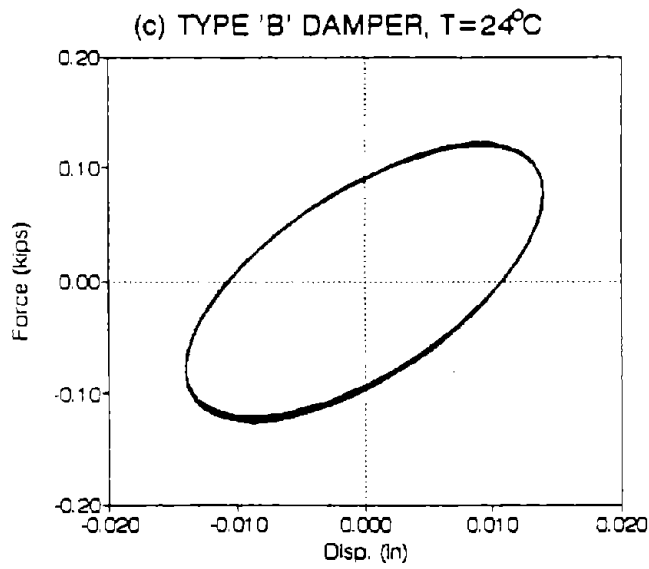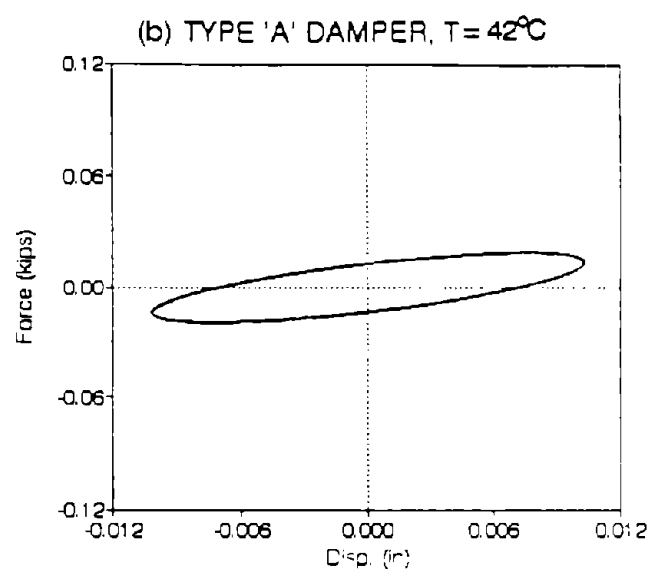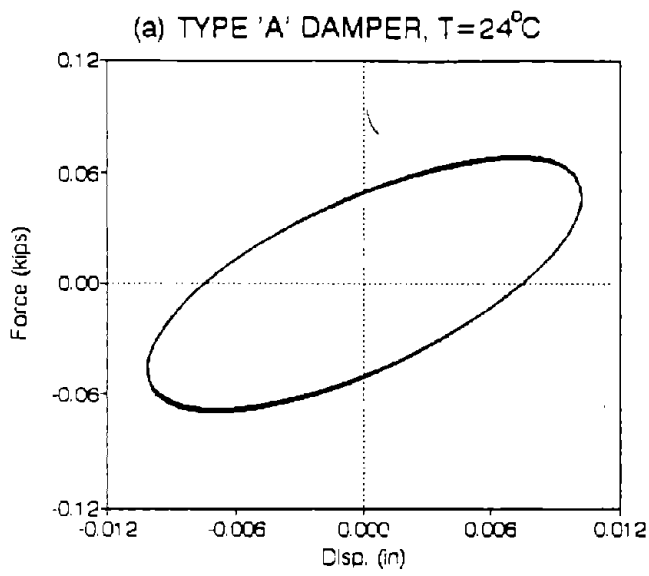
Fig. 2.5 Comparison of Force-Deformation Relationships
(5% Strain, 3.5Hz)

2-11

SECTION 3

SEISMIC TESTS OF VISCOELASTICALLY DAMPED STRUCTURE

3.1 Introduction

A 2/5-scale five-story steel structure [1] (Fig. 3.1) with and without added VE dampers was first tested using a shaking table [15] under 0.12g white noise and Hachinohe earthquake ground motions with precisely controlled ambient temperatures. The viscoelastically damped structure was then studied under strong earthquake ground motions of El Centro and Hachinohe earthquakes (Figures 3.2a,b and 3.3a,b) with peak ground accelerations scaled up to 0.6g.

All three types of the VE dampers reported in Section 2 were used in the experimental program. The seismic behavior of the model structure with added Type A dampers under various ambient temperatures has been discussed in detail [7]. This section will emphasize the seismic behavior of the model structure with added Type B dampers, especially under strong earthquake ground motions.

3.2 Inelastic Analysis of Test Structure without VE Dampers

In this section, analytical analyses of the test structure without added dampers are carried out under strong earthquake ground motions. The structure is then used to study the seismic response with added viscoelastic dampers under strong earthquake ground motions. It will also be used to illustrate the design procedure for applying viscoelastic dampers to structures as discussed in Section 4.

3.2.1 Description of the Structure

The structure used to illustrate the design process is a 2/5-scale five-story steel frame [15]. It was constructed under the US-China Cooperative Research Program on Dynamic Testing and Analysis. Overall dimensions of the test frame are 52.0″×52.0″ in plan and 224.0″ in height, as shown in Fig. 3.1. The cross-sectional properties of the members in the direction of earthquake ground motions are listed in Table 3.1.

A lumped mass system with weights of 1.27 kips for the first four floors and 1.31 kips for the fifth floor is used to simulate a prototype structure. By so doing, the model

Preceding page blank

structure will behave as a five-degree-of-freedom system when subjected to lateral loads. Detailed descriptions of the model structure can be found in [15].

3.2.2 Ground Motions used in Analytical Study

Based on previous studies, the range of natural frequencies of the model structure without adding VE dampers is between 3.1 to 3.2 Hz. When VE dampers are added to the structure, the natural frequency of the structure increases to between 3.25 Hz and 3.65 Hz, depending on the ambient temperature [7]. The damping ratio of the structure without added VE dampers is about 1%, while that with added VE dampers is about 15% at room temperature (25°C). Figures 3.2b and 3.3b show the time-scaled acceleration response spectra of El Centro and Hachinohe earthquakes, respectively, used in this study. It can be seen that, at 1% critical damping, the El Centro earthquake has a large energy concentration between frequencies of 3.4 Hz and 3.55 Hz, while the corresponding frequency range for the Hachinohe earthquake is between 3.15 Hz and 3.35 Hz. Increasing the structure's natural frequency to about 3.6 Hz may be quite beneficial to the structure when subjected to the Hachinohe earthquake at room temperature. However, at high ambient temperatures, the structure may be subjected to larger seismic input energy. The opposite is true when subjected to the El Centro earthquake. In these figures, they also show that, at 15% critical damping, the pseudo-acceleration is much lower than that at 1% critical damping. More importantly, irrespective of the type of energy content of a given earthquake the pseudo-acceleration at 15% critical damping is nearly constant across all frequency ranges. This indicates that providing extra damping to structures will be effective regardless of the type of input ground motions. In this study, analyses on the seismic response of the model structure subjected to the aforementioned earthquake records scaled to various levels of peak accelerations were carried out using DRAIN2D [17]. It should be noted that the model structure was overly designed to carry out a variety of research projects. With the weight used in this study to simulate the prototype structure, it is expected that very large ground motions are required to severely damage the structure.

3.2.3 Analytical Results

The calculated natural frequency of the model structure without added dampers corresponding to the first mode of vibration is 3.08 Hz. Comparisons between analytical simulation and experimental result of the structural response without added VE dampers under 0.12g El Centro and Hachinohe earthquake ground motions show that DRAIN2D

can describe the dynamic response of the model structure reasonably well in the elastic range.

Inelastic analysis on the model structure was carried out under 0.6g peak acceleration of the above two ground motions. Assuming yield stress of 36 ksi for the steel members, the plastic moments of the beams and columns used in the analysis are 59.5 in-kip and 41.04 in-kip, respectively. Figures 3.4a and 3.4b show the plastic hinges developed in the structure subjected to these two earthquake ground motions. This indicates that the structure, even though overly designed, may suffer substantial damage under these strong earthquakes.

Table 3.2 summarizes the results of inelastic analysis in terms of maximum lateral displacements and interstory drifts at each floor level. Values in this table will be used to assess the efficiency of VE dampers designed for this model structure subjected to strong earthquake ground motions.

3.3 Test Setup and Test Program

The test setup and instrumentation used in this study are identical to those reported in [7]. However, the temperature control devices were removed for tests under strong earthquake excitations because they might restrict heat transfer from the dampers to the environment.

The first phase of the test program was aimed at studying the effect of ambient temperature on seismic performance of the structure with three different types (Types A, B and C) of VE dampers. Earthquake simulation tests were carried out starting at the temperature of 25°C under the scaled 0.12g Hachinohe earthquake. The ambient temperature was then controlled to gradually increase up to 42°C in each subsequent test.

In the second phase of the test program, seismic simulation tests were conducted under Hachinohe and El Centro earthquake ground motions scaled in time and peak accelerations. Since analytical studies of the model structure without added VE dampers showed that the structure might be damaged under the above two earthquakes with peak ground accelerations greater than 0.24g, only the structure with added VE dampers was tested in this phase of the study. The tests started at a peak ground acceleration of 0.12g and continued up to 0.60g at room temperature of the laboratory (24°C). After each test, maximum strains in the columns and beams were monitored to assure that the test

structure remained elastic. Any possible damage to the dampers was also examined. As a result, 0.60g peak acceleration for both earthquake was chosen as the limit due to the shaking table's displacement capacity.

3.4 Effect of Ambient Temperature

3.4.1 Dynamic Structural Characteristics

Based on white noise tests, the natural frequency of the model structure without added VE dampers was found to be 3.17 Hz. When VE dampers were added to the structure, the natural frequency increased to between 3.26 Hz and 3.74 Hz, depending on the ambient temperature and the damper type. The corresponding damping ratio was between 5.1% and 15.8%. The temperature dependence of the natural frequency and equivalent damping ratio of the model structure with the three types of dampers are shown in Figs. 3.5a and 3.5b. They are consistent with those reported previously using Type A dampers [7]. As the ambient temperature increases, the VE material becomes softer and the energy dissipation capacity of the VE dampers decreases accordingly.

Figure 3.6a shows the transfer functions of the model structure with added Type B dampers under ambient temperatures of 25°C, 34°C and 42°C. It is apparent from the shapes of the transfer functions that the equivalent damping ratio of the viscoelastically damped structure decreases as the ambient temperature increases. In addition, the effect of higher vibration modes becomes insignificant with the addition of the VE dampers. This can be further illustrated in Fig. 3.6b where the transfer function of the model structure without added dampers is included for comparison. In this figure, the higher modes of the structure without added dampers appear to be significant and the corresponding structural damping is clearly much smaller than that of the structure with added VE dampers at all ambient temperatures. The existence of small peaks of the transfer function corresponding to the structure without added dampers is believed to be due to accidental torsion. They are completely eliminated when VE dampers are applied.

3.4.2 Seismic Structural Response

As was reported earlier [7], seismic response of the viscoelastically damped structure increases with increasing ambient temperatures. Similar observations are made for Type B and Type C dampers under the 0.12g Hachinohe earthquake. Figures 3.7a-c show a portion of the lateral displacement time history at the 5th, 3rd and 1st floor, respectively, of the model structure with Type B dampers under the ambient temperatures of 25°C

and 42°C. Also included in these figures are the corresponding response of the structure without added dampers. It can be seen that, compared with the no damper case, the addition of VE dampers effectively reduces the structural response as the ground motion starts. In addition, at 25°C, the response of the viscoelastically damped structure continues to decrease during the period that the response of the structure without added dampers increases. Similar observations can be made in the floor acceleration time histories as shown in Figs. 3.8a-c.

Seismic response envelopes of the model structure added with the three types of VE dampers under various ambient temperatures are shown in Figs. 3.9a-c. It can be seen that the temperature dependence of Type A and Type B dampers is similar while Type C damper is less affected by changes of the ambient temperature. All three types of dampers are effective in reducing the seismic response at all ambient temperatures as compared to the no damper case. However, when ambient temperature is as high as 42°C, the maximum damper deformation can be twice that at 25°C (Fig. 3.9d). Therefore, ambient temperature should be included as one of the design parameters for viscoelastically damped structures.

As indicated earlier, at higher temperatures the dampers will soften and deform more under the same earthquake ground motion. Figure 3.10 shows a portion of the damper deformation history at the second story under the 0.12g ground motions at ambient temperatures of 25°C, 34°C, and 42°C, respectively. As can be seen from this figure, damper deformation increases with increasing ambient temperature. However, the equivalent structural damping ratio becomes smaller as the ambient temperature increases (Fig. 3.5b). This indicates that the equivalent damping ratio of the viscoelastically damped structure does not depend on damper deformation alone. This phenomena may be explained by the modal strain energy concept that will be discussed in the next section.

3.5 Response under Strong Earthquake Ground Motions

3.5.1 Response Time Histories

Five different earthquake intensities (0.12g, 0.24g, 0.36g, 0.48g and 0.60g), expressed in terms of peak accelerations of the scaled Hachinohe and El Centro earthquake ground motions (Figs. 3.2a,b), were used as seismic inputs from the shaking table to study the performance of the model structure with added Type B dampers at room temperature.

Tests started at 0.12g peak acceleration and continued up to 0.60g in each subsequent test. At the end of each test, the structure is examined to assure elastic behavior and for possible damper damages. As indicated earlier, analytical results of the frame without added dampers are used to access the effectiveness of the viscoelastically damped structure under strong earthquake ground motions.

Figures 3.11a and 3.11b show the displacement time histories at the roof and the interstory drift at the second floor, respectively, of the model structure with and without added Type B dampers under the 0.6g Hachinohe earthquake. Figures 3.12a and 3.12b show the same information under the 0.6g El Centro earthquake. The structure without added dampers is expected to be severely damaged under these two ground motions, as indicated in the figures. It can be seen that the VE dampers effectively reduce the seismic response of the model structure. More importantly, the structure with added dampers remained elastic. Figures 3.13a or 3.13b show the strain time histories at the most critical section of the structure with added Type B dampers under these two earthquakes. The maximum strain is less than 0.06%, which is much less than the nominal yield strain of typical A-36 steel (0.12%) used to construct the model structure.

Figures 3.14a and 3.14b show the acceleration time histories of the model structure with and without added dampers subjected to the two earthquake ground motions. It can be seen that even though the structure without added dampers has been severely damaged in the numerical simulation under the 0.6g Hachinohe earthquake, the resulting floor acceleration is still much larger than that in the viscoelastically damped structure.

Figures 3.15a and 3.15b show lateral displacements and floor accelerations at the roof under the 0.24g Hachinohe earthquake for the structure without added dampers and the structures with added Type A, Type B and Type C dampers, respectively. It can be seen that all the dampers used in this study are similarly effective in reducing earthquake response under the same earthquake ground motion.

3.5.2 Effect of Earthquake Intensity

Figure 3.16a shows a portion of the VE damper deformation time histories at the second floor under 0.24g, 0.36g, 0.48g and 0.6g Hachinohe earthquakes. It can be seen that, in general, the fundamental frequency of the structure remains unchanged under different intensities of the ground motion. However, the damper efficiency is slightly lower under strong earthquakes as compared to that under moderate earthquakes. Figures 3.17a and 3.17b show the averaged transfer functions of the viscoelastically

damped structure under scaled Hachinohe and El Centro earthquakes. The damping ratio obtained from these transfer functions range from about 13% for the 0.6g Hachinohe earthquake to about 16% for the 0.24g El Centro earthquake. For the El Centro earthquakes, the earthquake intensity has very little effect on the damper efficiency (Fig. 3.17a) because the average damper deformation (Fig. 3.18a) and temperature rise within the damper material (2.2°C) are moderate. For the Hachinohe earthquakes, the damper efficiency is lower (Fig. 3.17b) because the average deformation (Fig. 3.18b) and the temperature increase within the damper material (4.5°C) are larger. However, the slight reduction in damper efficiency has very little effect on the structure's energy dissipation capacity, as can be seen from Fig. 3.16b and the structural responses are somewhat proportional to the intensities of the ground motions.

3.5.3 Response Envelope

Maximum response envelopes of relative lateral displacements, interstory drifts, story shear forces and overturning moments over the height of the model structure are shown in Figs. 3.19a-d and Figs. 3.20a-d. They are also summarized in Tables 3.3a,b. The maximum interstory drift ratios for the El Centro and the Hachinohe earthquakes are 0.46% and 0.5%, respectively. The reduction factors in the maximum base shear resulting from adding the dampers were 1.7 for both earthquakes. The reduction in the maximum interstory drift resulting from the inclusion of the dampers was by factors of 3.4 and 3.2 for the El Centro and the Hachinohe earthquake ground motions, respectively.

Figure 3.21 shows the response envelopes of the structure with (experimental result) and without (analytical simulation) added dampers under the 0.6g El Centro earthquake. Also shown in the figure is an analytical simulation of strengthening the structure without added damping. It can be seen that under this ground motion, simply adding more stiffness to the structure is not always beneficial because it may induce stronger vibrations. Using viscoelastic dampers not only adds stiffness to the structure but also provides a significant amount of damping which effectively reduces the excessive vibration due to strong earthquake ground motions.

Table 3.1   Cross-Sectional Properties of Structural Members

COLUMN	
Area (in^2)	2.41
I (in^4)	2.20
BEAM	
Area (in^2)	1.30
I (in^4)	3.28

Note: 1 in. = 25.4 mm

Table 3.2 Summary of Analytical Response Results

Maximum Response	Floor Level	0.6g El Centro	0.6g Hachinohe
Relative Floor Displacement (in)	5	2.150	3.490
	4	1.990	3.240
	3	1.650	2.700
	2	1.110	1.630
	1	0.390	0.470
Interstory Drift (in)	5-4	0.207	0.310
	4-3	0.365	0.599
	3-2	0.598	1.100
	2-1	0.721	1.185
	1-Base	0.394	0.470

Table 3.3a Summary of Inelastic Analysis (1% damping)

Ground Motion	Maximum Base Shear (kips)	Maximum Rotational Ductility	Maximum Overturning Moment (in-kip)	Interstory Drift Ratio (%)				
				1st	2nd	3rd	4th	5th
0.6g El Centro	7.604	2.73	967.8	1.1	1.5	1.3	0.8	0.4
0.6g Hachinohe	8.104	7.23	808.932	1.3	2.5	2.3	1.3	0.7

Table 3.3b Summary of Dynamic Response under 0.60g El Centro and Hachinohe Earthquakes

Maximum Response	Floor Level	No Damper (Inelastic Analysis)		With Type B Dampers (% Reduction of No Damper Case)	
		El Centro (0.60g)	Hachinohe (0.60g)	El Centro (0.60g)	Hachinohe (0.60g)
Relative Floor Disp. (inch)	5	2.150	3.490	0.766 (64.4)	0.823 (76.4)
	4	1.990	3.240	0.665 (66.6)	0.719 (77.8)
	3	1.650	2.700	0.529 (67.9)	0.579 (78.6)
	2	1.110	1.630	0.346 (68.8)	0.382 (76.6)
	1	0.390	0.470	0.143 (63.3)	0.148 (68.5)
Inter-Story Drift (inch)	5-4	0.207	0.310	0.104 (49.8)	0.111 (64.2)
	4-3	0.365	0.599	0.137 (62.5)	0.146 (75.6)
	3-2	0.598	1.100	0.187 (68.7)	0.201 (81.7)
	2-1	0.721	1.185	0.214 (70.3)	0.234 (80.3)
	1-0	0.394	0.470	0.143 (63.7)	0.148 (68.5)

52.0"   52.0"

4 @ 47.0"

36.0"

(a) Front View   (b) Side View
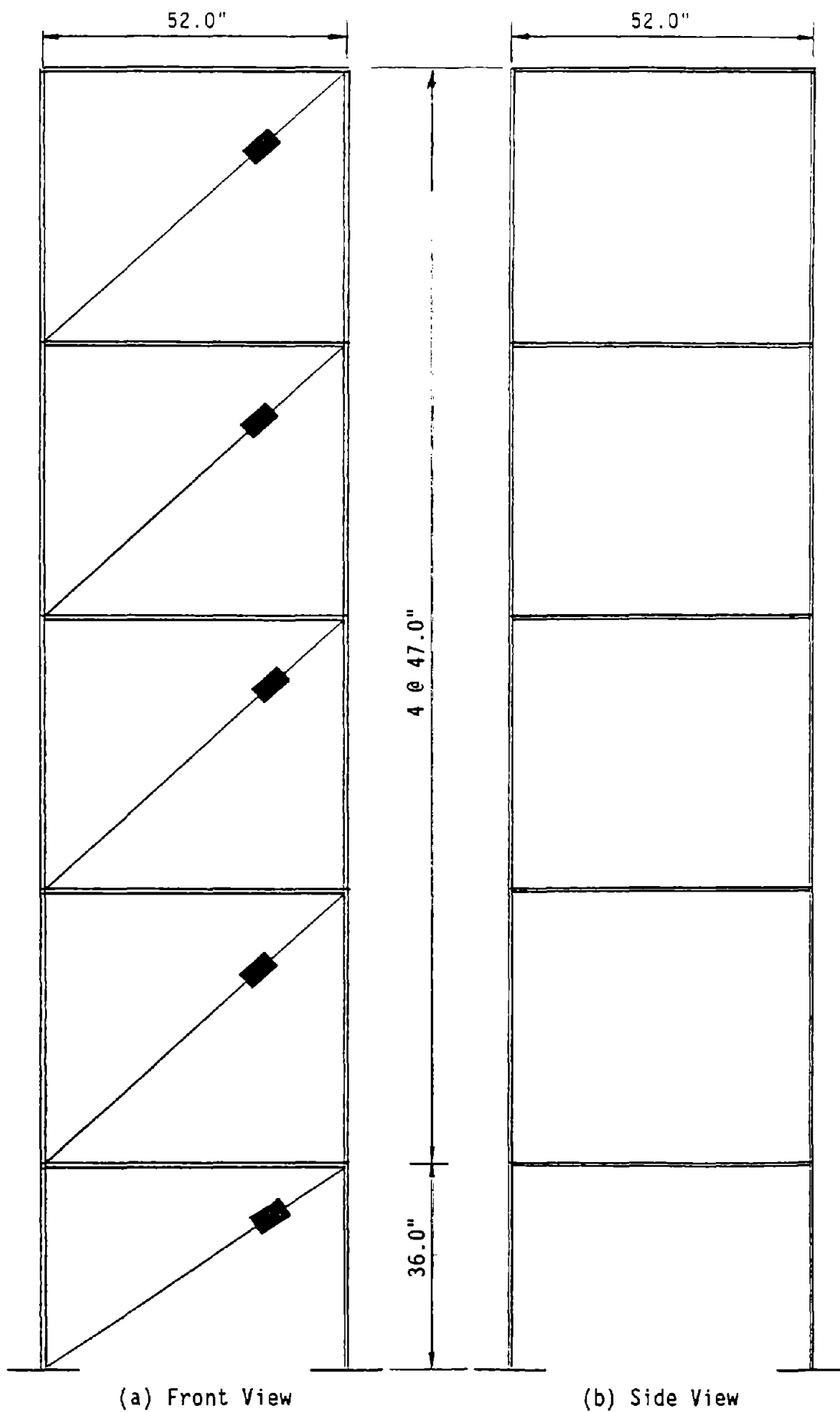
Fig. 3.1 Five-Story Steel Frame with Added VE Dampers
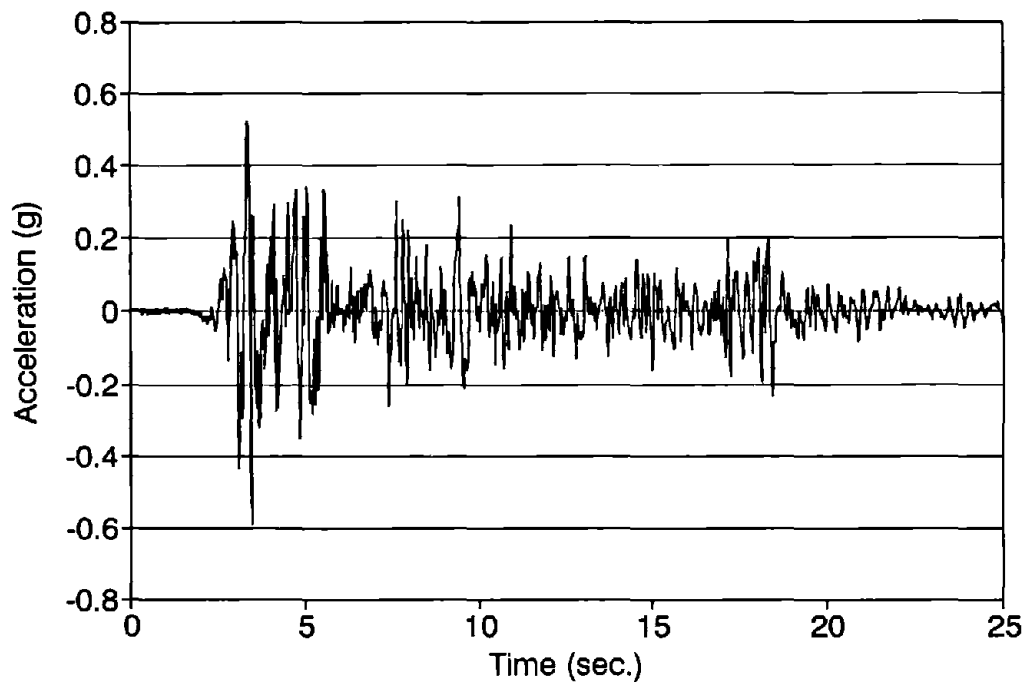
(a) Acceleration Time History
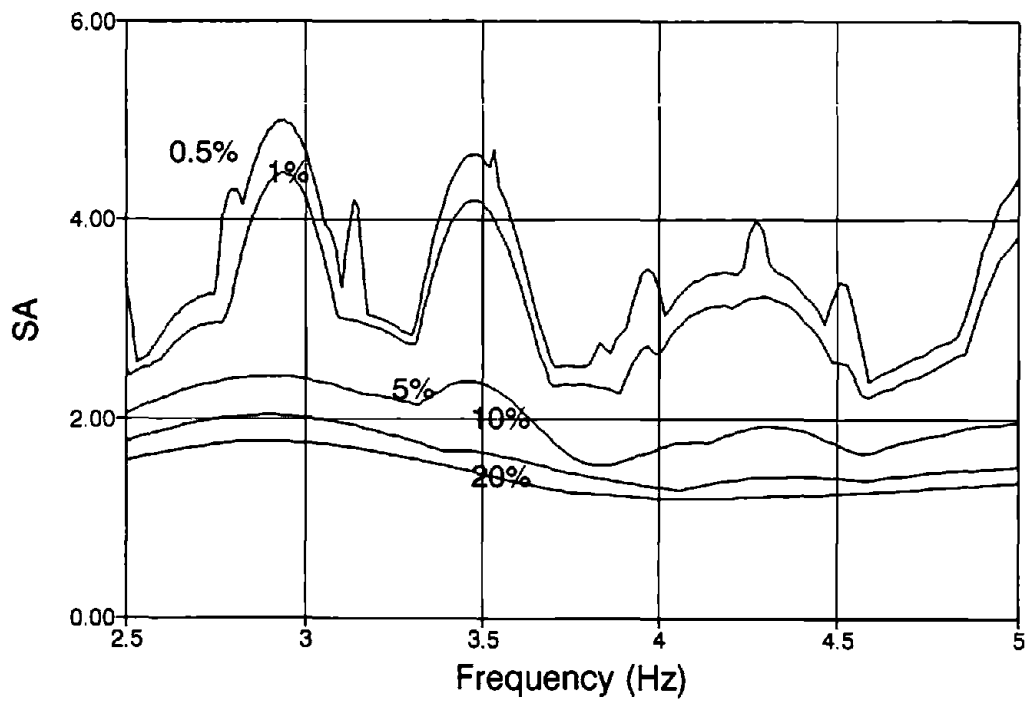
(b) Normalized Spectrum

Fig. 3.2   0.60g El Centro Earthquake
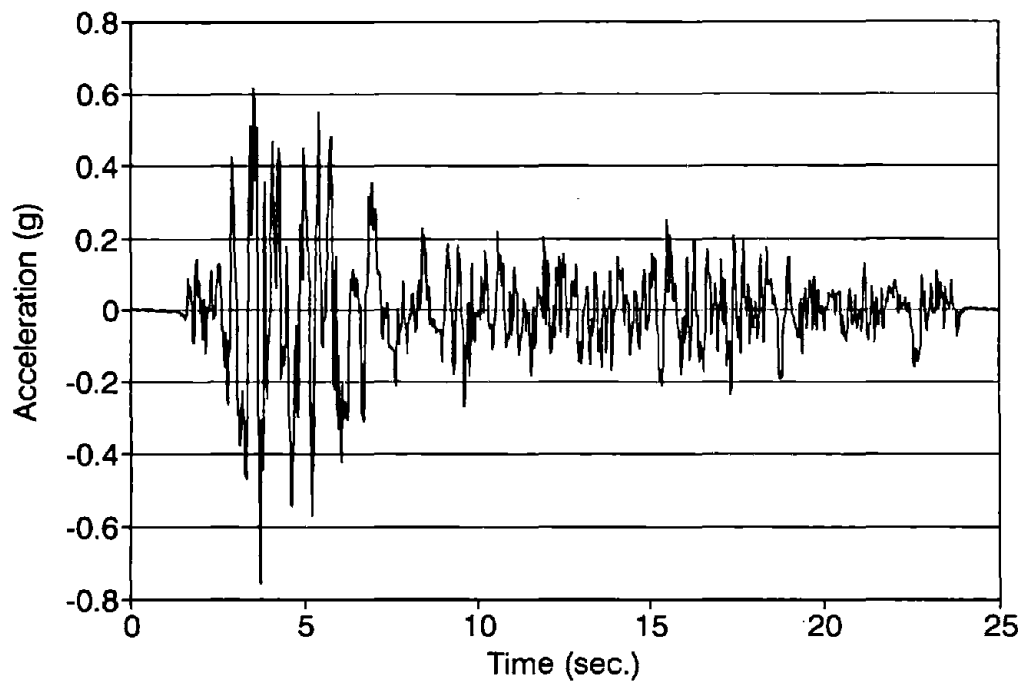
(a) Acceleration Time History
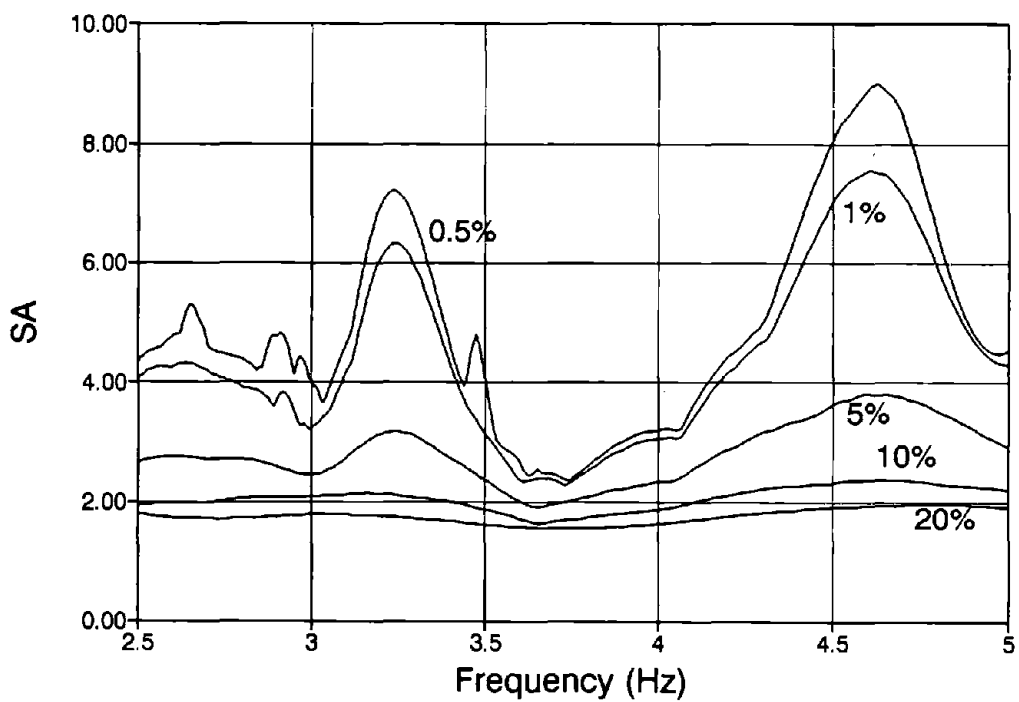
(b) Normalized Spectrum

Fig. 3.3   0.60g Hachinohe Earthquake

| 0.12g | 0.24g | 0.36g | 0.60g |
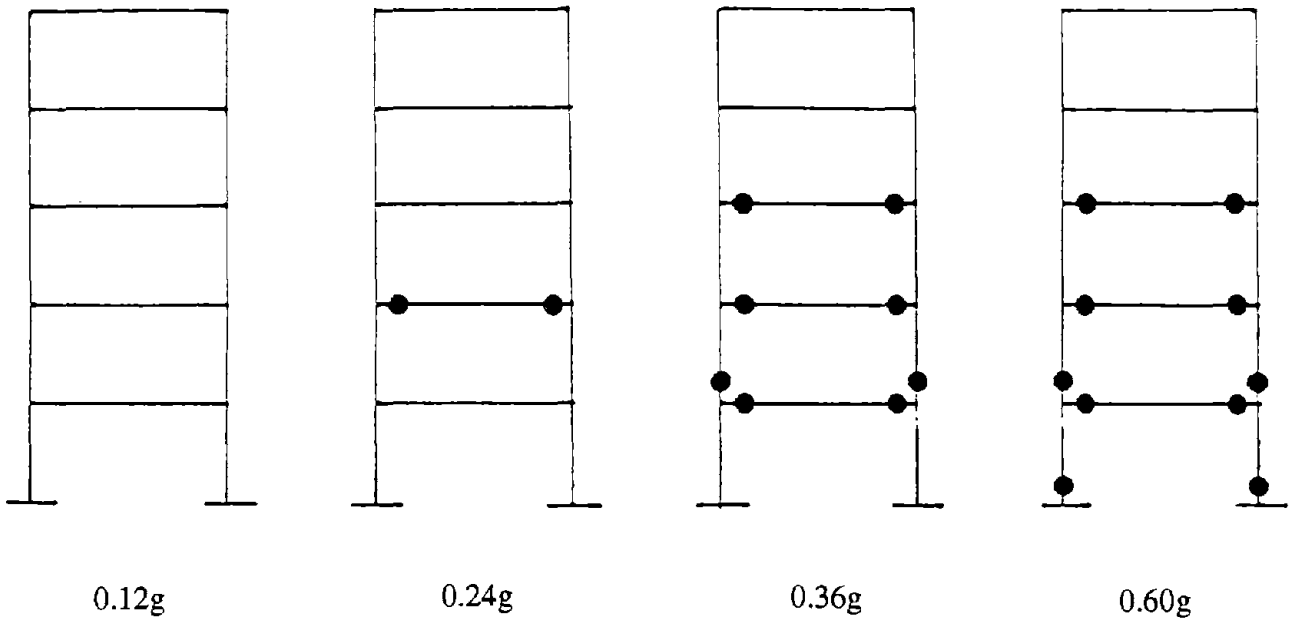
(a) Hachinohe Earthquake

| 0.36g | 0.48g | 0.60g |
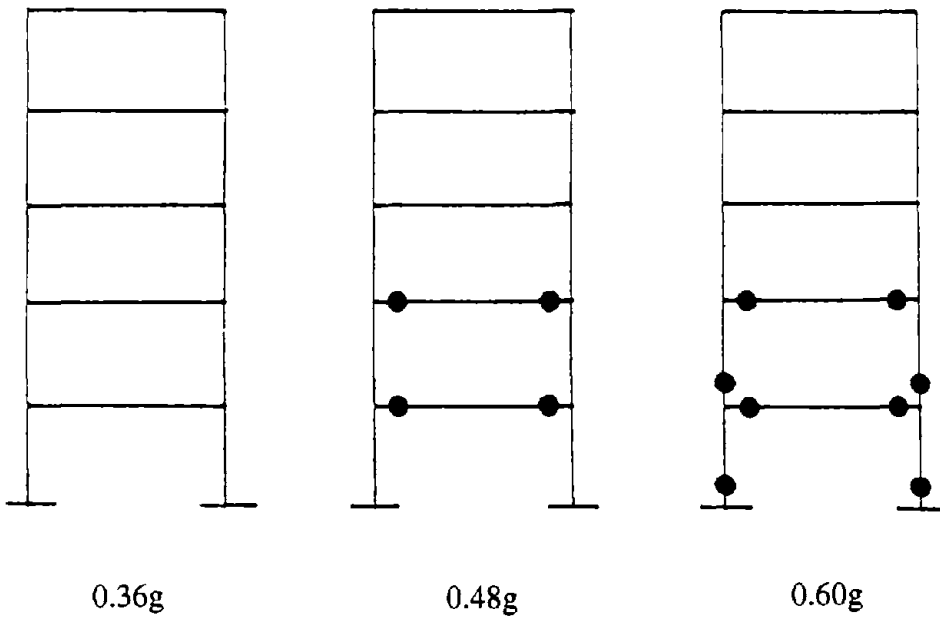
(b) El Centro Earthquake

Fig. 3.4 Plastic Hinge Formation Sequence

(a) Natural Frequency (Hz)

(b) Damping Ratio (%)
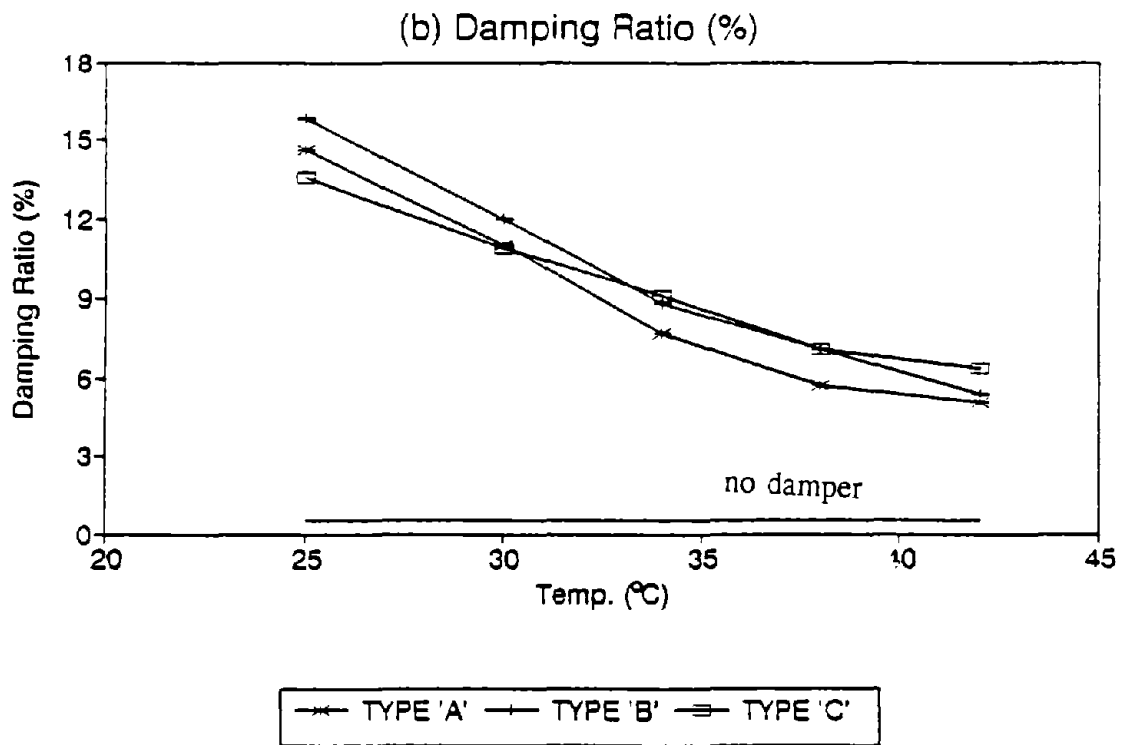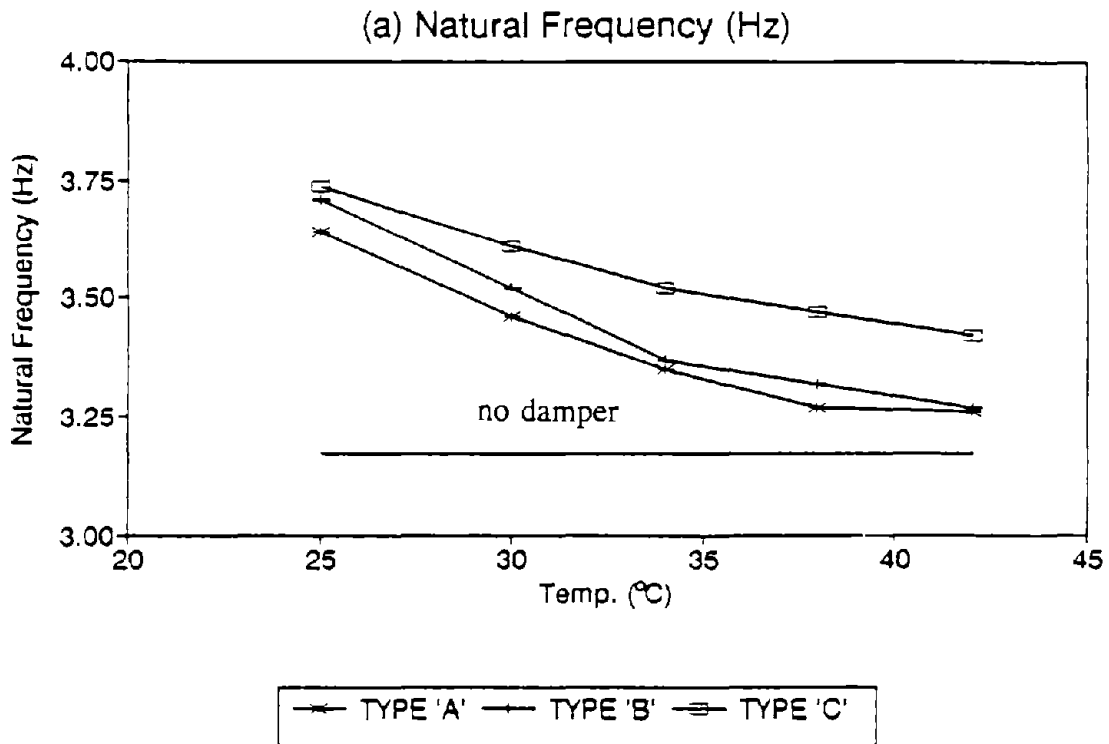
Fig. 3.5   Temperature Dependence of Structural Dynamic Characteristics
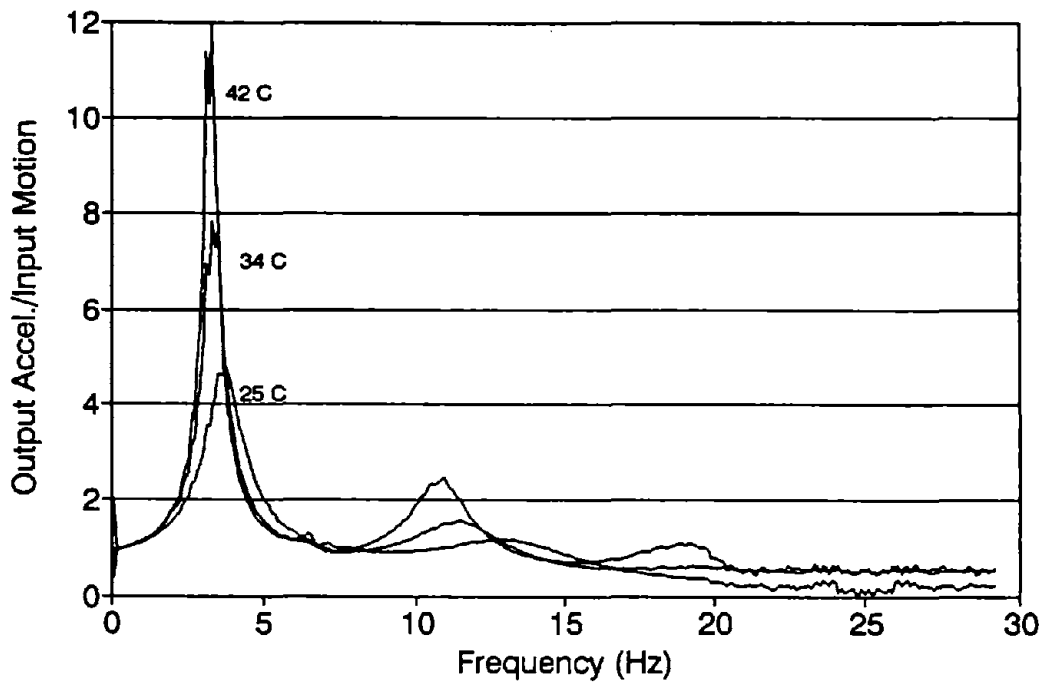
(a) Transfer Functions with Type B Dampers
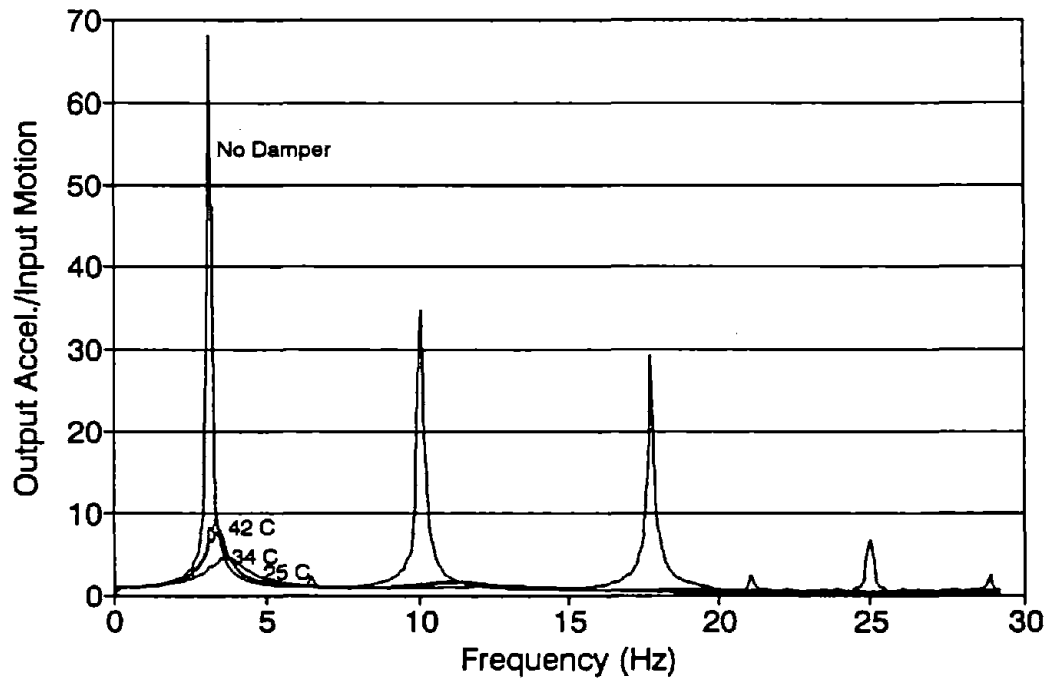
(b) Transfer Functions including No-damper Case

Fig. 3.6 Transfer Functions under Various Ambient Temperatures
(0.12g White Noise)

(a) Lateral Displacement at Roof
(0.12g Hachinohe Earthquake)

(b) Lateral Displacement at 3rd Floor
(0.12g Hachinohe Earthquake)

(c) Lateral Displacement at 1st Floor
(0.12g Hachinohe Earthquake)
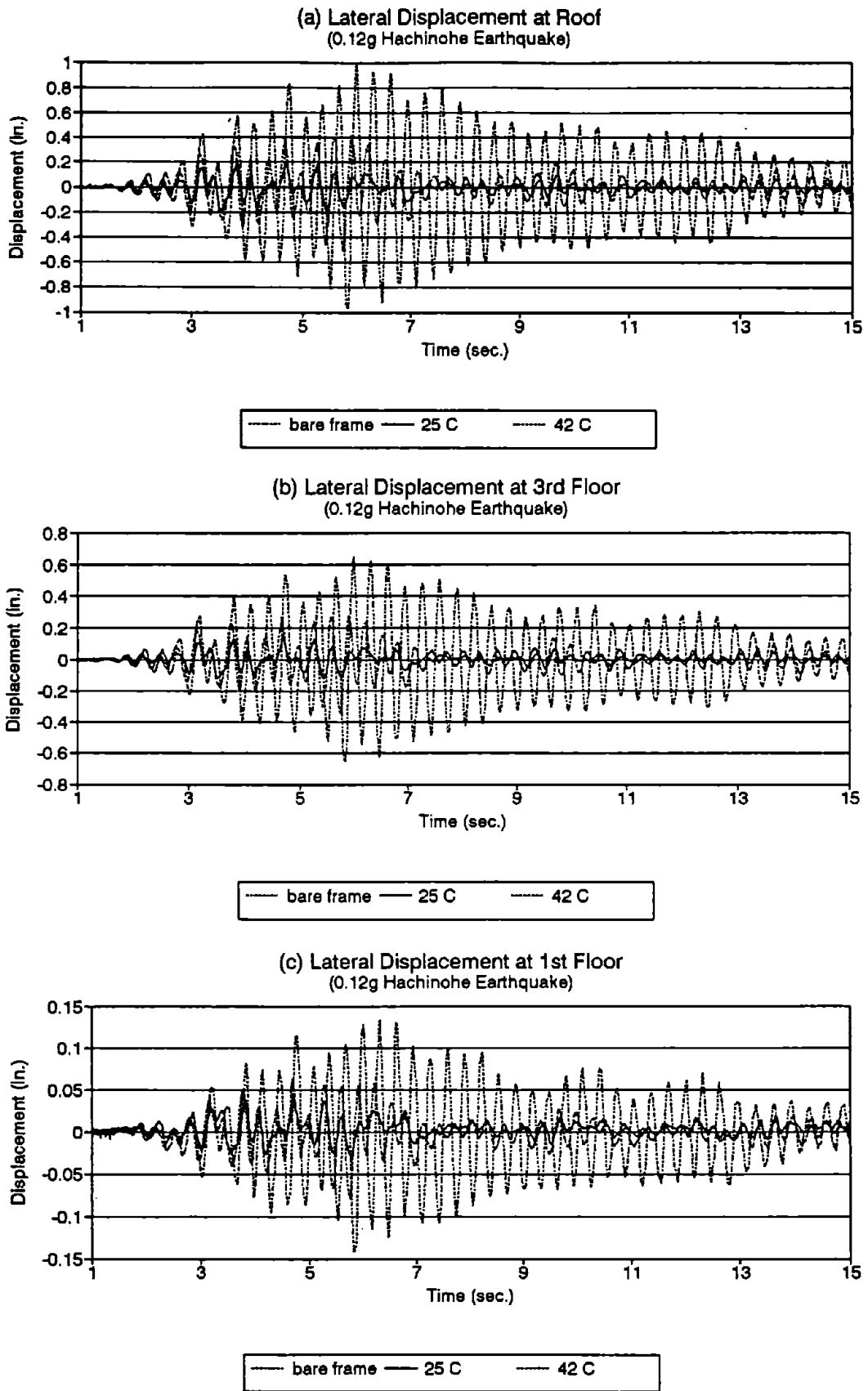
Fig. 3.7 Lateral Structural Displacement with and without Added VE Dampers at 25°C and 42°C

3-16
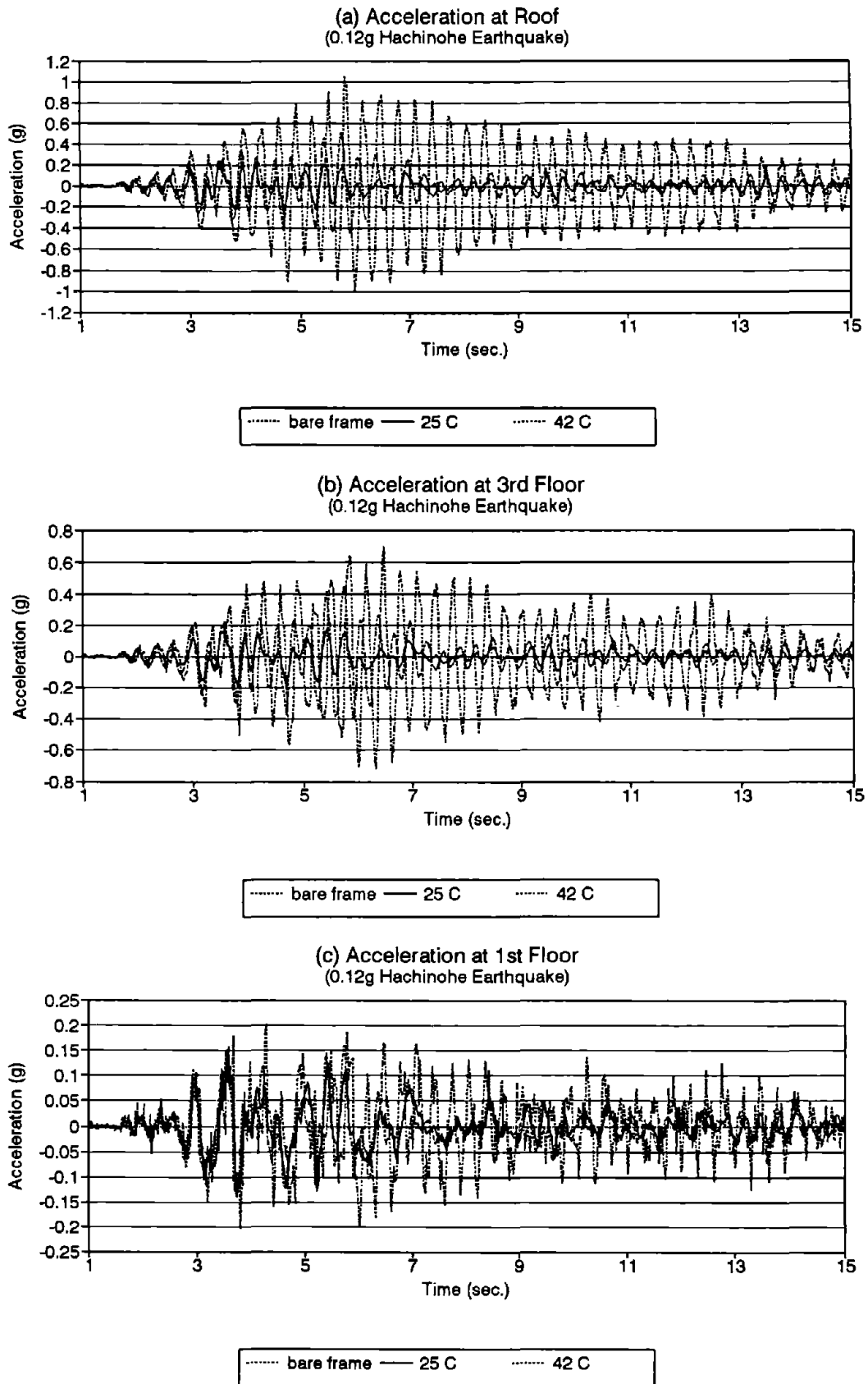
Fig. 3.8 Floor Accelerations with and without Added VE Dampers at 25°C and 42°C
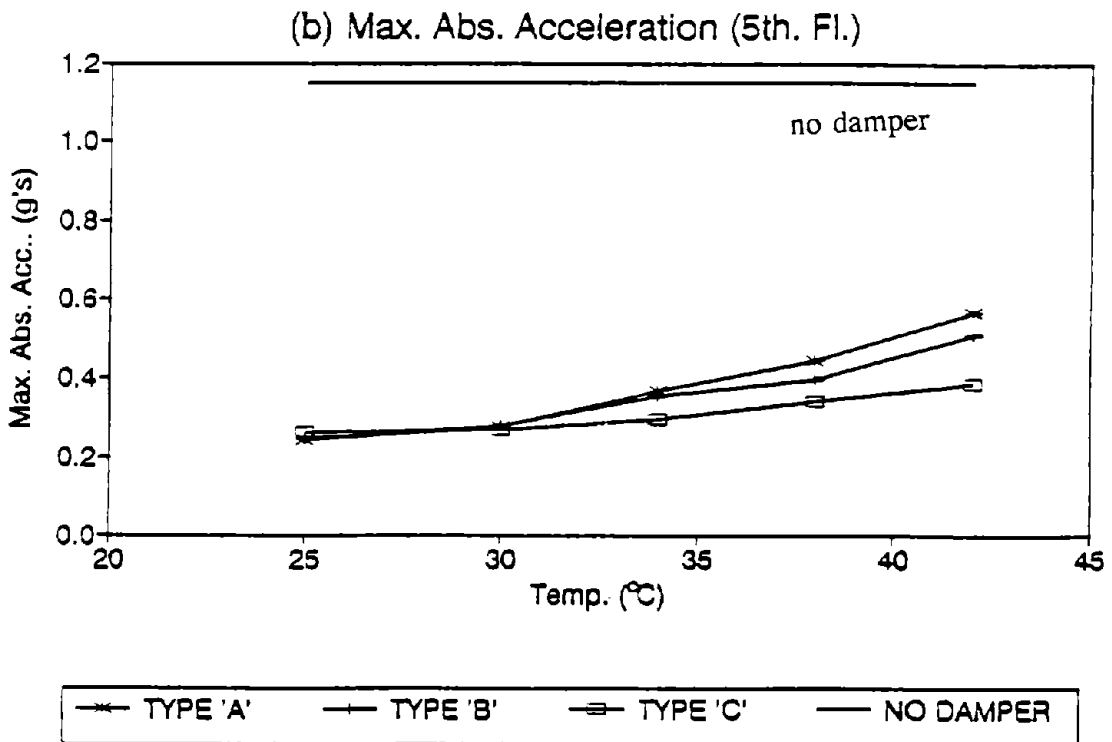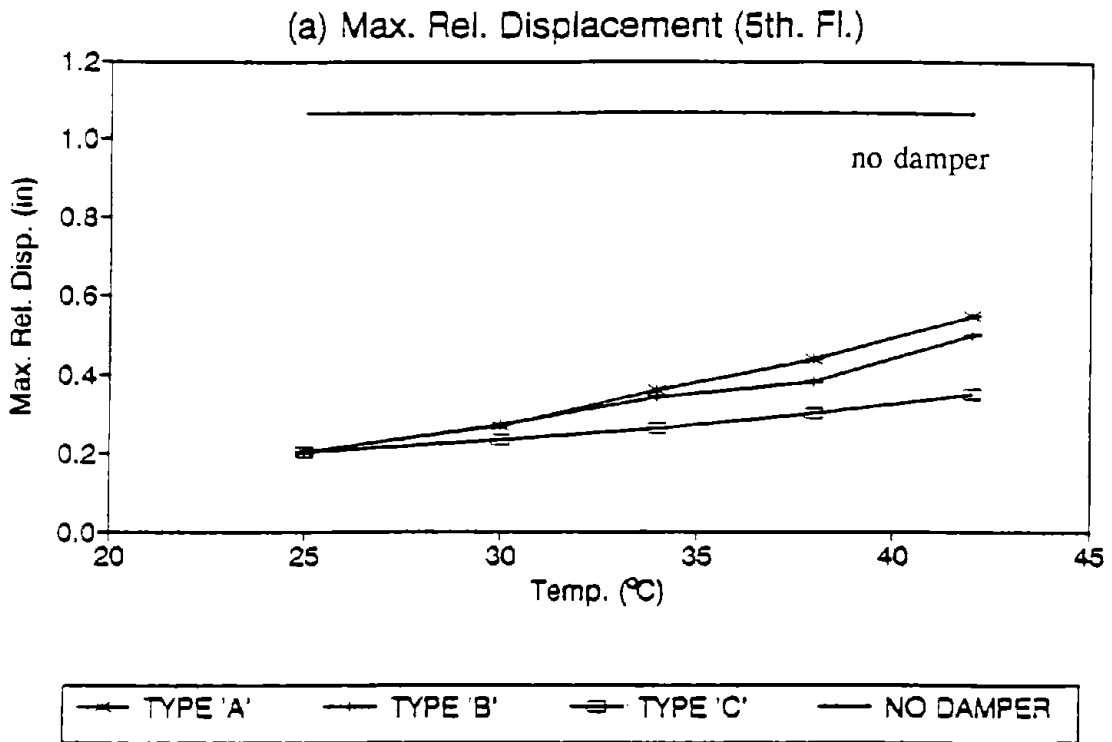
3-17

(a) Max. Rel. Displacement (5th. Fl.)

no damper

Max. Rel. Disp. (in)

Temp. (°C)

| —×— TYPE 'A' | —+— TYPE 'B' | —⊟— TYPE 'C' | —— NO DAMPER |

(b) Max. Abs. Acceleration (5th. Fl.)

no damper

Max. Abs. Acc.. (g's)

Temp. (°C)

| —×— TYPE 'A' | —+— TYPE 'B' | —⊟— TYPE 'C' | —— NO DAMPER |

Fig. 3.9 Temperature Dependence of Structural Response with Three Types of VE Dampers

(c) Max. Story Drift (1st-2nd Fl.)

no damper

Max. Story Drift (in)

Temp. (°C)

TYPE 'A'   TYPE 'B'   TYPE 'C'   NO DAMPER

(d) Max. Damper Strain (2nd Fl.)

Max. Damper Strain (%)

Temp. (°C)

TYPE 'A'   TYPE 'B'   TYPE 'C'
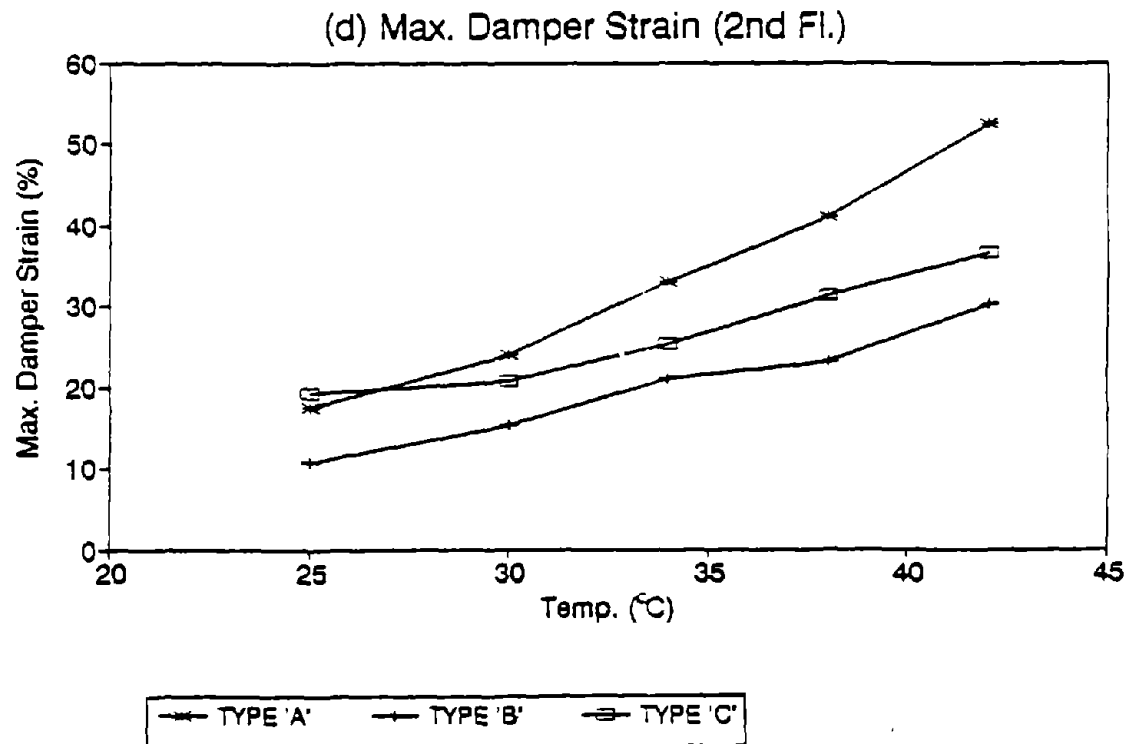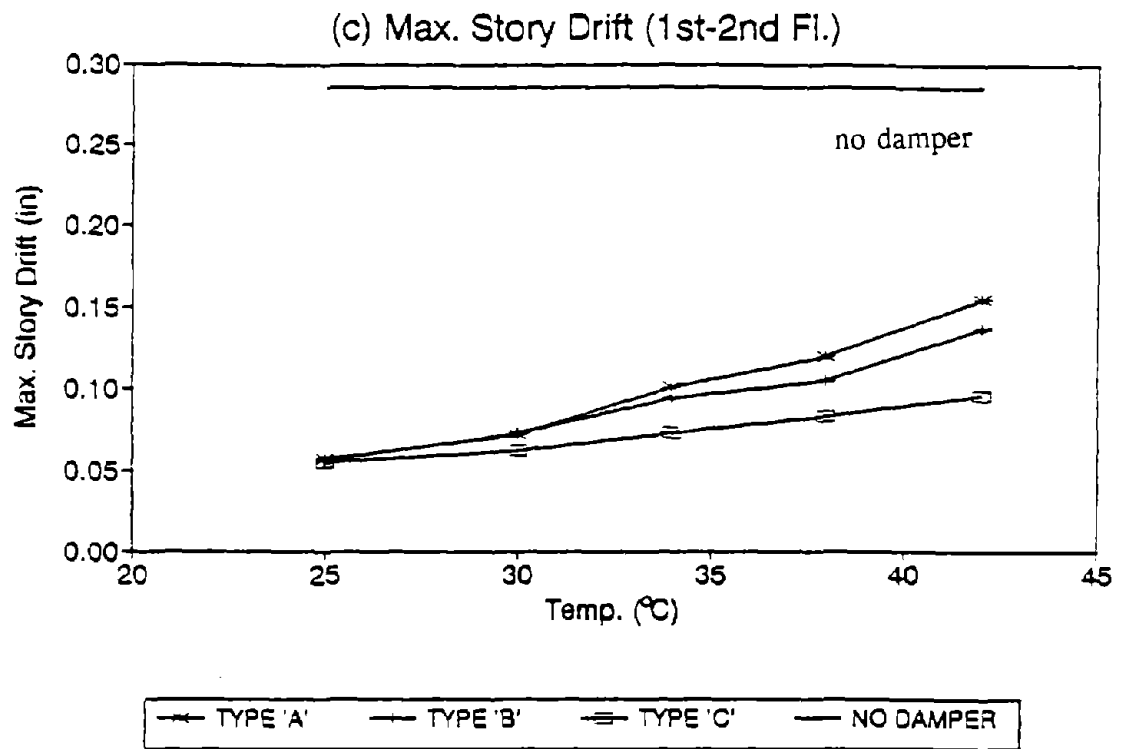
Fig. 3.9 Temperature Dependence of Structural Response with Three Types of VE Dampers (continued)
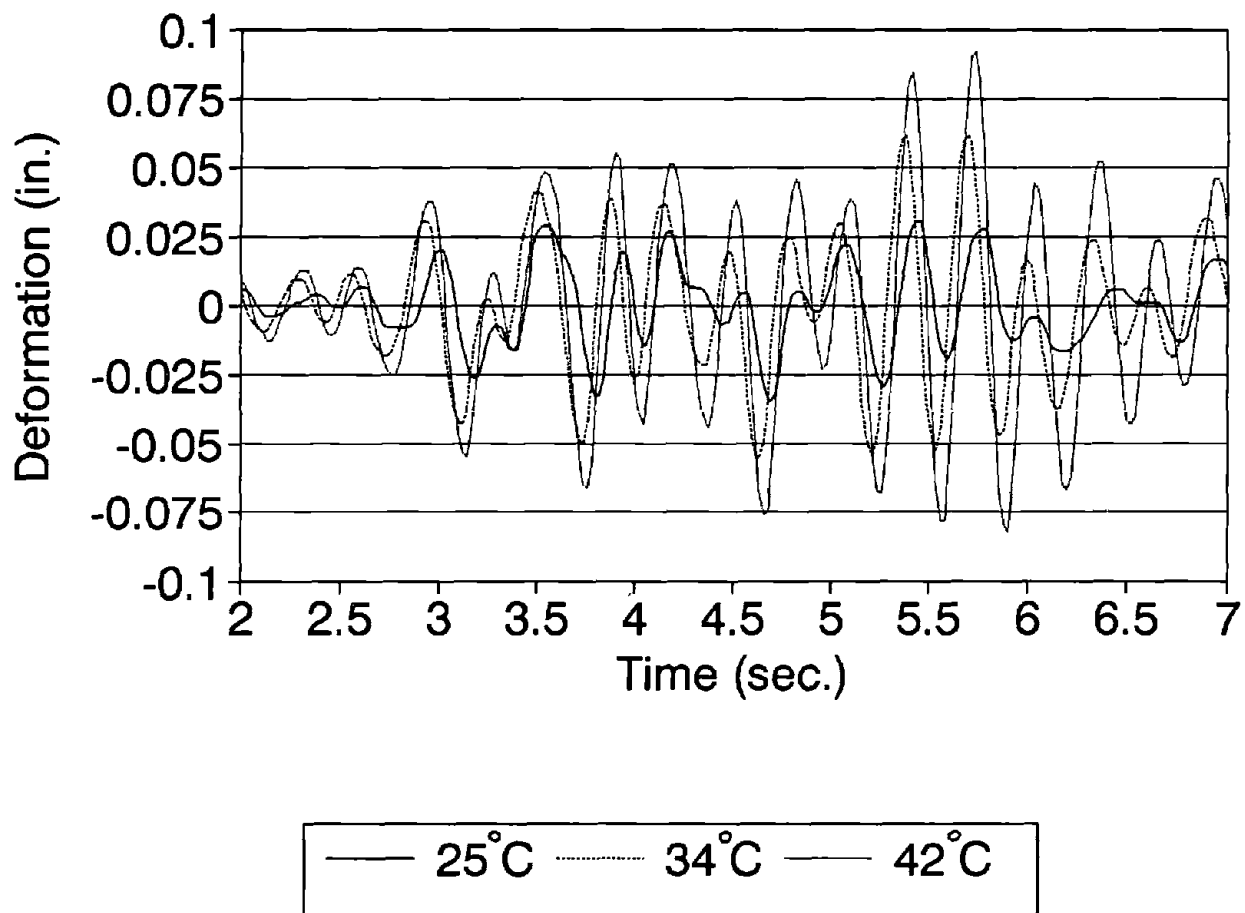
Fig. 3.10 Damper Deformation at 2nd Floor under Various Ambient Temperatures (0.12g Hachinohe Earthquake)

(a) Lateral Displacement at Roof
(0.6g Hachinohe Earthquake)

with damper ------ no damper

(b) Lateral Drift at 2nd Floor
(0.6g Hachinohe Earthquake)

with damper —— no damper
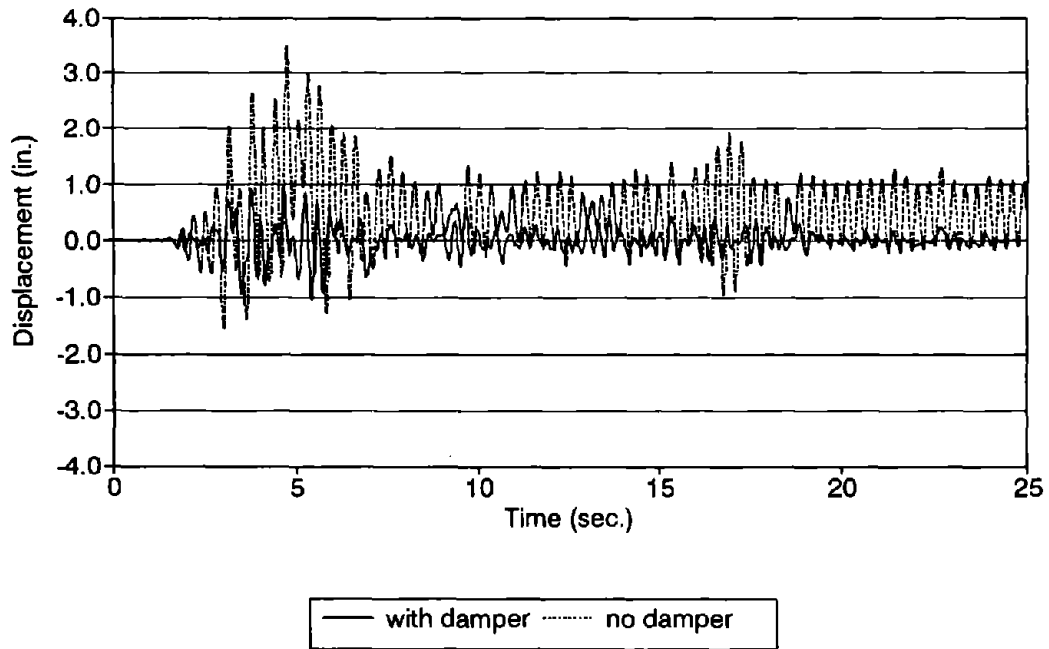
Fig.3.11 Lateral Structural Response with and without Added VE Dampers (0.6g Hachinohe Earthquake)

(a) Lateral Displacement at Roof
(0.6g El Centro Earthquake)

with damper ———   no damper ·······
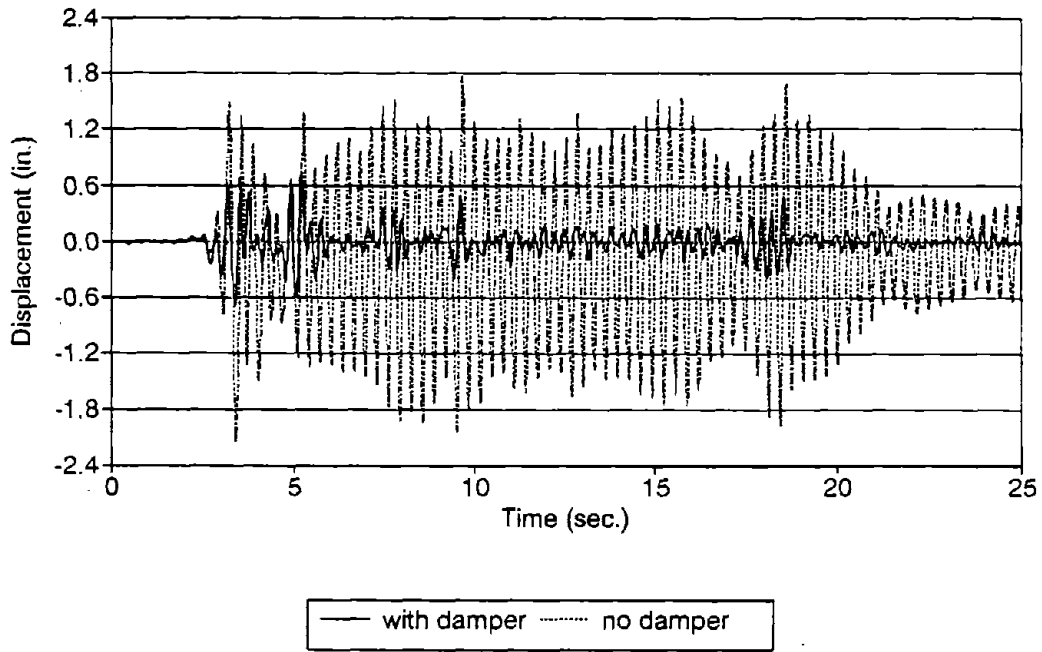
(b) Lateral Drift at 2nd Floor
(0.6g El Centro Earthquake)
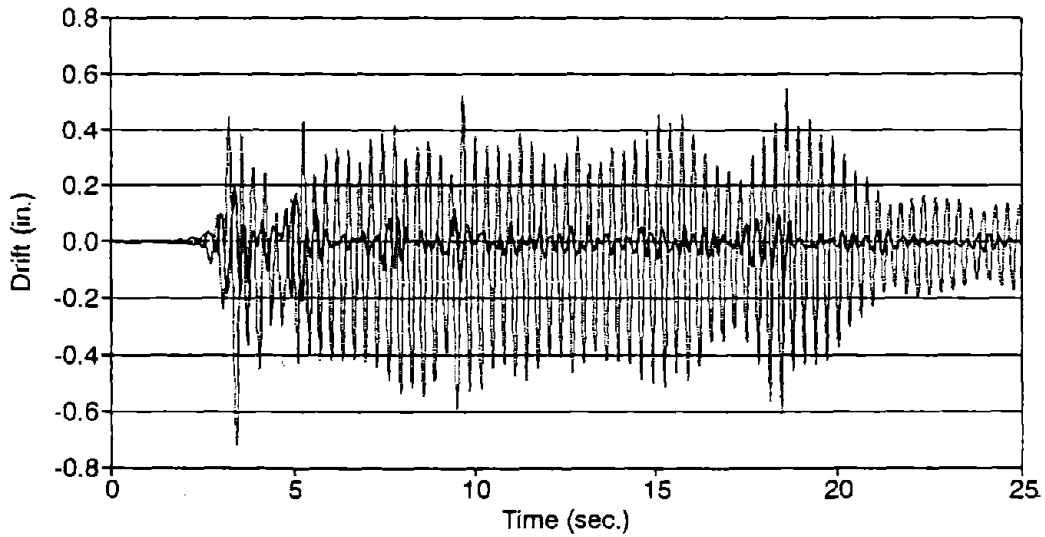
Fig.3.12 Lateral Structural Response with and without Added VE Dampers (0.6g El Centro Earthquake)

3-22
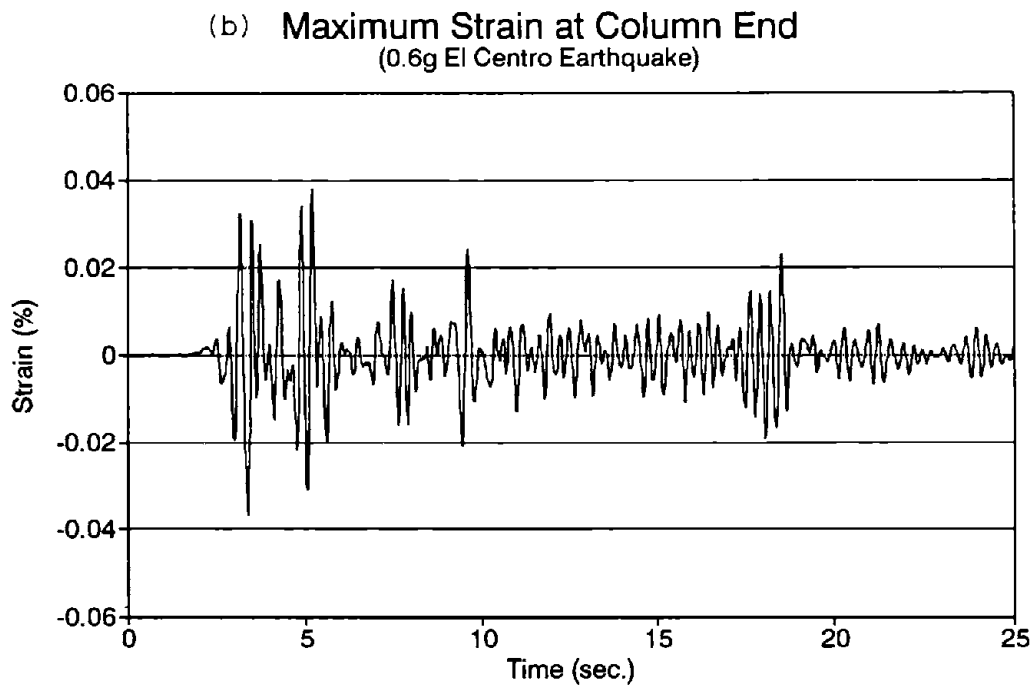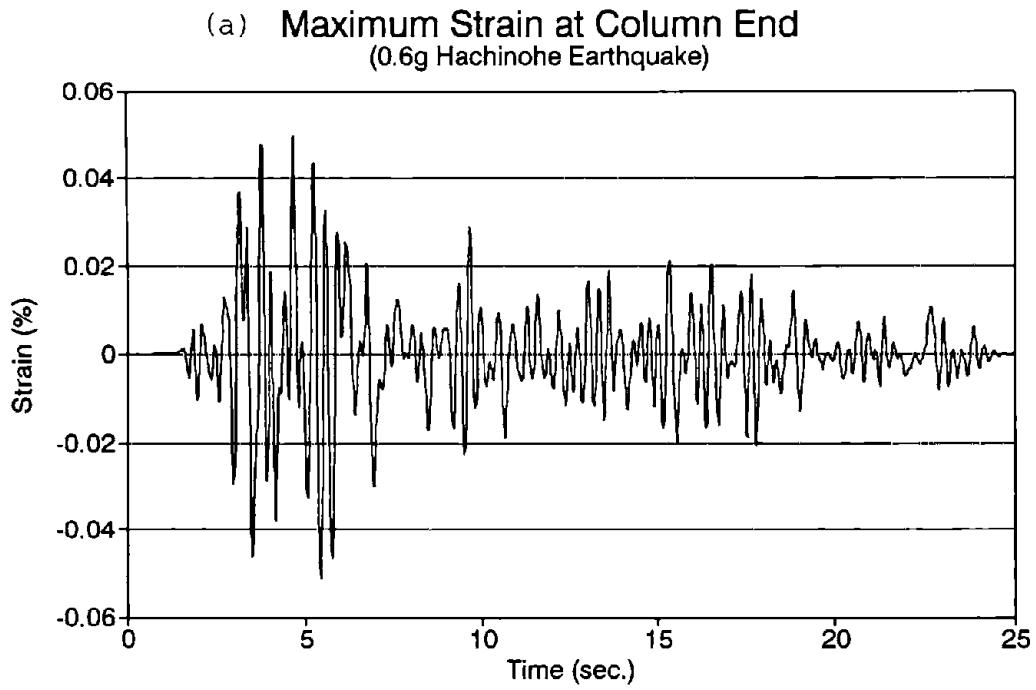
Figs.3.13 Maximum Strain at Column End under 0.6g Hachinohe and El Centro Earthquakes

(a) Acceleration at Roof
(0.6g Hachinohe Earthquake)

with damper ········ no damper

(b) Acceleration at Roof
(0.6g El Centro Earthquake)

with damper —— no damper
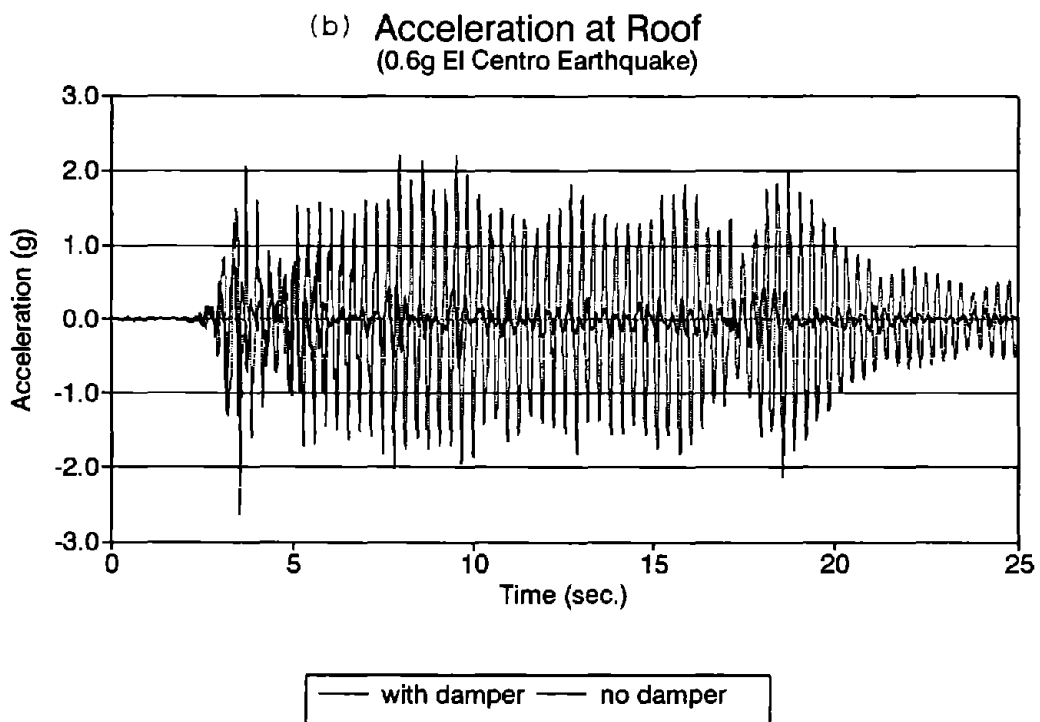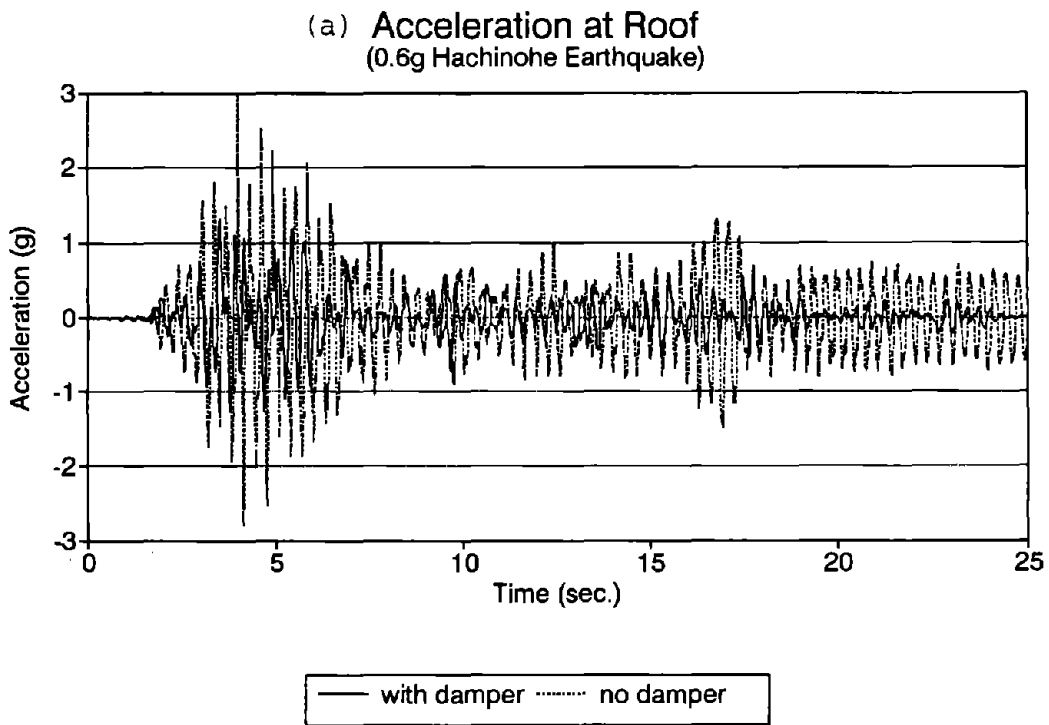
Fig. 3.14 Acceleration Histories at Roof under 0.6g Hachinohe and El Centro Earthquakes

(a) Roof Lateral Displacement
(0.24 Hachinohe Earthquake)

------- Type-A　　——— Type-B　　——— Type-C　　——— No Damper
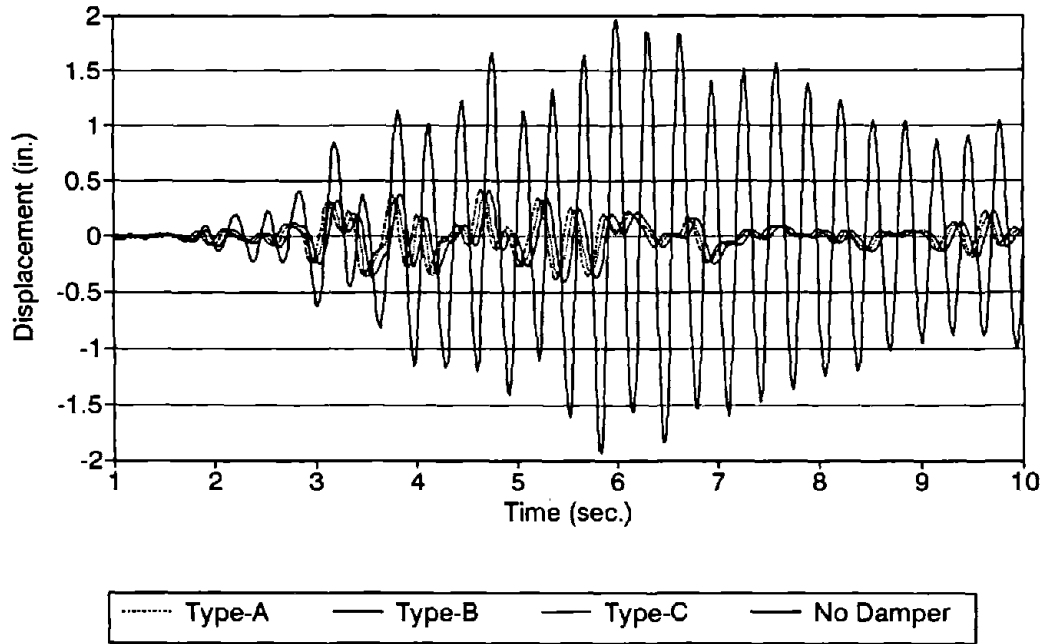
(b) Roof Absolute Acceleration
(0.24 Hachinohe Earthquake)
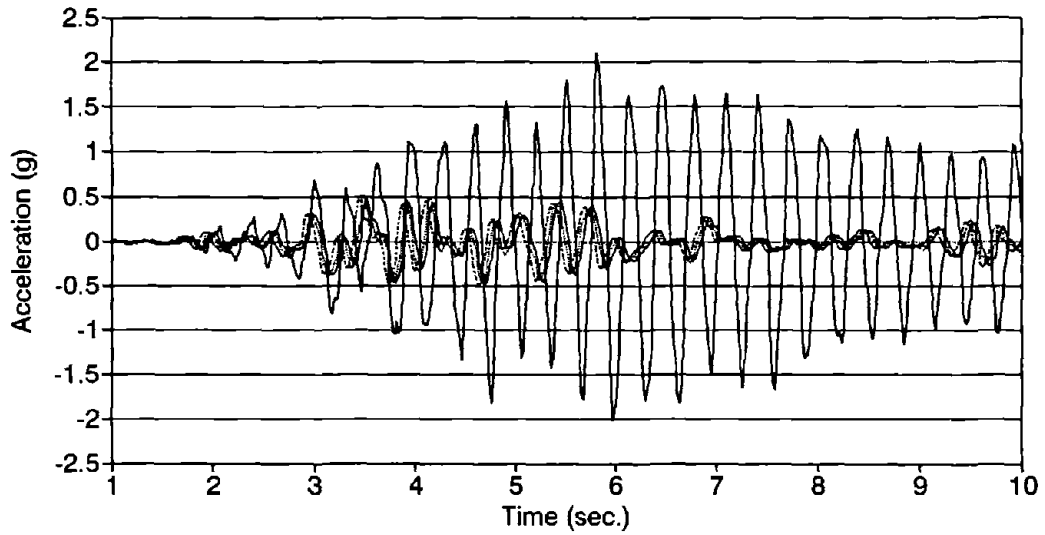
Fig. 3.15　Response Time-Histories with Different Types of Dampers
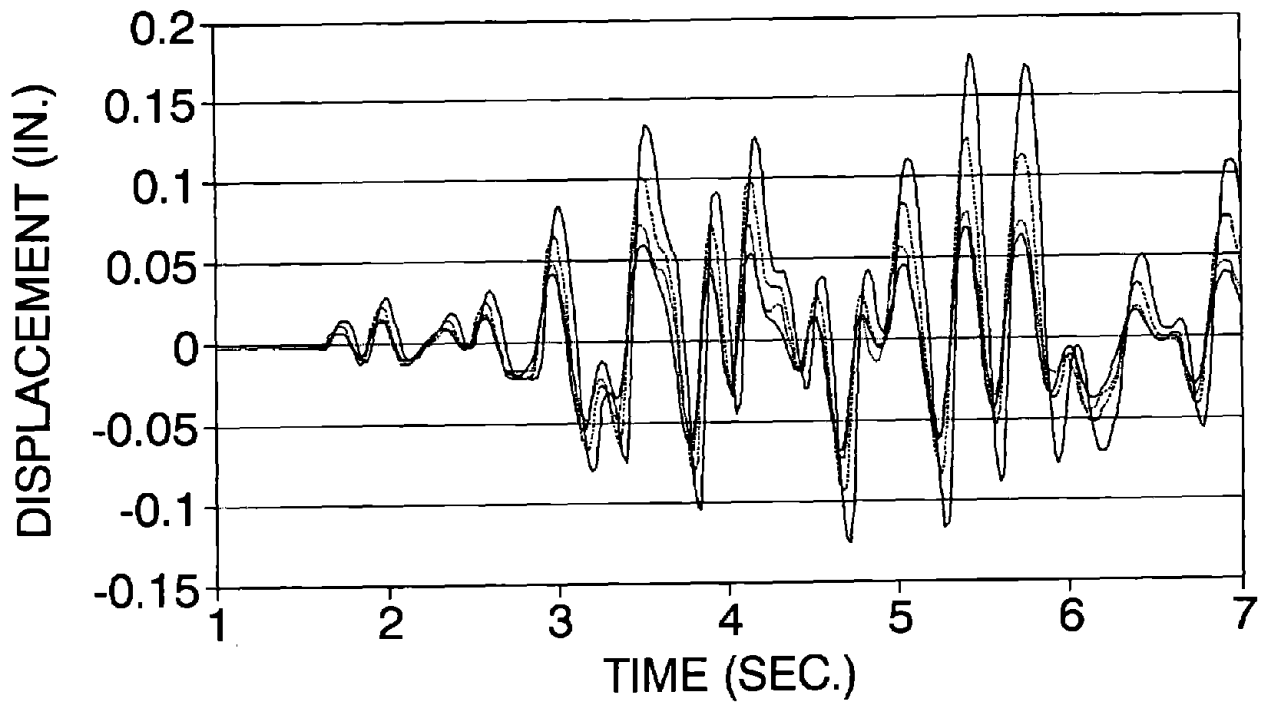
(a) Second Floor Damper Deformation
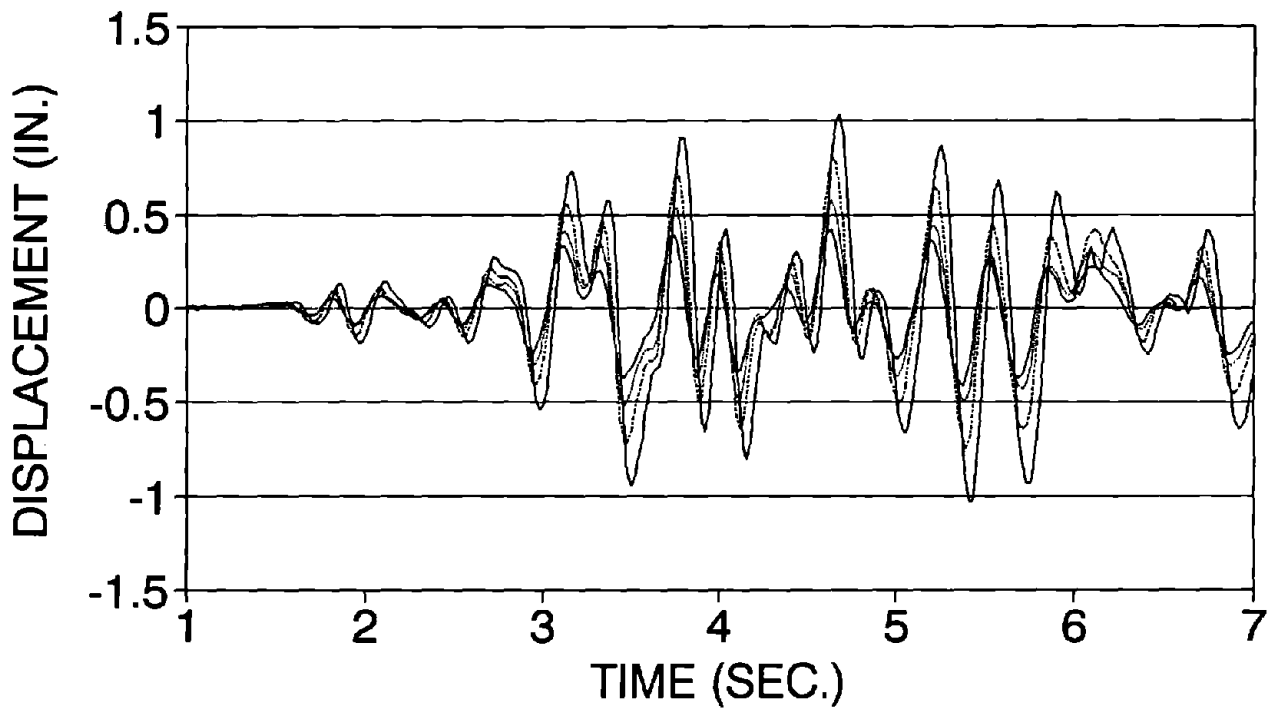
(b) Fifth Floor Lateral Displacement

```
——— .24g  ——— .36g  ·········· .48g  ——— .6g
```
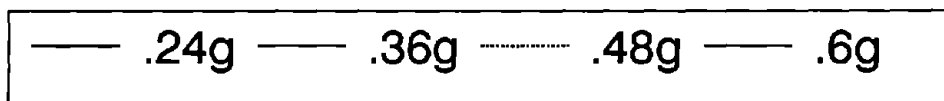
Fig. 3.16 Damper Deformation and Response Time Histories under 0.24 - 0.6g Hachinohe
Earthquakes

(a) Transfer Functions
(El Centro Earthquakes)

Legend: —— 0.24g ········ 0.6g
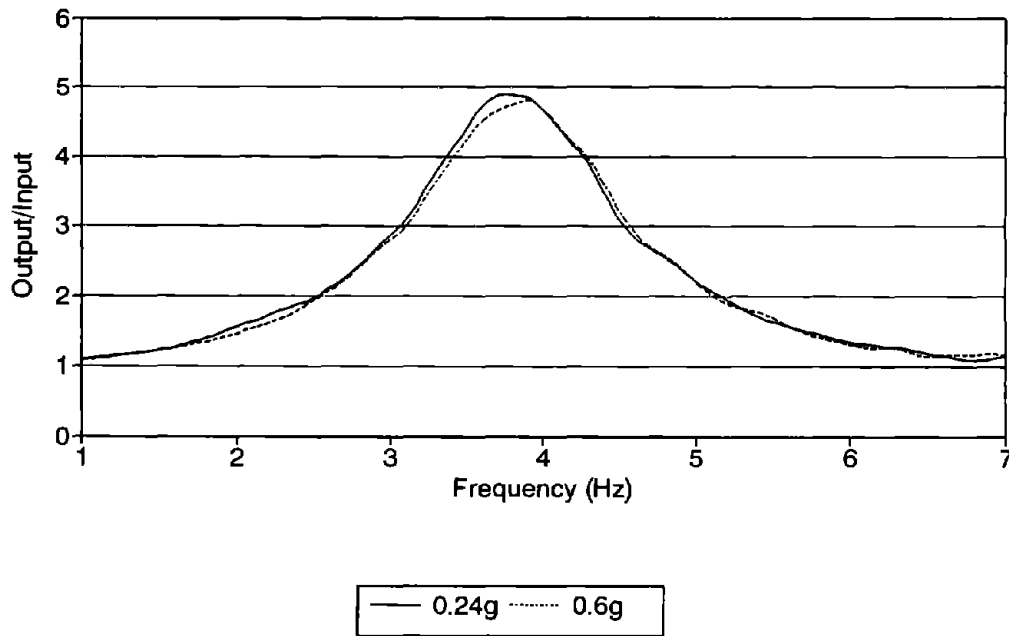
(b) Transfer Functions
(Hachinohe Earthquakes)

Legend: —— 0.24g ········ 0.6g
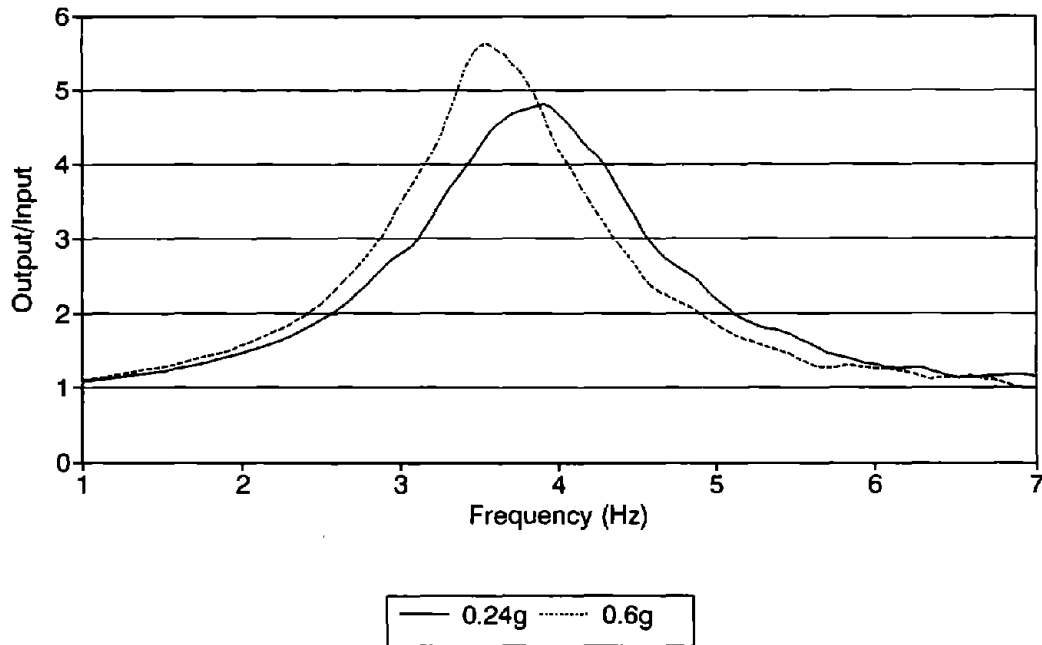
Fig. 3.17 Averaged Transfer Functions under 0.24 and 0.6g Hachinohe and El Centro Earthquakes
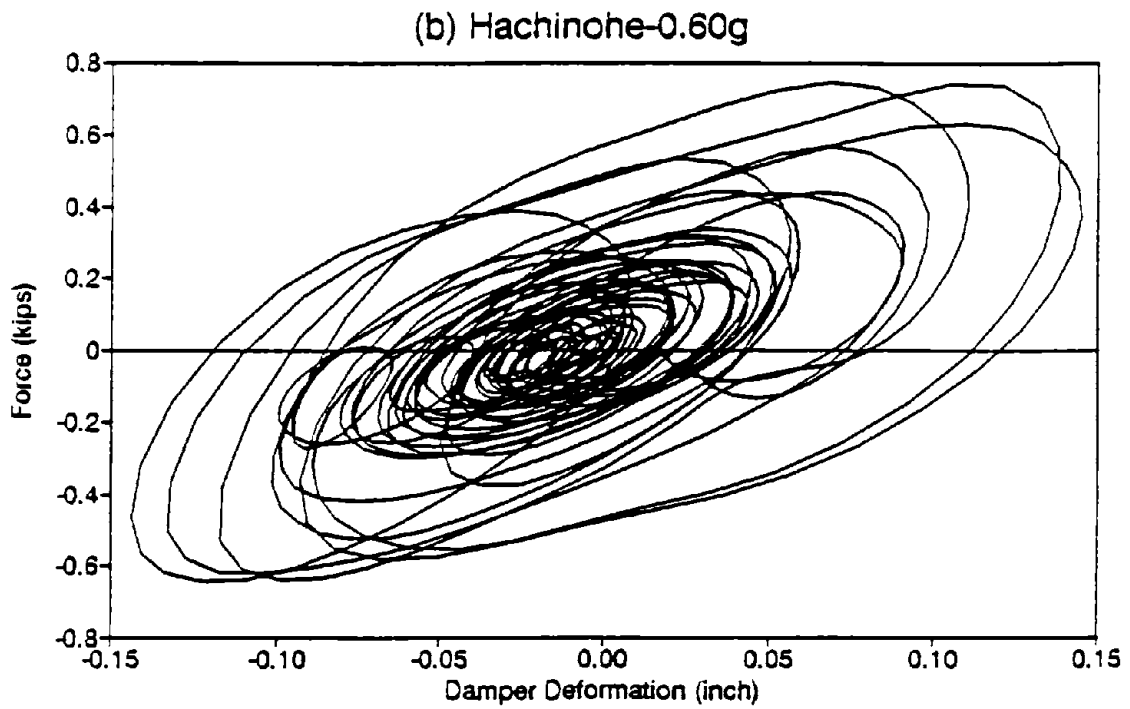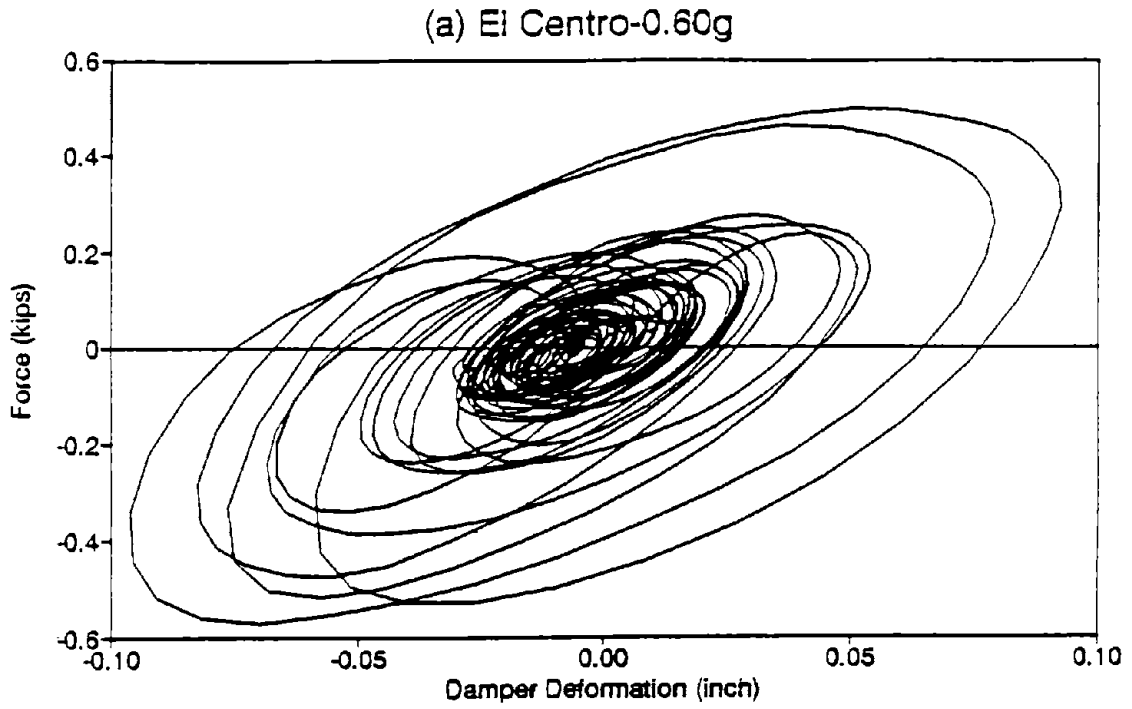
Fig. 3.18 Damper Force-Deformation Loops at 2nd Floor under 0.6g Hachinohe and El Centro Earthquakes
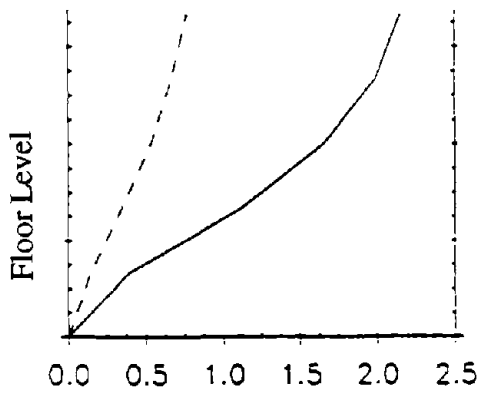
(a) Lateral Displacement (in)

(b) Interstory Drift (in)
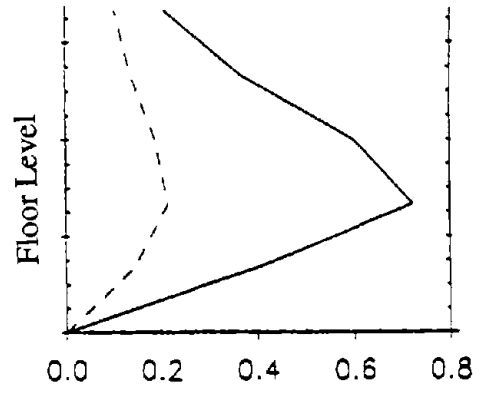
(c) Story Shear (kips)
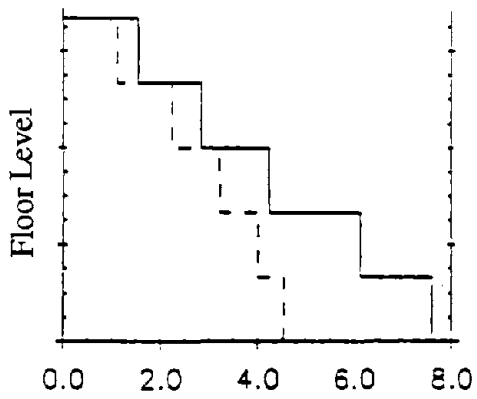
(d) Overturning Moment (×100 kip-in)
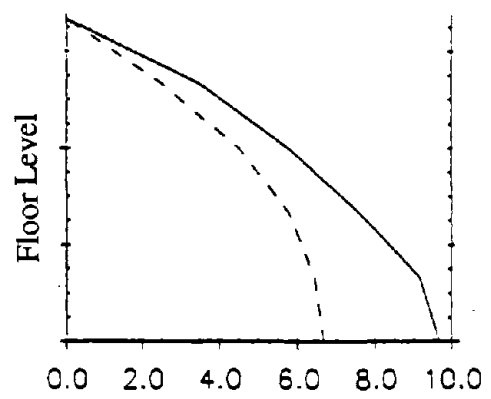
- - - - Added Damper ——— No Damper
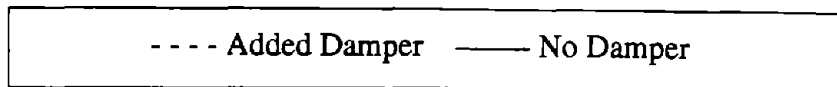
Fig. 3.19   Response Envelopes (0.6g El Centro Earthquake)

3-29

(a) Lateral Displacement (in)

(b) Interstory Drift (in)

(c) Story Shear (kips)

(d) Overturning Moment ($\times 100$ kip-in)
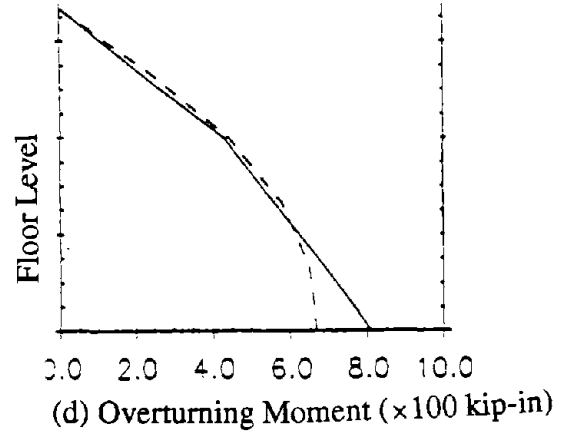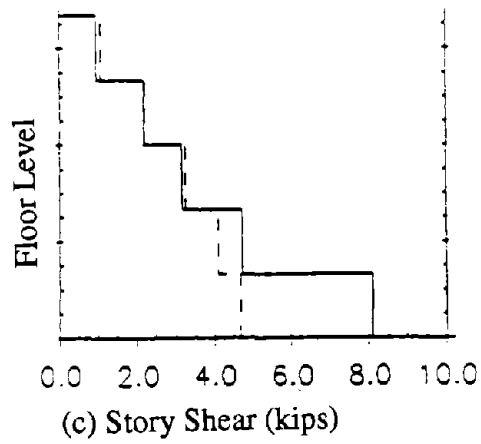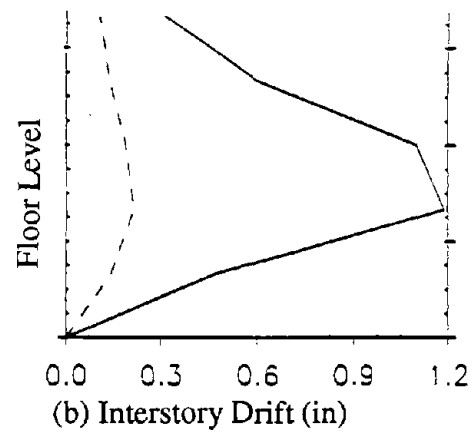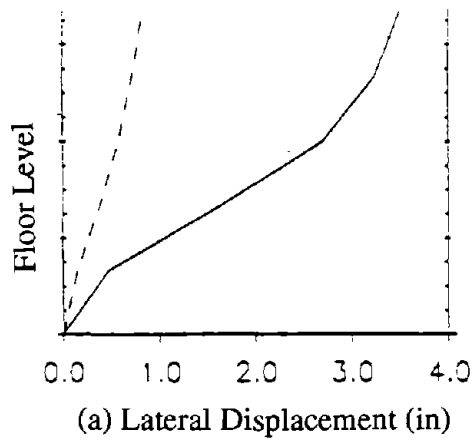
- - - - Added Damper ——— No Damper

Fig. 3.20 Response Envelopes (0.6g Hachinohe Earthquake)

(a) Displacement (in)

(b) Interstory Drift (in)
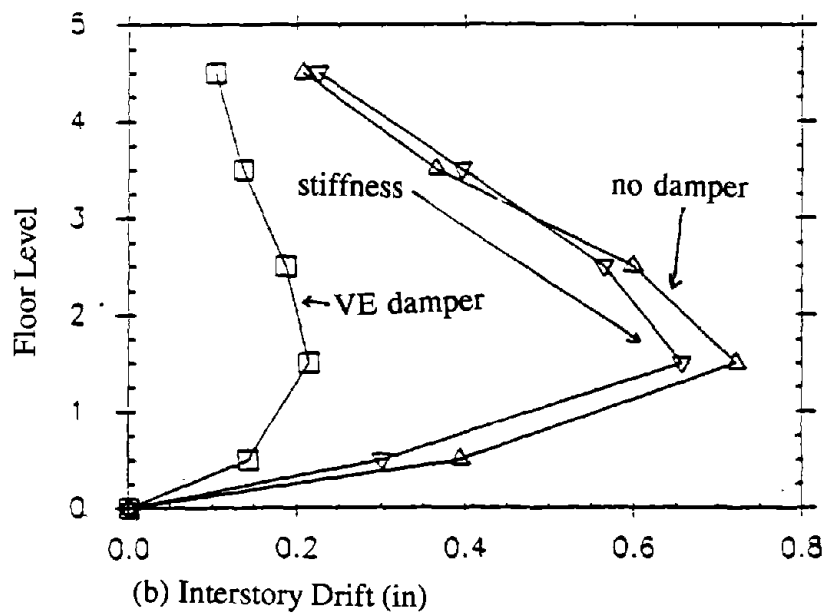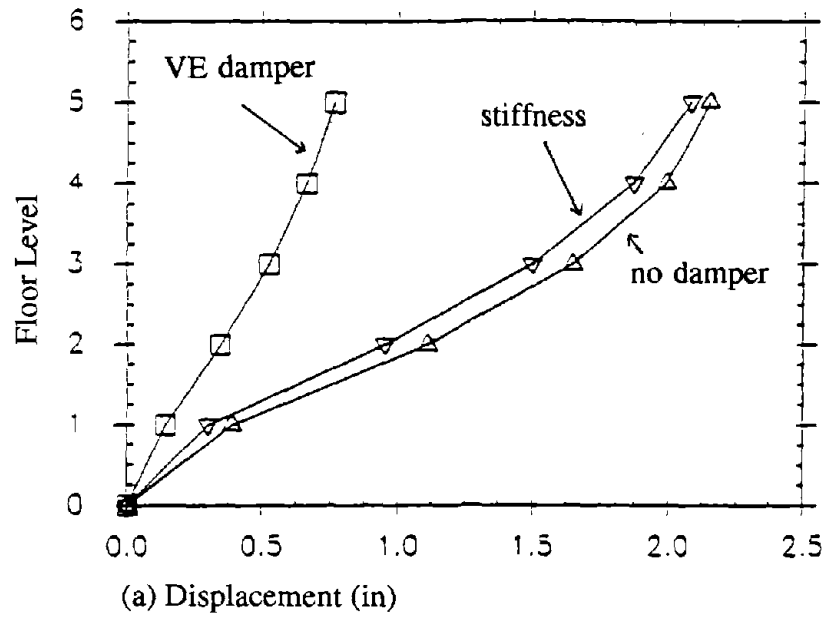
Fig. 3.21 Response Envelopes of No Damper Case, Added Stiffness Only and Added VE Dampers

SECTION 4

ANALYTICAL SIMULATIONS

4.1 Introduction

Viscoelastic dampers incorporated into the model structure behave linearly within a range of strains of the viscoelastic material. The dampers contribute to increased viscous damping as well as lateral stiffness of the structure.

The same mathematical idealizations and assumptions as used in Section 3.2 are used in this section to predict the dynamic behavior of the model structure with added dampers. The brace members incorporating the VE dampers are modeled as truss elements with stiffness equivalent to that of the VE dampers. The section properties of the brace members representing the brace and the viscoelastic damper together are determined based on the damper test results described in Section 2.

The lateral stiffness and mass matrices of the model structure without added dampers are given as

$$[K] = \begin{bmatrix} 47.42 & -14.74 & 0 & 0 & 0 \\ -14.74 & 29.47 & -14.73 & 0 & 0 \\ 0 & -14.73 & 29.47 & -14.73 & 0 \\ 0 & 0 & -14.73 & 29.47 & -14.73 \\ 0 & 0 & 0 & -14.73 & 14.74 \end{bmatrix} (K/in) \tag{4.1}$$

$$[M] = \begin{bmatrix} 1.12 & 0 & 0 & 0 & 0 \\ 0 & 1.27 & 0 & 0 & 0 \\ 0 & 0 & 1.27 & 0 & 0 \\ 0 & 0 & 0 & 1.27 & 0 \\ 0 & 0 & 0 & 0 & 1.31 \end{bmatrix} (kips) \tag{4.2}$$

4.2 Evaluation of Equivalent Structural Damping: Modal Strain Energy Method

Viscoelastically damped structures dissipate seismic input energy through added damping provided by the viscoelastic dampers. In order to insure the effectiveness of these dampers, it is very important to correctly estimate the amount of equivalent structural damping provided by the added dampers. In a recent study [4], by assuming a proportionally damped system, the resultant damping ratio for the ith mode of the structure with added dampers can be expressed as

$$\xi_i = \frac{E_d^i}{4\pi E^i} \tag{4.3}$$

Preceding page blank

where

ξ_i = structural damping ratio for the ith vibration mode

E_d^i = energy dissipated in one cycle by the dampers for the ith vibration mode

E^i = strain energy of the structure for the ith vibration mode

The above equation can also be expressed in terms of the modal strain energy [7,9,10]. In this approach, the viscoelastically damped structure can be represented in terms of the real natural modes of the associated undamped system if appropriate damping terms are inserted into the uncoupled modal equations of motion. One has

$$\ddot{Z}_i + \eta_i \omega_i \dot{Z}_i + \omega_i^2 Z_i = p_i(t) \tag{4.4}$$

$$u(t) = \sum_{i=1}^{N} \phi_i Z_i(t), \qquad i = 1, 2, 3, \ldots N \tag{4.5}$$

where

Z_i = ith modal coordinate

ω_i = natural frequency of the ith vibration mode

ϕ_i = ith mode shape vector of the associated undamped system

η_i = modal loss factor of the ith vibration mode ($= 2\xi_i$)

$u(t)$ = generalized coordinate

This implies that the damping matrix in the generalized coordinates can be uncoupled through the use of natural modes of the system. Therefore, the modal damping ratios of the structure equipped with viscoelastic dampers can be calculated using the mode shapes and the loss factor of the viscoelastic dampers. It can be shown that the equivalent damping of the viscoelastically damped structure can be expressed as

$$\eta_i = \eta_v \left[\frac{V_v^i}{V^i} \right] \tag{4.6}$$

where η_v is loss factor of the damper at the ith calculated resonant frequency, V_v^i/V^i is the fraction of elastic strain energy attributable to viscoelastic dampers when the structure deforms in the ith mode shape, and $\eta_i = 2\xi_i$.

A differential equation of the discrete-coordinate system for free vibration is

$$\ddot{M} + Ku = 0 \tag{4.7}$$

4-2

where the stiffness matrix K is constant but complex because of the addition of viscoelastic dampers. By assuming a solution of the form

$$u = \phi_i^* e^{i\omega_i^* t} \tag{4.8}$$

where ω_i^* and ϕ_i^* are the ith complex eigenvalue and eigenvector with

$$\phi_i^* = \phi_{Ri} + i\phi_{Ii} \tag{4.9}$$

$$\omega_i^* = \omega_i \sqrt{1 + i\eta_i} \tag{4.10}$$

$$(\omega_i^*)^2 = \omega_i^2 (1 + i\eta_i) \tag{4.11}$$

The term η_i is the modal loss factor of the ith mode. From Eqs. (4.7) and (4.8),

$$K\phi_i^* = (\omega_i^*)^2 M\phi_i^* \tag{4.12}$$

A Rayleigh quotient corresponding to Eq. (4.12) is

$$(\omega_i^*)^2 = \frac{\phi_i^{*T} K \phi_i^*}{\phi_i^{*T} M \phi_i^*} \tag{4.13}$$

The stiffness matrix K in Eq. (4.13) is in a complex form as

$$K = K_R + iK_I \tag{4.14}$$

From Eqs. (4.9), (4.11), and (4.12),

$$(\omega_i^*)^2 = \frac{\phi_i^{*T} K_R \phi_i^*}{\phi_i^{*T} M_R \phi_i^*} + i\frac{\phi_i^{*T} K_I \phi_i^*}{\phi_i^{*T} M_I \phi_i^*} \tag{4.15}$$

Approximating the complex eigenvector ϕ_i^* by the real eigenvector ϕ_i, an approximate value for η_i can be obtained. Equating real and imaginary parts of Eq. (4.15) to their counterparts in Eq. (4.11) gives

$$\omega_i^2 = \frac{\phi_i^T K_R \phi_i}{\phi_i^T M \phi_i} \tag{4.16}$$

$$\omega_i^2 \eta_i = \frac{\phi_i^T K_I \phi_i}{\phi_i^T M \phi_i} \tag{4.17}$$

$$\eta_i = \frac{\phi_i^T K_I \phi_i}{\phi_i^T K_R \phi_i} \tag{4.18}$$

On the other hand, the stiffness matrix K consists of two parts. The first one, K_e, is the structural stiffness matrix without damper contributions. The second, K_d, is obtained from the structural stiffness matrix due to damper contributions alone. Both parts are matrices of the same order as K, which can thus be represented by

$$K = K_e + K_d \tag{4.19}$$

where K_e is real but K_d is complex, whose real and imaginary parts have the ratio of $1 : \eta_v$, where η_v is the loss factor of the viscoelastic dampers. Thus

$$K_d = K_{dR} + iK_{dI} \tag{4.20}$$

Then, Eq. (4.19) becomes

$$k_{dI} = \eta_v K_{dR} \tag{4.21}$$

$$K = K_e + K_{dR} + iK_{dI} \tag{4.22}$$

Substituting Eqs. (4.21) and (4.22) into Eq. (4.18) gives

$$\eta_i = \eta_v \frac{\phi_i^T K_{dR}\phi_i}{\phi_i^T K_R\phi_i}$$

$$= \eta_v \frac{\phi_i^T K_{dR}\phi_i}{\phi_i^T (K_e + K_{dR})\phi_i} \tag{4.23}$$

The modal loss factor in terms of elastic energies is given by Eq. (4.6). Hence, Eq. (4.23) can be written as

$$\eta_i = \frac{\phi_i^T K_{dR}\phi_i}{\phi_i^T K_R\phi_i}$$

$$= \eta_v \frac{\phi_i^T (K_R - K_e)\phi_i}{\phi_i^T K_R\phi_i}$$

$$= \eta_v \left(1 - \frac{\phi_i^T K_e\phi_i}{\phi_i^T K_R\phi_i}\right) \tag{4.24}$$

where matrix K_R is a structural stiffness matrix including contribution of the dampers ($= K_e + K_{dR}$). Finally, the modal damping ratio of the ith mode can be calculated as

$$\xi_i = \frac{\eta_v}{2} \left(1 - \frac{\phi_i^T K_e\phi_i}{\phi_i^T K_R\phi_i}\right) \tag{4.25}$$

where ξ_i = structural damping ratio for the ith vibration mode.

If the change of vibration mode shapes due to the addition of VE dampers can be neglected, Eq. (4.25) can be further reduced to

$$\xi_i = \frac{\eta_v}{2}\left(1 - \frac{\omega_i^2}{\omega_{si}^2}\right) \tag{4.26}$$

where ω_i and ω_{si} are the ith natural frequencies of the structure without and with added dampers, respectively.

4.3 Prediction of Structural Damping Ratio

4.3.1 Effect of Ambient Temperature

Table 4.1 shows the damper properties used in the numerical study. These values were obtained from the damper tests corresponding to a 5% damper strain. The natural frequency and the predicted structural damping ratio using Eqs. (4.25) and (4.26) and those measured experimentally are shown in Figs. 4.1a,b and 4.2a,b and are summarized in Table 4.2. As can be seen, the same degrees of accuracy as that reported previously [7] are obtained.

4.3.2 Effect of Different Damper Placements

The amount of damping provided by energy dissipating devices is controllable and adjustable. The way in which these dampers are distributed throughout the structure may have a significant effect on the effectiveness of response control. By varying the location of the dampers, different dynamic responses are obtained. The problem of the optimum distribution of supplemental damping has been studied by several researchers. Recently, Zhang and Soong [18] made an attempt to extend the concept of degree of controllability used in active control applications to finding the optimal locations of passive dampers.

Seven different cases of damper placements were experimentally studied as shown in Fig. 4.3. These include two extreme cases for the purpose of comparison, which are Case 1, all floors equipped with dampers, and Case 7, bare frame without any dampers. Type A dampers were used in all the cases and the simulated 0.12g Hachinohe earthquake was considered as the input motion. Damper properties used in the numerical simulation are summarized in Table 4.3. These values are obtained from the empirical formulae by assuming a 5% strain.

The measured and predicted first-mode natural frequencies and structural damping according to the configurations of damper placements, Case 1 through Case 7, are shown

in Figs. 4.4a and 4.4b, respectively, as well as in Table 4.4. It can be seen that the natural frequencies and damping ratios can be predicted very well. Again, Eq. (4.26) gives less accurate estimated results as compared to Eq. (4.25).

In general, the natural frequency and equivalent structural damping of a viscoelastically damped structure with various damper distributions can be satisfactorily predicted using the modal strain energy method.

4.4 Prediction of Structural Response

4.4.1 Effect of Damper Placement

The maximum floor displacement and maximum interstory drift were taken as representatives of response prediction with various damper placements. The predicted maximum responses were compared with the experimental ones in Table 4.5 for seven tested cases using the Hachinohe earthquake records as the input motion. It can be seen that, in general, the predicted results closely match those obtained from the experiments. The time histories of the floor displacements for Cases 2, 3 and 5 are shown in Figs. 4.5a-4.7b.

4.4.2 Response under Strong Earthquake Ground Motions

The input accelerograms based on the Hachinohe and El Centro earthquakes but scaled up to a peak acceleration of 0.60g were selected for numerical simulations of the viscoelastically damped structure under strong earthquake ground motions. Type B dampers were originally installed in the test structure for the shaking table tests. The analytical response results are compared with the experimentally obtained floor displacements, interstory drifts and floor accelerations.

Tables 4.6-4.8 show the damper properties together with analytical and experimental results on structural properties and peak responses under these ground motions. Figures 4.8a-c show the analytical and experimental response time histories at the roof, the third floor and the first floor, respectively, of the structure with added Type B dampers under the 0.6g Hachinohe earthquake. Figures 4.9a-c show the same information under the 0.6g El Centro earthquake. It can be seen that, in general, lateral displacement response of the viscoelastically structure can be satisfactorily predicted by conventional linear dynamic theories provided proper damper stiffness and damping ratio are used. Similar conclusions can be made for the interstory drifts, as shown in Figs. 4.10a and

4.10b. The predicted floor acceleration, is, however, less accurate, as can be observed from Figs. 4.11a and 4.11b.

Table 4.1   Damper Properties used in Numerical Simulation,
Ambient Temperature Effect

Damper Type	Temp. (°C)	ω (Hz)	K_d (lb/in)	η
'A'	24	3.61	4421	1.12
	28	3.46	2804	1.11
	32	3.33	2044	1.11
	36	3.27	1569	1.10
	40	3.26	1248	1.09
'B'	25	3.71	5571	1.37
	30	3.50	3578	1.36
	34	3.37	2683	1.33
	38	3.32	2077	1.30
	42	3.27	1648	1.27
'C'	25	3.74	7169	0.85
	30	3.61	5775	0.75
	34	3.52	4977	0.69
	38	3.47	4376	0.64
	42	3.42	3894	0.59

Table 4.2   Comparison of Dynamic Characteristics, Ambient Temperature Effect

Damper Type	Temp. (°C)	Experimental		Analytical	
		ω (Hz)	ξ (%)	ω (Hz)	ξ (%)
'A'	24	3.61	14.6	3.53	14.2
	28	3.46	11.0	3.36	10.0
	32	3.33	7.7	3.28	7.7
	36	3.27	5.7	3.23	6.0
	40	3.26	5.1	3.20	4.9
'B'	25	3.71	16.1	3.62	18.4
	30	3.50	12.0	3.43	13.7
	34	3.37	8.8	3.34	10.4
	38	3.32	7.1	3.28	8.0
	42	3.27	5.4	3.23	6.2
'C'	25	3.74	13.6	3.71	14.9
	30	3.61	10.9	3.58	11.4
	34	3.52	9.1	3.51	9.5
	38	3.47	7.1	3.45	8.0
	42	3.42	6.4	3.41	6.8

Table 4.3 Damper Properties used in Numerical Simulation,
Damper Placement.

Damper Placement	ω (Hz)	K_d (lb/in)	η
Case 1	3.61	4338	1.12
Case 2	3.59	4321	1.12
Case 3	3.46	4212	1.13
Case 4	3.37	4136	1.14
Case 5	3.31	4085	1.14
Case 6	3.19	3982	1.16
Case 7	3.17	-	-

Table 4.4 Comparison of Dynamic Characteristics, Damper Placement

Damper Placement	Experimental		Analytical	
	ω (Hz)	ξ (%)	ω (Hz)	ξ (%)
Case 1	3.61	14.34	3.62	13.28
Case 2	3.59	10.20	3.55	11.22
Case 3	3.46	8.10	3.46	9.06
Case 4	3.37	8.00	3.41	8.54
Case 5	3.31	3.36	3.27	4.36
Case 6	3.19	2.00	3.20	2.11
Case 7	3.17	0.54	3.17	-

Table 4.5 Comparison of Dynamic Response, Damper Placement

Damper Placement	Experimental		Analytical	
	Max. Disp. (in)	Max. Story Drift (in)	Max. Disp. (in)	Max. Story Drift (in)
Case 1	0.194	0.061	0.182	0.055
Case 2	0.223	0.066	0.216	0.070
Case 3	0.259	0.069	0.262	0.072
Case 4	0.291	0.099	0.285	0.098
Case 5	0.565	0.176	0.578	0.186
Case 6	0.766	0.223	0.697	0.210
Case 7	0.984	0.272	0.964	0.280

Table 4.6 Damper Properties used in Numerical Simulation, Strong Earthquake Excitation

Earthquake	ω (Hz)	γ (%)	K_d (lb/in)	η
Hachinohe : 0.60g	3.61	15.0	4895	1.34
ElCentro : 0.60g	3.71	10.0	5550	1.36

Table 4.7 Comparison of Dynamic Characteristics, Strong Earthquake Excitation

Earthquake	Experimental		Analytical	
	ω (Hz)	ξ (%)	ω (Hz)	ξ (%)
Hachinohe : 0.60g	3.61	14.9	3.66	15.30
ElCentro : 0.60g	3.71	14.1	3.73	16.80

Table 4.8 Comparison of Dynamic Response under Strong Earthquake Motions

Earthquake	Experimental		Analytical	
	Max. Disp. (in)	Max. Story Drift (in)	Max. Disp. (in)	Max. Story Drift (in)
Hachinohe : 0.60g	1.127	0.295	1.070	0.319
ElCentro : 0.60g	0.755	0.211	0.734	0.215
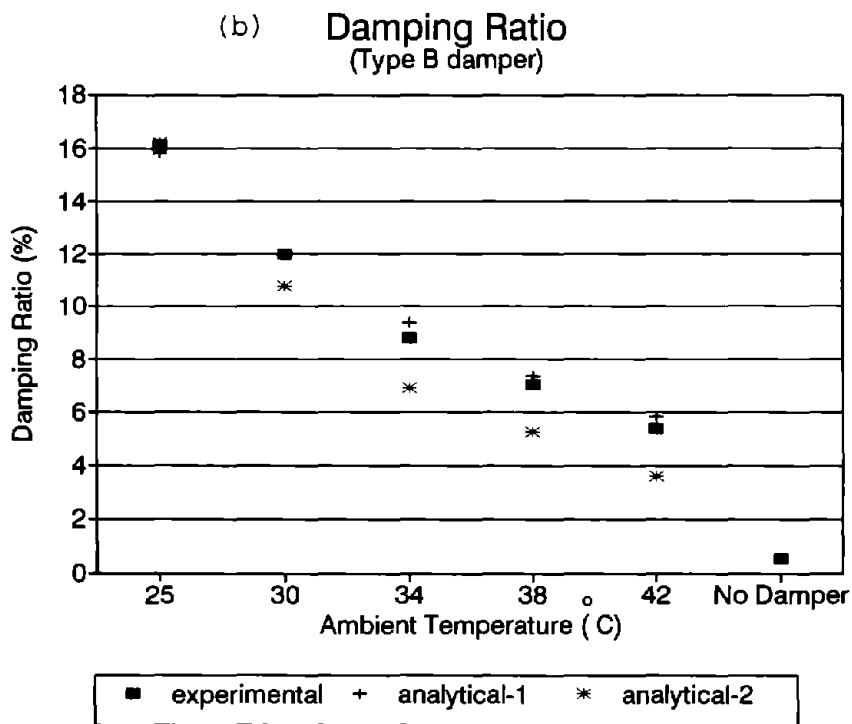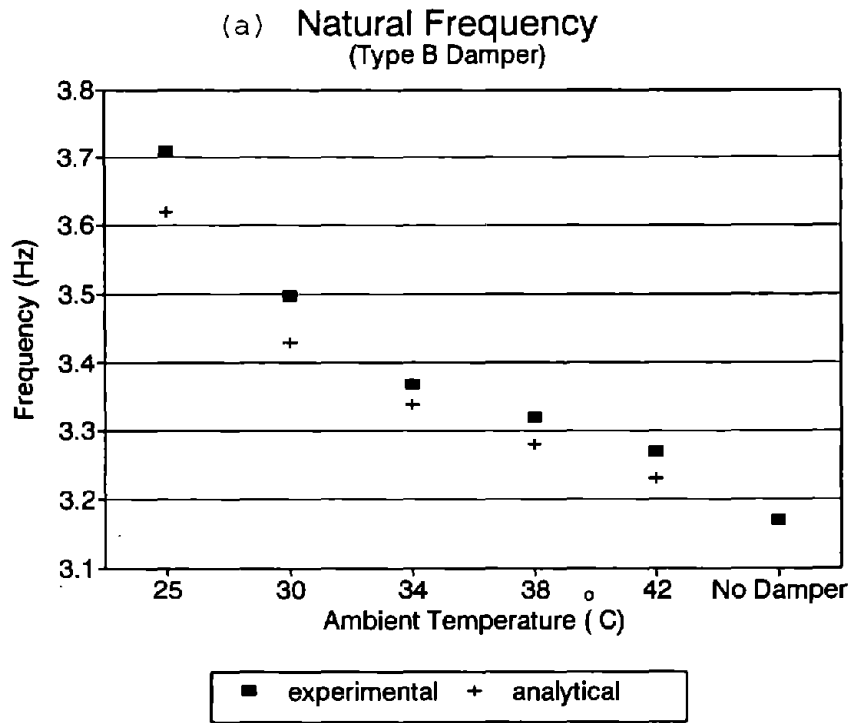
Fig. 4.1 Predicted Dynamic Characteristics using Modal Strain Energy Method (Type-B Dampers)

(a) Natural Frequency
(Type C Damper)
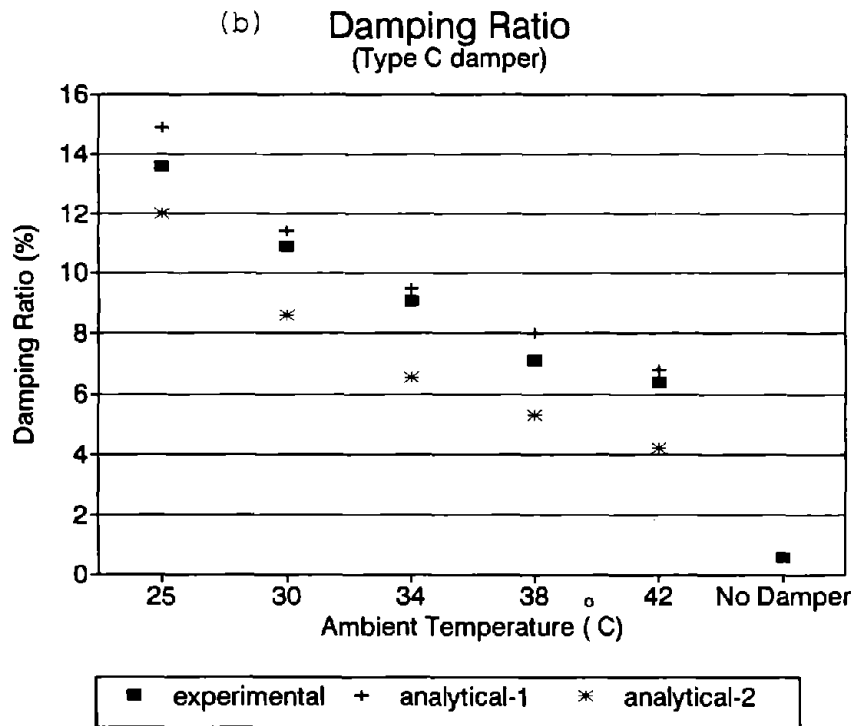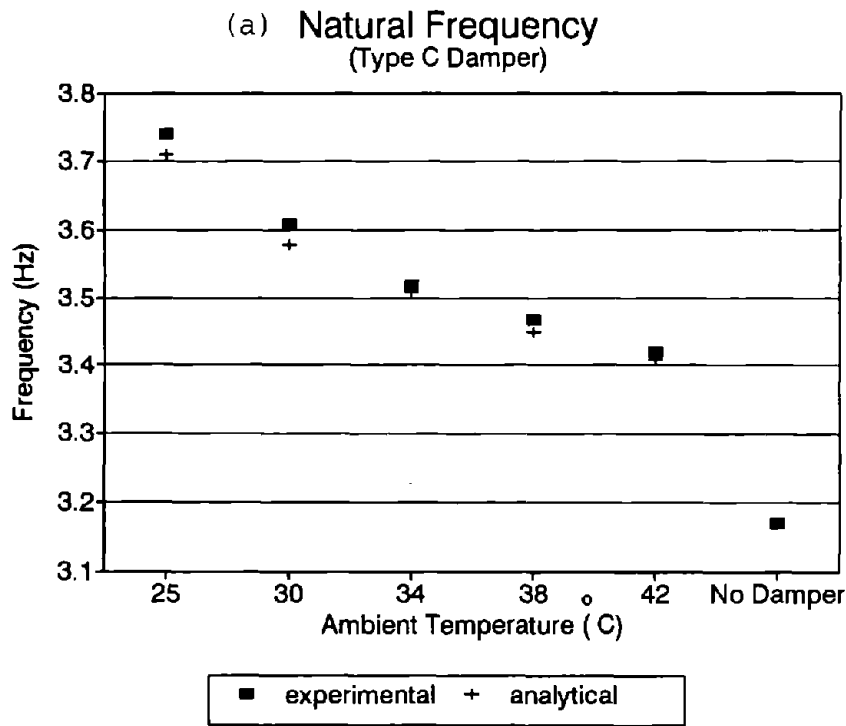
Fig. 4.2 Predicted Dynamic Characteristics using Modal Strain Energy Method (Type-C Dampers)

Case 1   Case 2   Case 3   Case 4   Case 5   Case 6   Case 7

Fig.4.3 Different Damper Placement Cases

(a) Natural Frequency

(b) Damping Ratio
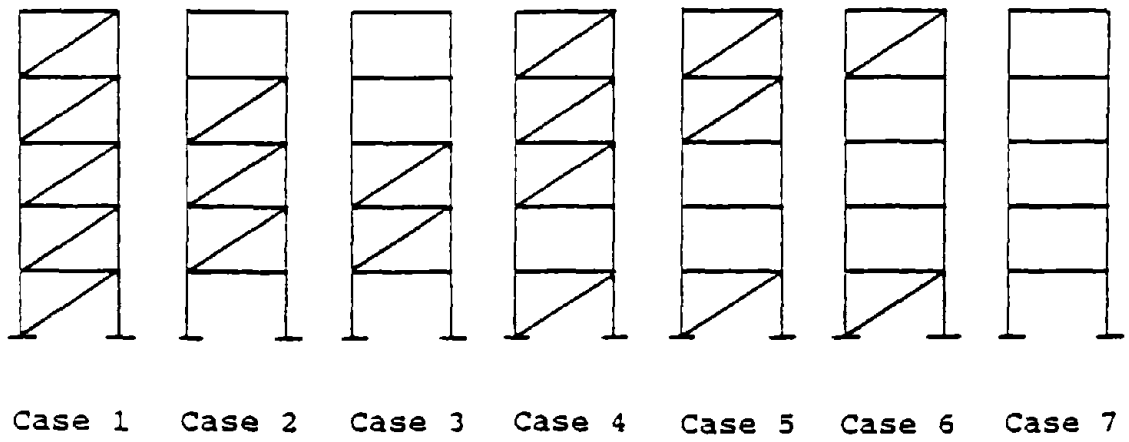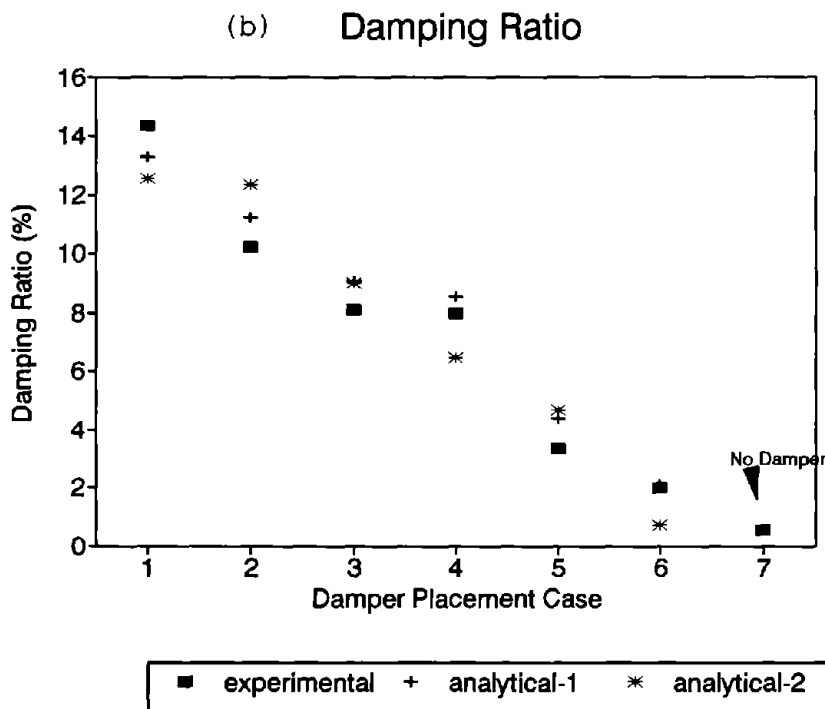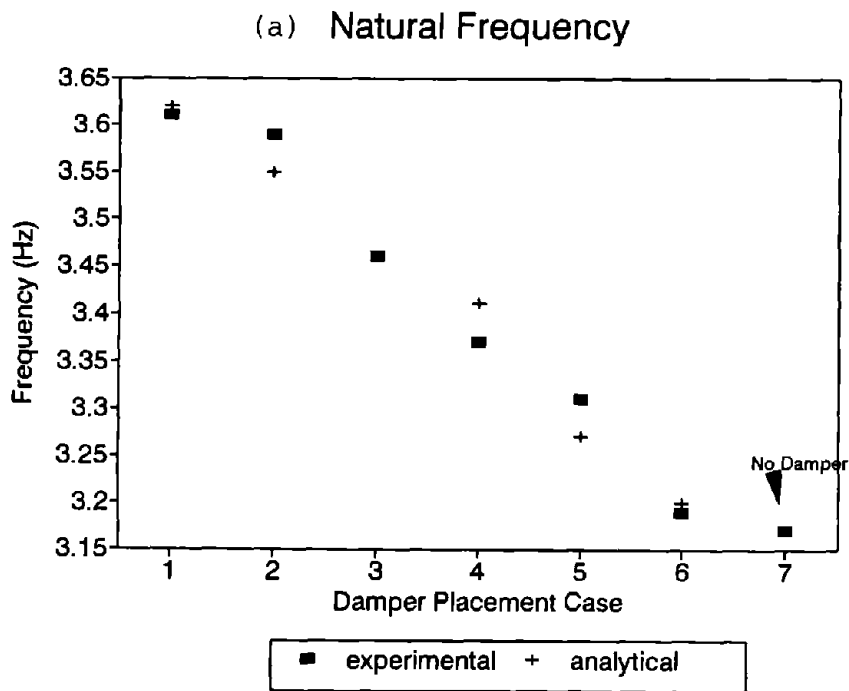
Fig. 4.4 Predicted Dynamic Characteristics using Modal Strain Energy Method (Different Damper Placement Cases)

(a) Experimental
(Damper Placement Case 2)

(b) Analytical
(Damper Placement Case 2)
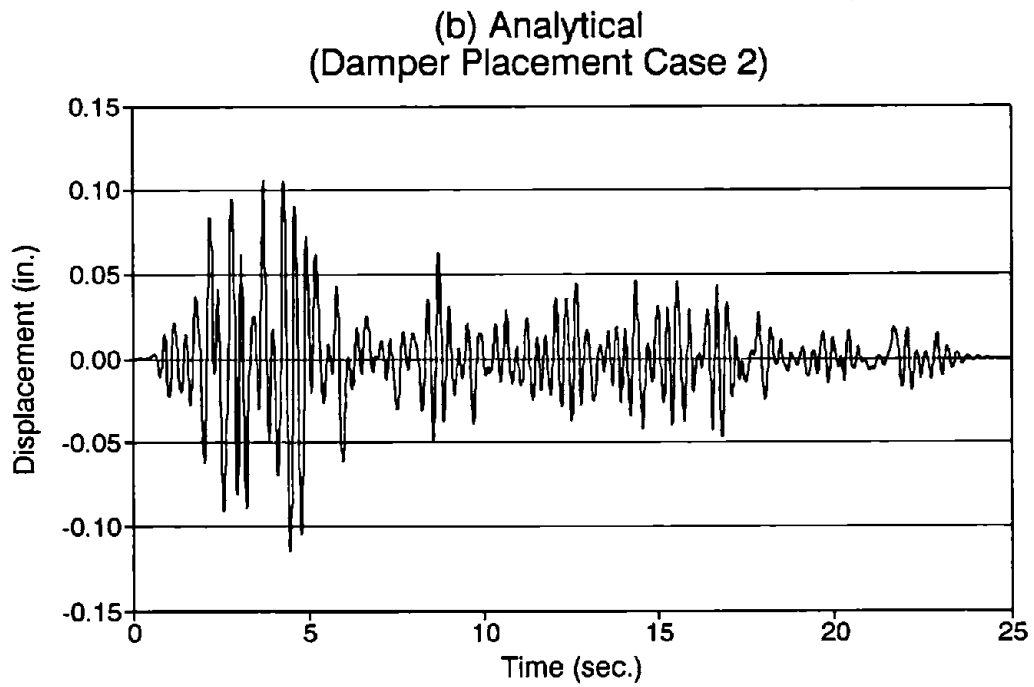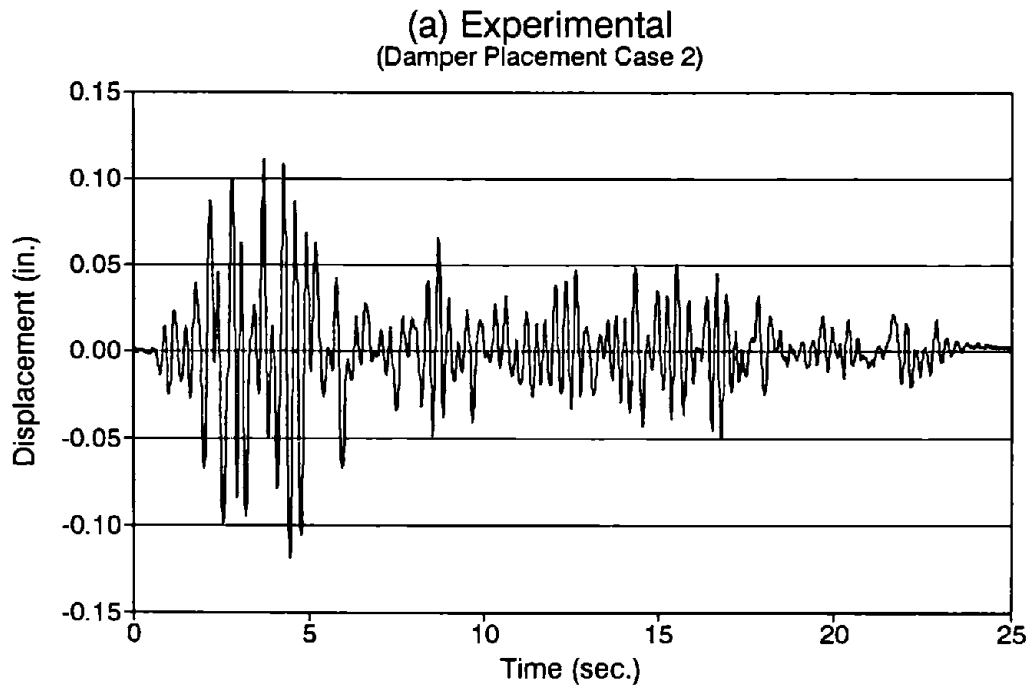
Fig. 4.5   Experimental and Analytical Response of Damper Placement Case 2

(a) Experimental
(Damper Placement Case 3)

(b) Analytical
(Damper Placement Case 3)
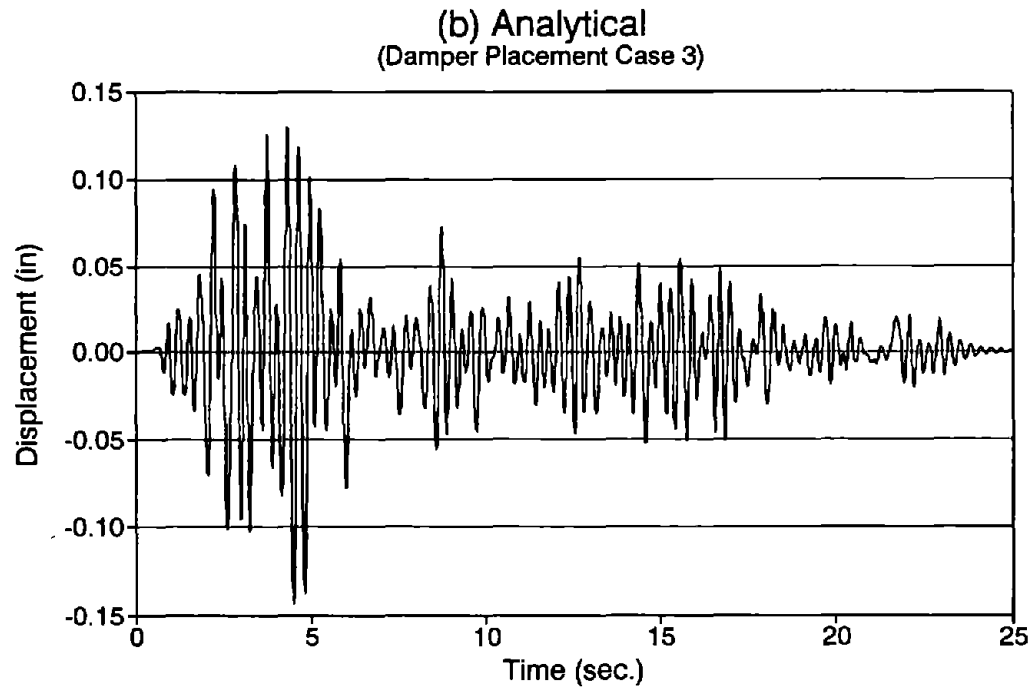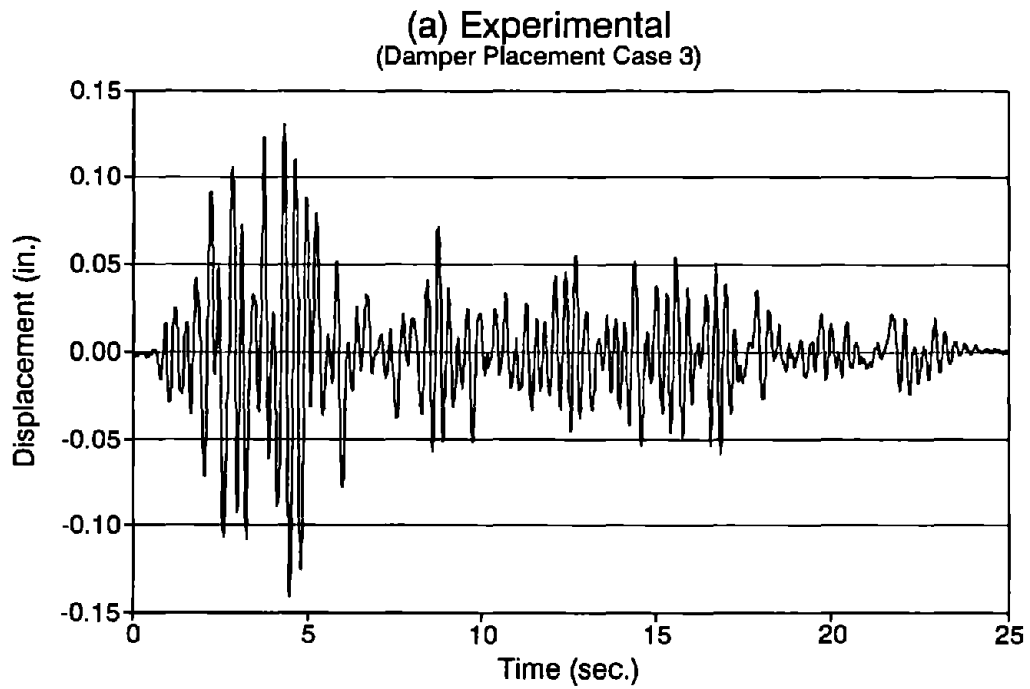
Fig. 4.6   Experimental and Analytical Response of Damper Placement Case 3

(a) Experimental
(Damper Placement Case 5)

(b) Analytical
(Damper Placement Case 5)
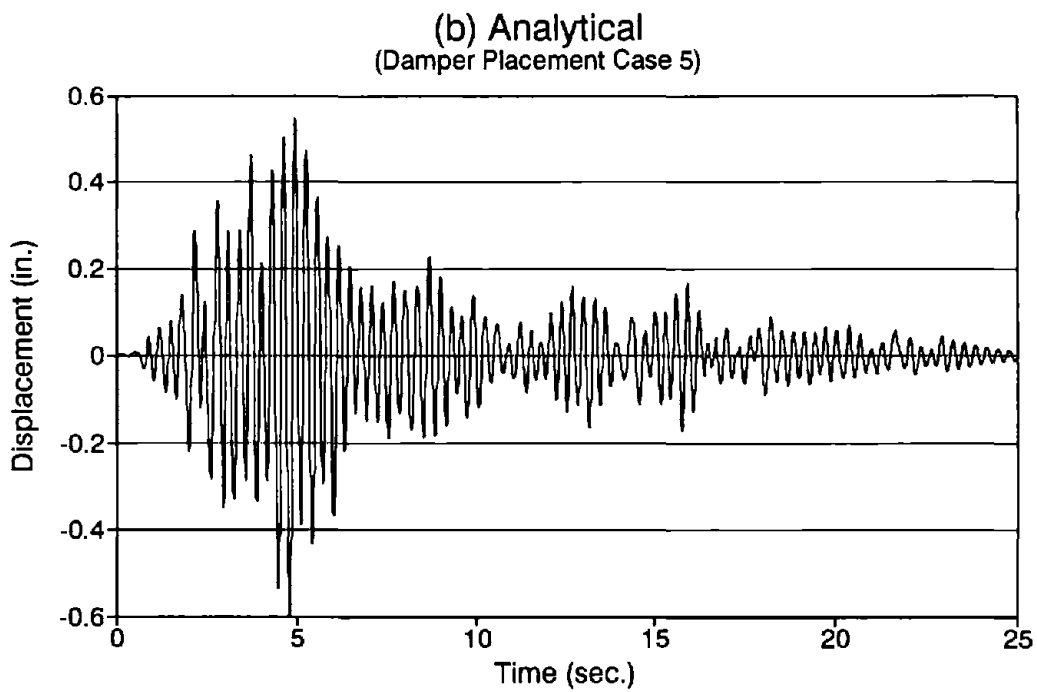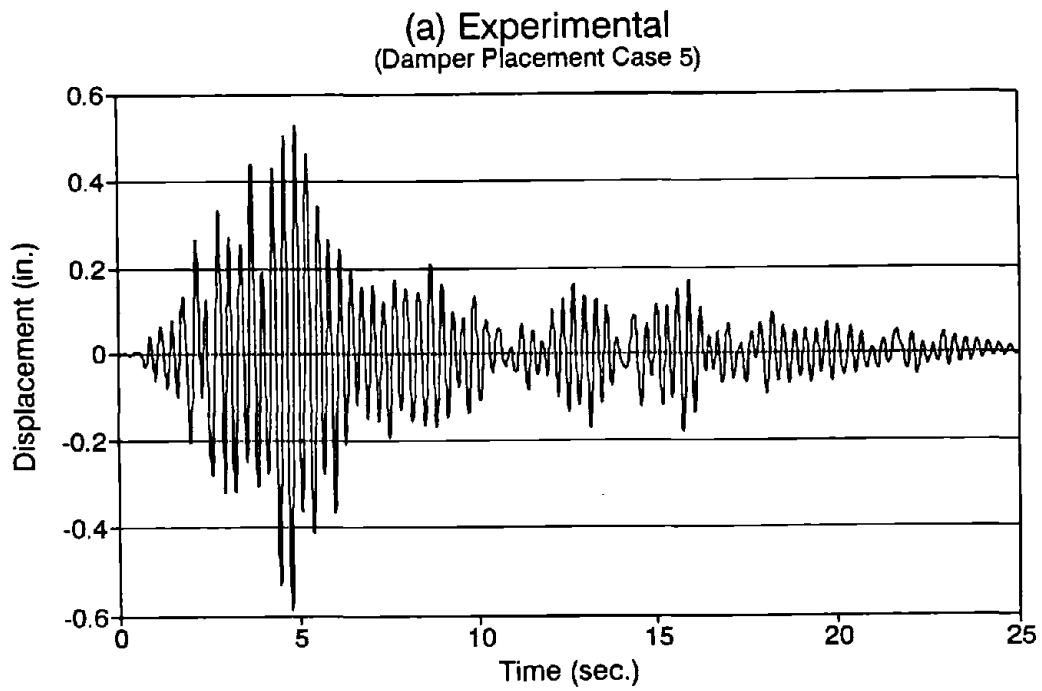
Fig. 4.7   Experimental and Analytical Response of Damper Placement Case 5

4-17
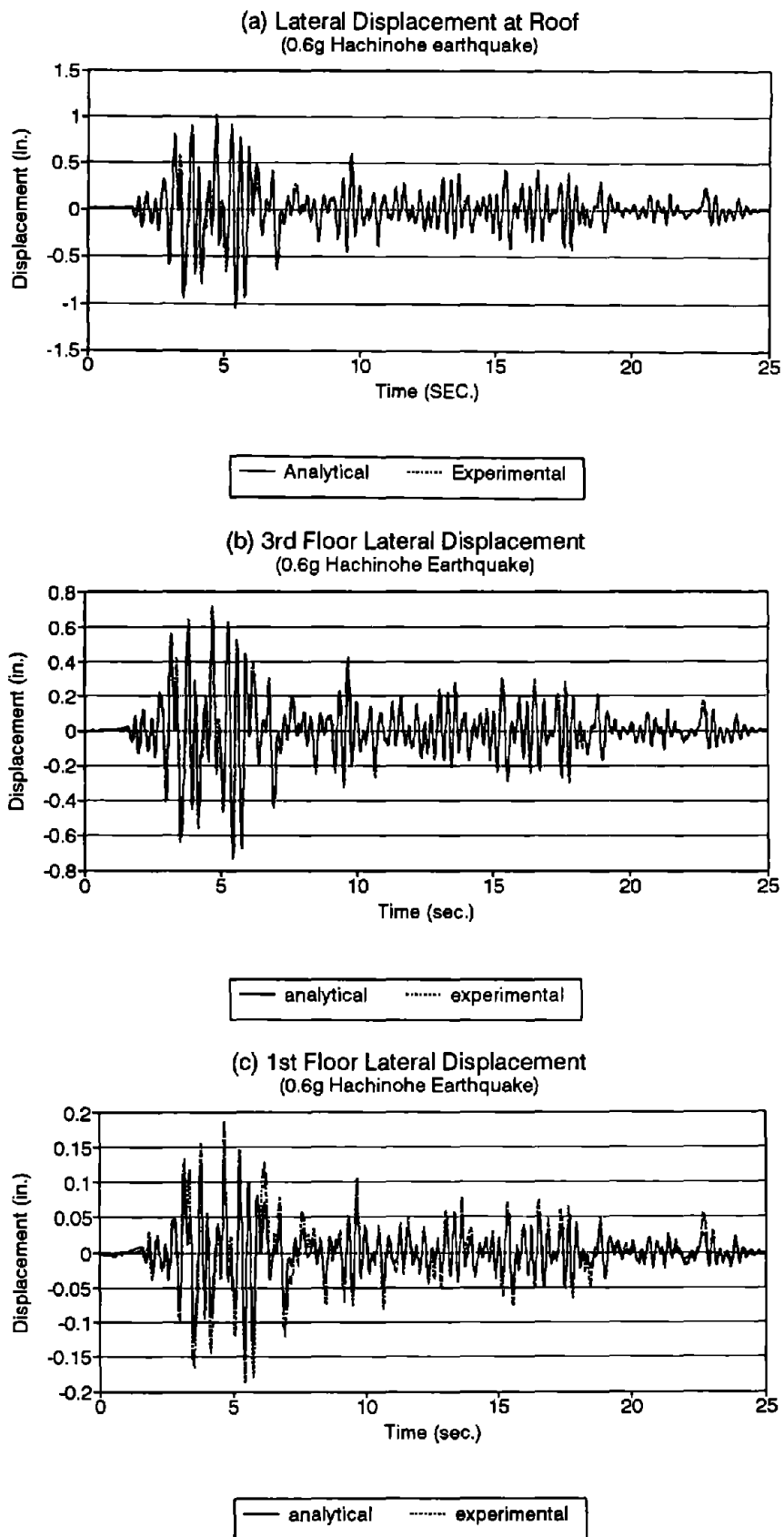
Fig. 4.8 Response Prediction of Floor Displacements under 0.6g Hachinohe Earthquake

(a) Lateral Displacement at Roof
(0.6g El Centro Earthquake)

—— analytical   ······ experimental

(b) Lateral Displacement at 3rd Floor
(0.6g El Centro Earthquake)

—— analytical   ······ experimental

(c) Lateral Displacement at 1st Floor
(0.6g El Centro Earthquake)

—— analytical   ······ experimental
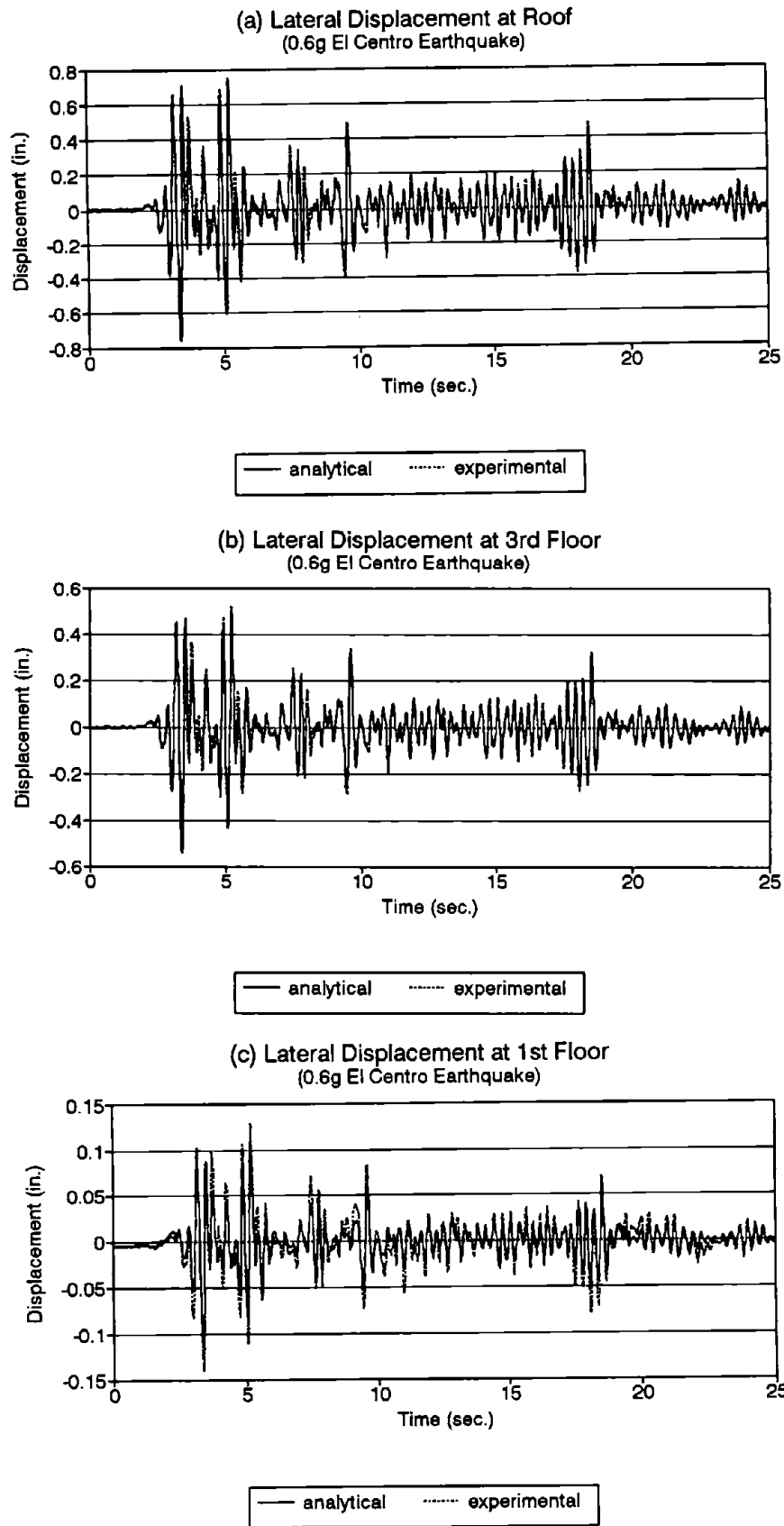
Fig. 4.9 Response Prediction of Floor Displacements under 0.6g El Centro Earthquake

4-19

(a) Story Drift at 2nd Floor
(0.6g Hachinohe earthquake)

—— Analytical   ········ Experimental

(b) Story Drift at 2nd Floor
(0.6g El Centro Earthquake)

—— analytical   ········ experimental
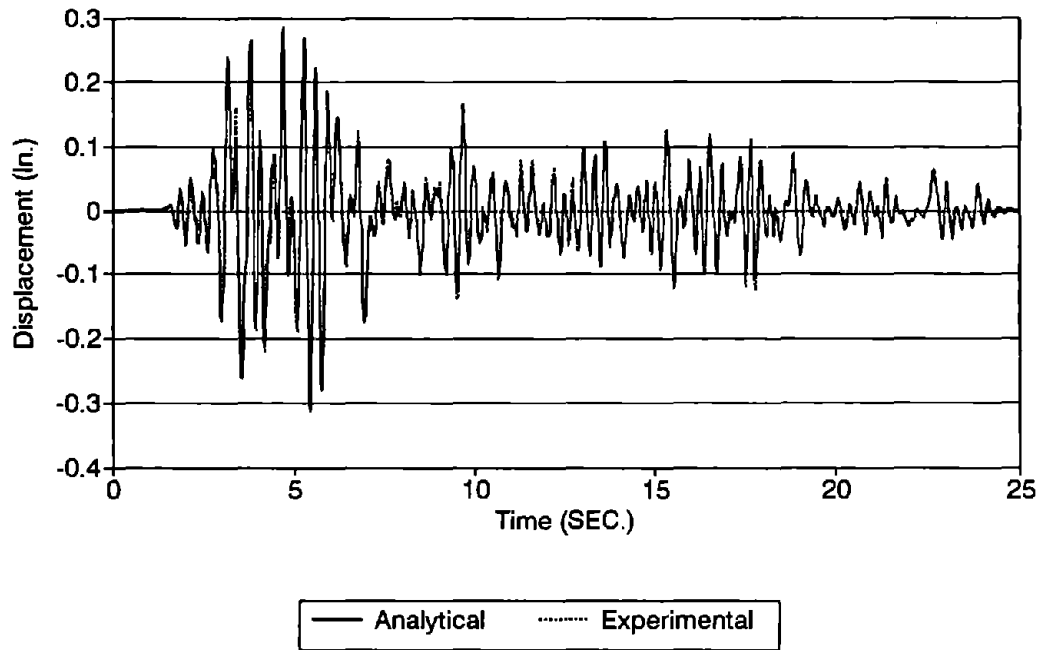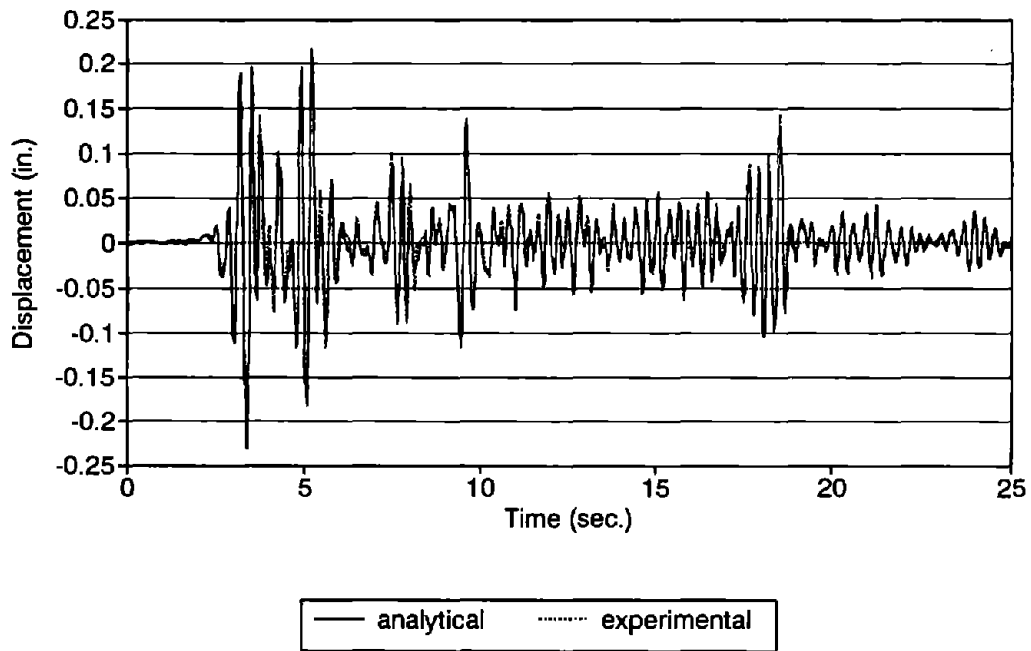
Fig. 4.10   Response Prediction of Story Drift
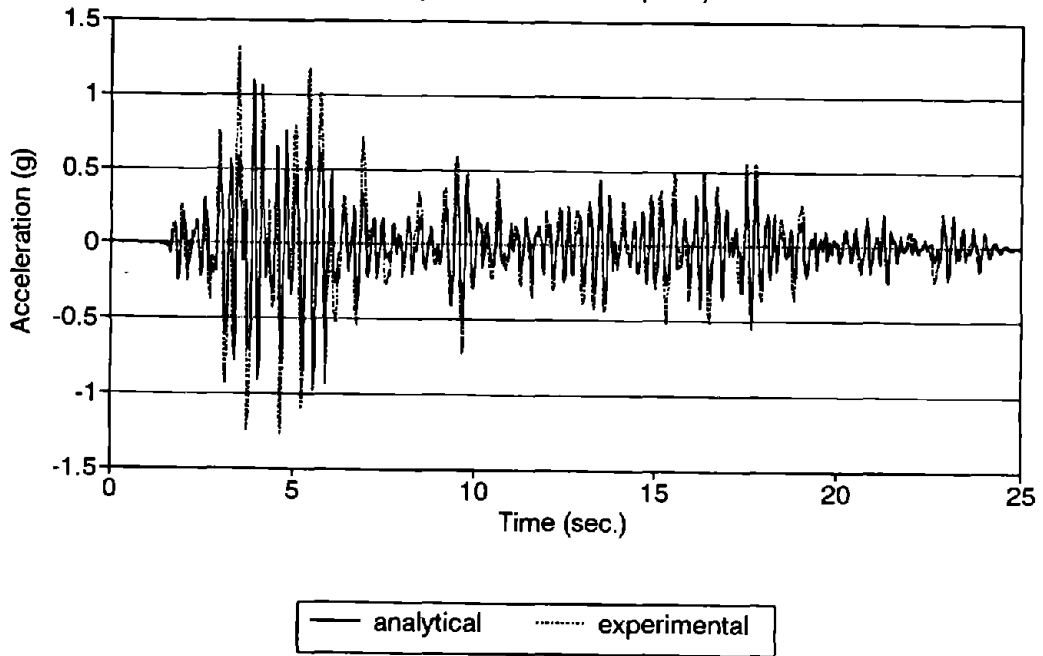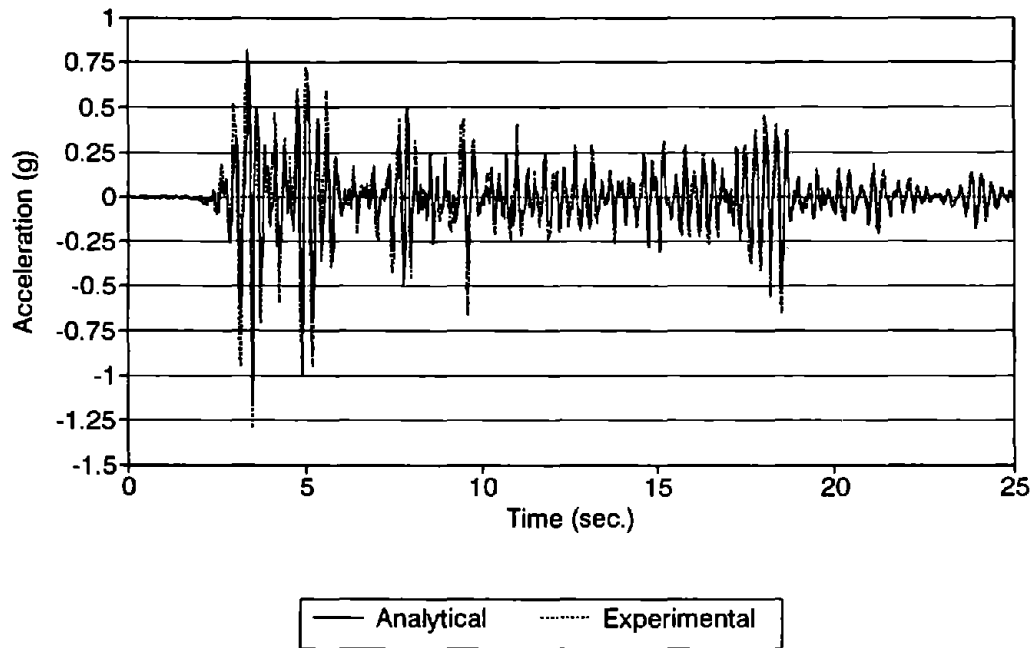
Fig. 4.11   Response Prediction of Roof Acceleration

SECTION 5

DESIGN OF STRUCTURES WITH ADDED VISCOELASTIC DAMPERS

5.1 Design Procedure

One of the fundamental requirements in structural design is to reliably predict the designed structural response under specified loading conditions. Current state-of-the-practice enables the engineers to correctly analyze the structures they design, provided all the design parameters are properly given. In designing structures with added VE dampers, the most important design parameter is the damping ratio. By properly incorporating the modal strain energy method into the design flow chart, the design of structures with added VE dampers can be accomplished with minimum modifications to the current design procedure.

As in many other design problems, the design of viscoelastically damped structures is in general an iterative process. First, an analysis of the structure without added dampers should be carried out. Then the required damping ratio becomes the primary design parameter for adding VE dampers to the structure. The design will normally contain the following steps which may be repeated to update the structural properties after each design cycle: (a) design the primary structure without added dampers; (b) determine the desired damping ratio; (c) select available damper locations in the building; (d) design the dampers; (e) calculate the equivalent damping ratio using the modal strain energy method; and (f) perform structural analysis using the designed damping ratio. When steps (e) and (f) satisfy the desired damping ratio and structural performance criteria, the design is completed. Otherwise, a new design cycle will proceed which may lead to new structural properties, damper locations or damper dimensions and properties.

5.2 Design Example

The following example is considered:

Sample Structure: 2/5 scaled steel frame [6]

Design Earthquakes: Scaled El Centro and Hachinohe earthquakes with 0.6g peak accelerations

Design Requirement: (1) $\delta/h \leq 0.5\%$ and (2) structure remains elastic under the design earthquakes

Preceding page blank

Operating Temperature: 25°C

(a) Analysis of the Structure.   Analytical results using DRAIN2D show that plastic hinges will form over the structure under the specified design earthquakes. The story drifts under the scaled 0.6g Hachinohe and El Centro earthquakes are 2.5% and 1.53%, respectively. In order to achieve the design requirement, VE dampers will be used.

(b) Determination of the Required Damping Ratio.   The required damping ratio in general can be determined from the response spectra of the design earthquakes. In this example, it is determined that an equivalent structural damping ratio of 15% will be the initial goal.

(c) Select Desirable and Available Damper Locations.   VE dampers can be placed in any available locations which allow shear deformations to occur within the dampers. In this example, dampers will be placed as diagonal braces. The angle θ between the bracing members and the floor is 42.1° except for the first floor.

(d) Design the VE Dampers.   The selection of damper stiffness k' and loss factor η can be a trial and error procedure. They can also be determined based on the principle that the added stiffness from the VE dampers be proportional to the story stiffness of the primary structure. This is obtained from modifying the modal strain energy method for each story as

$$k_{di} = \frac{2\xi}{\eta - 2\xi} k_i \tag{5.1}$$

where k_{di} and k_i are the contributions of damper stiffness and the structural story stiffness without added dampers at the ith story, respectively. For a VE material with known G' and G'' at the designed frequency and temperature, the area of the damper, A, can be determined as

$$A = \frac{k'h}{G'} \tag{5.2}$$

where k' is the damper stiffness equal to $k_d / \cos \theta$ in this example.

For this design example, the typical story stiffness without dampers, k_i, is 14.73 kip/in. Assuming $\eta = 1.1$, the damper stiffness at a typical story, k_{di}, can be determined from Eq. (5.1) as $k_{di} = 5.52$ kip/in. If two dampers are used in each story, the required damper stiffness, k', can be determined to be 3.72 kip/in.

The thickness of the VE material, h, can be determined from the maximum allowable damper deformation to insure that the maximum strain in the VE material is smaller than

the maximum allowable value. In this example, the maximum damper deformation is $0.005 \times 47 \times \cos\theta = 0.174$ in. If the maximum damper strain of 60% is allowed, the damper thickness h is determined as 0.3 in. The damper properties can be determined based on one-third of that of the maximum damper strain, or 20%. In this example, $G' = 250$ psi. Finally, if two VE layers are used, the area of the VE dampers can be obtained from Eq. (5.2) as $A = k'h/2G' = 3.01$ in². The dimensions of the damper are then 2×2 in $\times 1.5$ in $\times 0.3$ in with $A = 3.0$ in².

(e) <u>Estimate the Structural Damping Ratio</u>. Following the modal strain energy method with the damper properties corresponding to 25°C, 20% strain and 3.5 Hz, the damping ratio of the viscoelastically damped structure is about 15%. If the calculated damping ratio at this stage is lower than the required value, more dampers or larger dampers may have to be used.

(f) <u>Perform Dynamic Analysis of the Viscoelastically Damped Structure under the Design Earthquake</u>. In this example, it shows that the structure behaves elastically and the maximum story drift is less than 0.5%. The above design has also been verified through shaking table tests. some of the test results can be found in [7].

5.3 Discussion

In this example, the structure with added dampers behaves elastically under the design earthquake. If inelastic deformation is allowed in the structure, the demand in VE damping can be reduced.

SECTION 6

FULL-SCALE STRUCTURAL TESTS

6.1 Introduction

In order to verify the test results obtained and the damper design procedure developed from the reduced scaled models, the full-scale prototype structure of the 2/5-scale model with and without added VE dampers were studied experimentally and analytically. The structure, constructed by the Beijing Polytechnic University of Beijing, China, was a product of the US-China cooperative research program [15].

The modal strain energy method used for the 2/5-scale model was employed to design the dampers and predict the added damping to the prototype structure by the dampers. Dynamic scaling factors between the model and prototype structures with the added VE dampers were carefully considered.

Two eccentric mass vibration generators, one on the ground floor and the other on the roof, were used to sinusoidally excite the structure. In addition, free-decay tests were conducted at different ambient temperatures.

6.2 Prototype Structure

The prototype structure was designed and constructed by using the proper dynamic scaling factors. A brief description of the structure is provided in this section. The damper design procedure is then illustrated to determine the size of the dampers for desired added damping for the prototype structure.

6.2.1 Dynamic Scaling Law

The dynamic scaling factors between the model and prototype structures are shown in Table 6.1. The scaling factors of acceleration and modulus of elasticity are chosen to be one. The scaling factor for the damping ratio, which is a non-dimensional parameter, is also one.

Since the damping ratio of a viscoelastically damped structure is related to stiffness of the dampers, in order to obtain the same damping ratio as in the model structure, one can simply increase the damper stiffness of the model structure by 2.5 times to obtain

the required damper stiffness for the prototype assuming the damper loss factor does not change. This will be further discussed in the following sections.

6.2.2 Structural Properties

Using the scaling factors given in Table 6.1, the full-scale five-story steel frame structure was constructed and its dimensions are shown in Fig. 6.1. It is single-bay structure with cast-in-situ floor slabs [15]. The center to center distance between columns is 3.3 m. The first floor height is 2.175 m and the floor height is 3.0 m for the rest of floors. The columns extend out 0.215 m above the center line of the roof beam. The total height is 14.915 m. The foundation plate is cast-in-place reinforced concrete. All the columns are of the same size and all the beams have the same dimensions. The cross section of the column is 308×250×14×10 in mm. The web and flange of the columns are fabricated by welding. The beam is hot-rolled 25b I-shaped A3 steel. The cross-section is 40×118×10×13 in mm. All the beam-column joints are welded and bolted to transfer moments as rigid connections.

The braces for installing the VE dampers are concurrent at the beam-column center lines joint and installed in the weak axis (N-S direction). Each set of bracing members consists of two double angles with equal legs L50×50×5 in mm. The VE damper is connected at the lower 86 cm part of the brace. The diagonal bracing member with the viscoelastic damper is bolted to the gusset plates which are welded to the center of the beam flange and column web. The stiffness of the brace is 27 ton/cm.

The structural floor weight for the first through fourth is 2180 Kg. The fifth floor weighs 2700 Kg due to addition of the model QZJ-1 vibrator on the roof. The ground soil layers under the foundation plate are (1) 40 cm light loam, (2) 115 cm heavy loam, and (3) microscopic sand. The dominant period of the test site is 0.4 second [19,20] from the ambient vibration test.

6.2.3 VE Damper Theory and Design Curves

Before the dampers can be designed for a given structure, one needs to relate the dampers and structural properties to the added damping. Since the finite stiffness of the braces connecting the dampers to the structure will affect the damper efficiency, we shall view the braces as a part of the damper system. The effective stiffness, k'_{v-b}, and loss factor, η_{v-b}, of a brace-damper system in series can be calculated using complex

variables as [21]

$$\frac{1}{k'_{v-b} + jk''_{v-b}} = \frac{1}{k'_{v-b} + j\eta_{v-b}k'_{v-b}} = \frac{1}{k'_v + jk''_v} + \frac{1}{k_b} = \frac{1}{k'_v + j\eta_v k'_v} + \frac{1}{k_b} \qquad (6.1a)$$

where k'_v is the damper storage stiffness, η_{v-b} and η_v are the loss factors of the damper-brace system and VE damper itself, respectively, and k_b is the brace stiffness. The loss factors are defined as

$$\eta_{v-b} = \frac{k''_{v-b}}{k'_{v-b}} \quad \text{and} \quad \eta_v = \frac{k''_v}{k'_v} \qquad (6.1b)$$

For instance, if the stiffness ratio of the brace to the damper is 18 and the damper loss factor is 1.4, the effective damper storage stiffness will remain approximately the same as the original damper storage stiffness but the effective loss factor reduces to 1.2.

For simplicity, the subscript $v-b$ representing the damper-brace system will be replaced by v only in the following sections unless noted otherwise. The damper stiffness and loss factor will be referring to the effective damper stiffness and effective loss factor.

As proposed for the model structure [7,10,11], the added structural modal damping ratio can be calculated from the structural properties and damper stiffness and loss factor as

$$\zeta = \frac{\eta_v}{2} \frac{SE'_v}{SE_s} \qquad (6.2a)$$

$$= \frac{\phi^T K''_v \phi}{2\phi^T K_s \phi} \qquad (6.2b)$$

$$= \frac{\eta_v}{2} \frac{\phi^T K'_v \phi}{\phi^T K_s \phi} \qquad (6.2c)$$

$$= \frac{\eta_v}{2} \left(1 - \frac{\phi^T K_o \phi}{\phi^T K_s \phi}\right) \qquad (6.2d)$$

$$\approx \frac{\eta_v}{2} \left(1 - \frac{\omega^2}{\omega_s^2}\right) \qquad (6.2e)$$

where K''_v is the stiffness matrix constructed using the pure loss (viscous) stiffness of the dampers, SE'_v and SE_s are the elastic strain energy in the dampers and the structural modal strain energy including the dampers, respectively, ϕ^T is the transpose of the mode shape vector, K'_v is the stiffness matrix due to the damper storage (elastic) stiffness, and K_o and K_s are, respectively, the stiffness matrices of the structure without and with the dampers. The damper storage stiffness can be represented by adding a spring or steel brace with desired stiffness to the structure.

6-3

The structural damping ratio is usually normalized by the loss factor of the viscoelastic material as seen from Eq. (6.2a), which is given by

$$\frac{2\zeta}{\eta_v} = \frac{SE'_v}{SE_s} \tag{6.3}$$

It is equal to the strain energy ratio of the dampers to the structure.

As shown in Eq. (6.2a), the added structural damping ratio is proportional to the strain energy in the dampers with a certain damper loss factor and structural strain energy. In order to maximize the damper strain energy, the dampers should be placed in locations experiencing large displacements. Equation (6.2e) provides a quick estimate of added damping in the viscoelastically damped structures [11]. Equations (6.2a-e) also show that the maximum structural damping ratio that can be obtained using VE dampers is

$$\zeta = \frac{\eta_v}{2} \tag{6.4}$$

which is one-half of the damper loss factor.

The equations given above provide the calculation of the modal damping ratio assuming that the inherent structural damping ratio is zero. When the inherent structural damping ratio is not zero, the calculation of the total damping ratio can be very complicated depending on the mechanism of inherent damping. Here we assume that the energy dissipated by the inherent damping is uniformly distributed in the structure and the total dissipated energy can be expressed as [22]

$$K_I = 2\zeta_o K_o + \eta_v K'_v \tag{6.5}$$

Substituting K_I for K''_v in Eq. (6.2b), the total modal damping ratio becomes

$$\zeta = \frac{\phi^T K_I \phi}{2\phi^T K_s \phi} \tag{6.6a}$$

$$= \zeta_o + \frac{(\eta_v - 2\zeta_o)}{2} \frac{\phi^T K'_v \phi}{\phi^T K_s \phi} \tag{6.6b}$$

$$= \zeta_o + \frac{(\eta_v - 2\zeta_o)}{2} \left(1 - \frac{\phi^T K_o \phi}{\phi^T K_s \phi}\right) \tag{6.6c}$$

$$\approx \zeta_o + \frac{(\eta_v - 2\zeta_o)}{2} \left(1 - \frac{\omega_o^2}{\omega_s^2}\right) \tag{6.6d}$$

The normalized loss factor or the strain energy ratio is

$$\frac{2(\zeta - \zeta_o)}{\eta_v - 2\zeta_o} = \frac{\phi^T K'_v \phi}{\phi^T K_s \phi} \tag{6.7}$$

6-4

For the present study, the viscoelastic dampers are in pairs at each level of the full-scale structure in the weak direction and are installed in the diagonal bracing elements near the end as shown in Fig. 6.2. Ten viscoelastic dampers are used in the full-scale structure. The damper stiffnesses and sizes used are the same.

Assuming no inherent damping, the normalized structural damping ratio, $2\zeta/\eta_v$, can be calculated using Eq. (6.2d) against different damper storage stiffnesses as shown in Fig. 6.3. It is interesting to note that the normalized prototype structural damping can be obtained either by the finite element analysis (FEA) or by scaling up stiffness 2.5 times from the model structure. The structural modal frequency with the added dampers can also be calculated as shown in Fig. 6.4.

From the damper design curve, damping versus stiffness, one can then locate the damper storage stiffness for the desired damping ratio when the damper loss factor is determined. The damper loss factor is usually a constant and can be obtained from the damper manufacturer.

6.2.4   Viscoelastic Damper Properties and Dimensions

When the effective damper-brace storage stiffness k'_{v-b} is located from the design curve, the actual damper storage stiffness, k'_v, can be calculated from Eq. (6.1a). The total VEM shear area, A, can be calculated from

$$A = \frac{k'_v h}{G'}$$

(6.8)

where G' is the shear storage modulus of the VEM and h is the thickness. The thickness of the VEM has to be large enough to withstand the credible strain and fatigue posed in the VEM.

The shear storage modulus of the VEM is usually a function of frequency and temperature. The frequency at which the damper operates is approximately the same as the structural modal frequency and can be obtained from Fig. 6.4.

The damper size can also be scaled up from that used in the model structure. The thickness should be increased by the scaling factor to retain the designed strain in the VEM as

$$h_{\text{prototype}} = h_{\text{model}}/\lambda$$

(6.9a)

6-5

Since the stiffness has to be increased by the scaling factor $1/\lambda$, the area of the VEM has to be increased by $1/\lambda^2$, i.e.,

$$A_{\text{prototype}} = \frac{A_{\text{model}}}{\lambda^2} f_v \qquad\qquad (6.9b)$$

where f_v is a constant greater than one. The damper stiffness is usually frequency-dependent; the lower the frequency is, the lower the stiffness will be. The damper area needs to be further increased from the scaled-up area by f_v to obtain the designed stiffness because the natural frequency of the prototype structure is smaller. Here we assume that the loss factors for the model damper and prototype damper are the same. If the natural frequencies of the two structures are very different, the loss factors will be different and the damper size has to be further adjusted.

The VE dampers used in the full-scale structural tests consist of two layers of 3M ISD 110 VEM bonded to steel plates as shown in Fig. 6.5. This VEM was used in the dampers for the model structure. The vibrational energy in the structure is dissipated by shearing of the VEM. The VEM thickness is scaled up to 1.2 cm. The total area of the VEM is 56.7×2 cm², which was calculated from Eq. (6.3) with the following information: (a) the design damping ratio is 10% at 24°C, (b) the effective damper loss factor is 1.2 and the normalized structural damping is 0.18, (c) from Fig. 6.3, the storage stiffness is 1.45 tons/cm, (d) from Fig. 6.4, the structural modal frequency is 2.2 Hz, and (e) the VEM storage shear modulus is 1.5×10⁶ Pascal (220 psi).

The original damper storage stiffnesses and loss factors at different temperatures used in this study are shown in Table 6.2. With the braces, the effective damper storage stiffnesses remained about the same. However, the effective loss factors were all reduced to 1.2 which was used for design. The damper stiffness does not change significantly in this narrow frequency range of 2.1 to 2.2 Hz. The strain is 10%.

6.3 Full-Scale Structural Vibration Tests

The test set-up and experimental details as well as test results are described and discussed in this section. The main purpose of the vibration tests was to obtain modal parameters, i.e., modal damping ratio, mode shape and frequency, of the full-scale structure with and without viscoelastic dampers at different ambient temperatures. Both forced and free vibration tests were conducted. The test results are compared to the analytical ones.

6.3.1 Instrumentation

As shown in Fig. 6.6, a total of six precision accelerometers, Model V401R, were installed on the floors to measure the floor acceleration responses. The relative displacement of the VE damper on the second floor was monitored by a displacement transducer, Model WCY-2. Two vibrators were used, one at a time, to excite the structure. Vibrator QZJ-1 [19] was installed on the roof and vibrator TQJ-4 [20] was installed on the ground floor. The acceleration and displacement signals were fed into a multi-channel tape recorder as well as a PC with a Data Translation data acquisition board.

6.3.2 Free Vibration Tests

Free vibration tests were carried out by pulling and suddenly releasing the test structure. Modal frequencies and damping ratios for the damped and undamped cases at different temperatures were calculated by curve-fitting the measured decay acceleration time histories with simple linear viscous damping model as

$$\ddot{x}(t) = \frac{x_o}{\cos\phi} e^{-\zeta\omega_n t}\omega_n^2 \left\{ \cos(\omega_d t - \phi) + 2\zeta\sqrt{1 - \zeta^2}\sin(\omega_d t - \phi) \right\} \tag{6.10}$$

where x_o is the initial lateral displacement and ω_n is the undamped natural frequency. Equation (6.10) is obtained from differentiating the displacement time history twice. The displacement and velocity are defined as follows

$$x(0) = x_o, \quad \dot{x}(0) = 0 \tag{6.11}$$

$$x(t) = \frac{x_o}{\cos\phi} e^{-\zeta\omega_n t}\cos(\omega_d t - \phi), \quad \phi = \tan^{-1}\frac{\zeta}{\sqrt{1 - \zeta^2}}, \quad \omega_d = \omega_n\sqrt{1 - \zeta^2} \tag{6.12}$$

A stationary post was constructed 20 meters away from the structure for the free-decay tests as shown in Fig. 6.7. Steel cables along with a load rod and pulleys were used to pull the structure. The structure was suddenly released by breaking the load rod. The maximum lateral displacement at the roof level was approximately 10 mm.

The experimental as well as curve-fitted results are shown in Figs. 6.8a-f. It is interesting to note that Eq. (6.10) using the simple linear viscous model can describe the free-decay responses with and without the VE dampers very well. This greatly simplifies the design and analysis of viscoelastically damped structures. The first natural frequencies and damping ratios from curve-fitting the experimental data are shown in Table 6.3 for different ambient temperatures.

The damping ratio was increased from 1.3% to 11.4% at 24°C. The damping ratio was reduced as the ambient temperature increased. This is due to the decrease in the damper storage stiffness at higher ambient temperatures. The natural frequency of the structure increased only slightly at all temperatures. The dampers were able to sufficiently increase the damping in the structure without greatly changing the original structural stiffness.

Figure 6.9a shows that the normalized measured loss factors at different temperatures correlate quite well with the prediction, which is the design curve. As shown in Fig. 6.9b, the measured natural frequency of the structure with and without dampers are also in good agreement with the prediction. These master design curves can be used to design dampers for different sizes and ambient temperatures for the structure.

The frequency shift given by Eq. (6.6d) was also used to calculate the damping ratios using the measured frequencies as shown in Fig. 6.10. Again, the correlation is quite good. These results demonstrate that the modal strain energy method developed from the model structures is applicable to the full-scale structure.

6.3.3 Forced Vibration Tests

Forced vibration tests were conducted using two different vibrators. Each vibrator had two equal eccentric weights rotating in opposite directions, which generated a unidirectional force varying sinusoidally with time. The output force, $F(t)$, of the vibrator can be calculated as

$$F(t) = 2m\omega^2 R \sin \omega t \qquad (6.13a)$$

$$= 79mf^2 R \sin 2\pi ft \quad (N) \qquad (6.13b)$$

where m is the mass of the eccentric weight, ω is the circular frequency, R is the eccentric distance, and f is the frequency in Hz.

Vibrator TQJ-4 was located on the foundation plate. The force generated by the vibrator would excite the foundation, soil and the structure. The amplitude of the force is

$$F = 5710f^2 \quad (N) \qquad (6.14)$$

The vibration in the structure generated by this vibrator was small due to the large weight and stiffness of the foundation and soil, although the output force was large. In

order to obtain larger displacements, Vibrator QZJ-1 was located on the roof. The force amplitude generated by this vibrator is

$$F = 445f^2 \quad (N) \tag{6.15}$$

which is 12.8 times smaller than that produced by the vibrator on the foundation plate.

The swept sine tests were conducted to identify the damping ratio and natural frequency of the structure at different ambient temperatures. The results obtained from these tests were very close to those obtained from the free-decay tests. The structure was then excited at the natural frequency by the two vibrators.

Figure 6.11 shows the measured roof acceleration without and with dampers at 25° and 30°C ambient temperatures with the vibrator on the foundatin plate. Without dampers, the roof acceleration was approximately 7.5 and 5 times larger than those at 25° and 30°C, respectively. The dampers were very efficient in reducing resonance responses. Since the response is inversely proportional to the damping ratio when the structure is vibrating at resonance, the damping ratios for the structure with dampers at 25° and 30°C should be

$$\zeta_{25°C} = 1.3 \times 7.5 = 9.8\% \qquad \text{and} \qquad \zeta_{30°C} = 1.3 \times 5 = 6.5\%$$

which are consistent with values obtained from the prediction and free-decay tests. The inherent structural damping ratio was still assumed to be 1.3%.

The accelerations on the other floors were also measured and are shown in Fig. 6.12 as response envelopes. It is seen that the acceleration was reduced by the dampers on all floors.

When the vibrator was on the roof, the structural response increased approximately 15 times compared to that using the other vibrator as shown in Fig. 6.13. The structural response without dampers is not presented because the vibration became so violent that the vibrator was jammed and could not work properly.

These response envelopes also approximate the mode shapes of the structure with and without dampers. Figure 6.14 shows that the normalized acceleration envelopes illustrated in Figs. 6.12 and 6.13 collapse into one curve with small variations. This is the mode shape of the structure which is not significantly changed with and without the dampers.

6.4 Discussion

The results of the analytical and experimental study on the full-scale structure can be summarized as follows:

(1) The damper design procedure developed from the model structures can be readily applied to the full-scale structure. For the scaling rules used in this study, the size of the damper material for the full-scale structure can be simply scaled up by the scaling factor for the VEM thickness and square of the scaling factor for the area. Some further increase in the area may be needed when the difference in the natural frequencies is large between the model and prototype structures. This study provides an important link between the design and analysis of the model and full-scale structures using viscoelastic dampers. The use of the extensive data base generated from the testing of the reduced scaled models for the full-scale structures can now be better justified.

(2) The experiments show that the visocelastic dampers are quite efficient in reducing the vibration as demonstrated in the model structure. The linear viscoelastic theory is still applicable to the full-scale structure. This simplifies the damper design and the dynamic structural analysis.

(3) The modal strain energy method used for the 2/5-scale model structure can also be used for the full-scale structure to predict the structural damping and dynamic response at various ambient temperatures.

Table 6.1   Dynamic Scaling Factors

Parameter	Scaling	Value
length	λ	0.4 (1:2.5)
Time	$\lambda^{1/2}$	0.63
Frequency	$\lambda^{-1/2}$	1.58
Acceleration	1	1
Modulus of elasticity	λ_E	1
Force	$\lambda^2 \lambda_E$	0.16
Moment of inertia	λ^4	0.0256
Displacement	λ	0.4
Stiffness	$\lambda \lambda_E$	0.4
Damping	1	1

Table 6.2   Measured VE Damper Storage Stiffnesses and Loss Factors

Temperature ($^\circ C$)	Stiffness ton/cm	Loss Factor	Effective Loss Factor
24	1.5	1.4	1.2
25	1.3	1.4	1.2
26	1.2	1.4	1.2
30	0.71	1.35	1.2
32	0.58	1.3	1.2
34	0.48	1.25	1.2

Table 6.3   First Natural Frequencies and Damping Ratios from Experiment

Temperature ($^\circ C$)	Damping ratio (%)	Natural Frequency (Hz)
No dampers	1.3	2.03
24	11.4	2.24
25	10.8	2.22
26	8.56	2.16
30	6.04	2.09
32	4.88	2.09
34	4.84	2.09
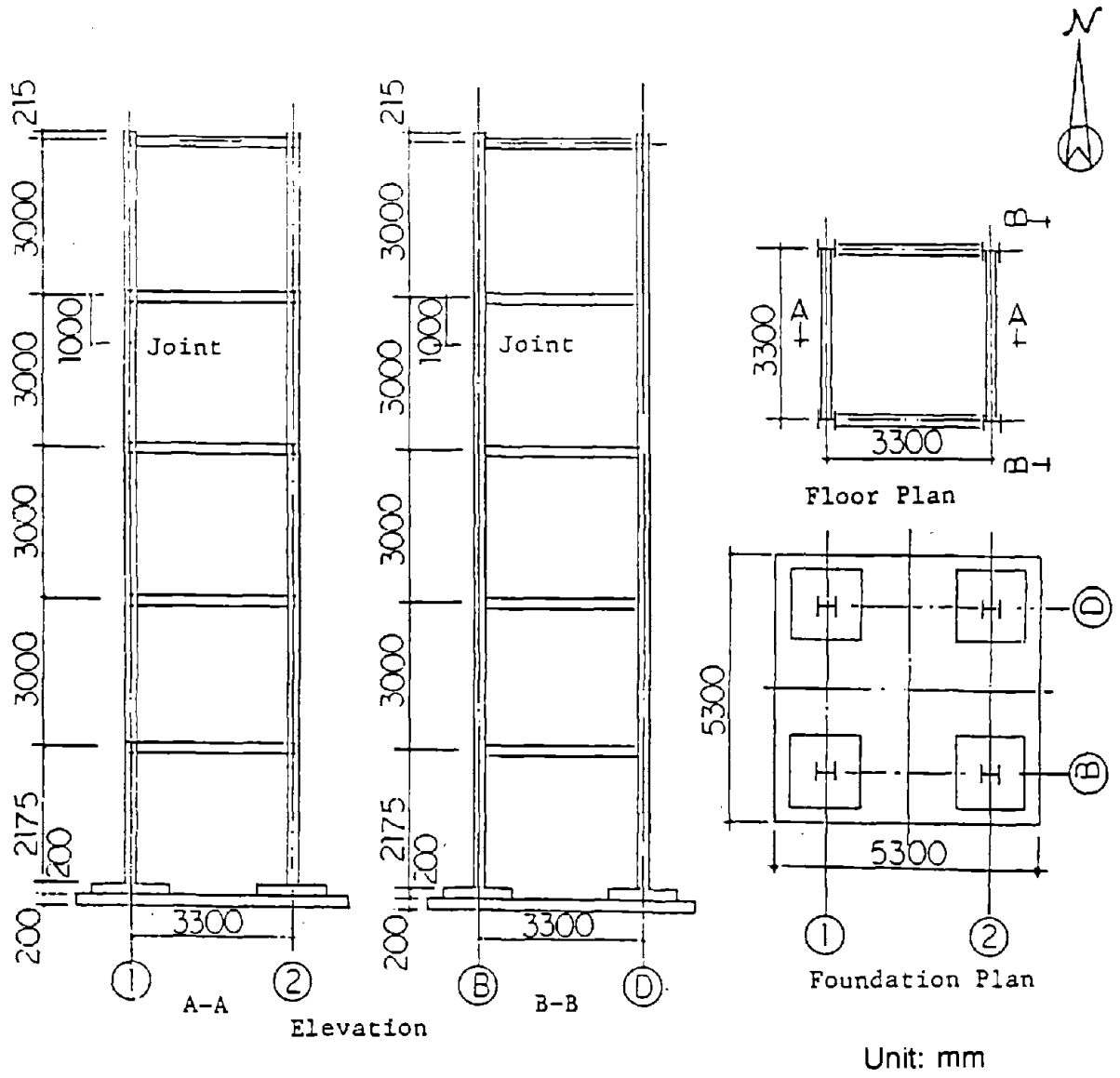
Fig. 6.1   Full-scale Five-story Steel Frame
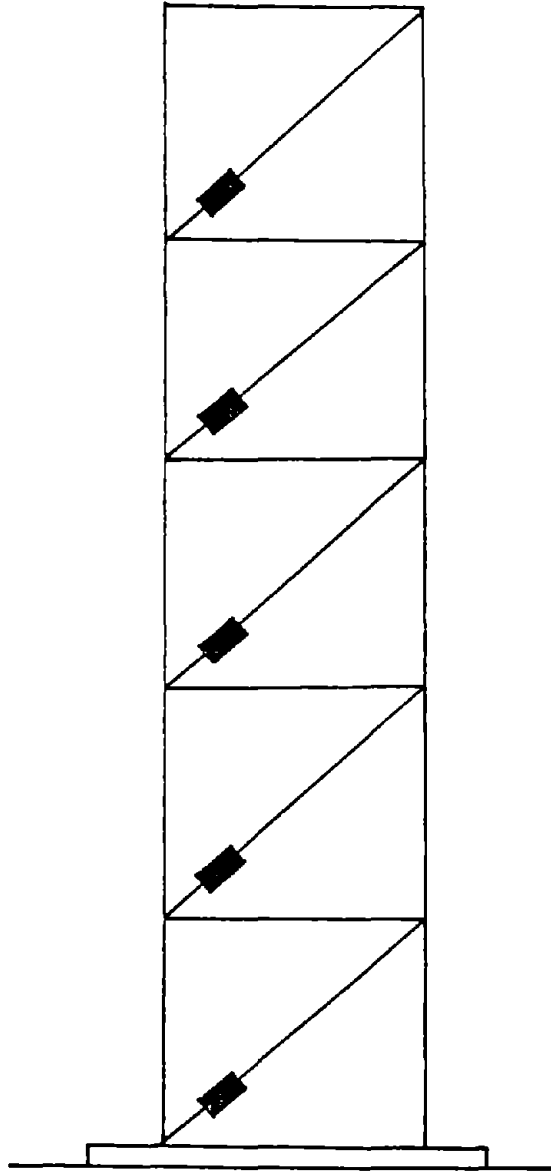
Fig. 6.2   Five-story Prototype Steel Frame with Added VE Dampers
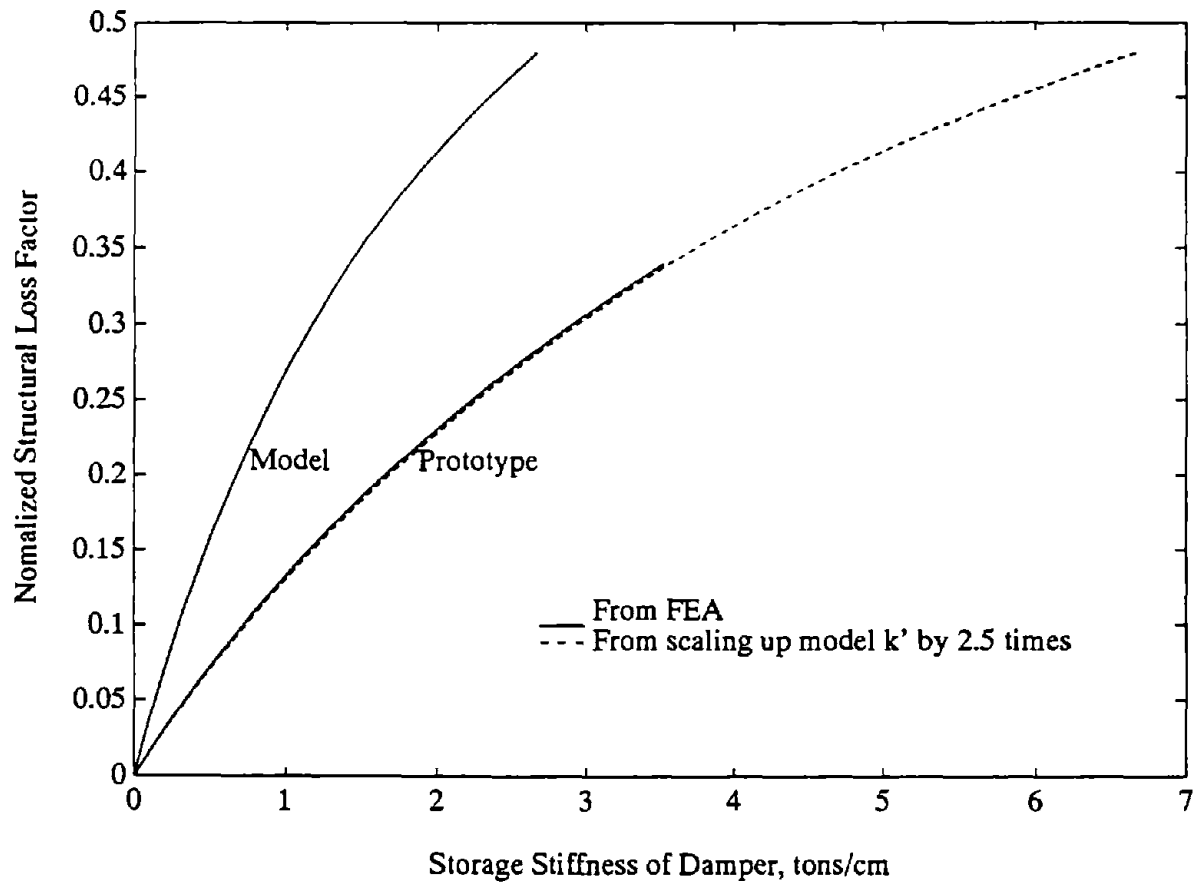
Fig. 6.3 Normalized Structural Loss Factor vs. Damper Storage Stiffness for
2/5-scale Model and Full-scale Prototype
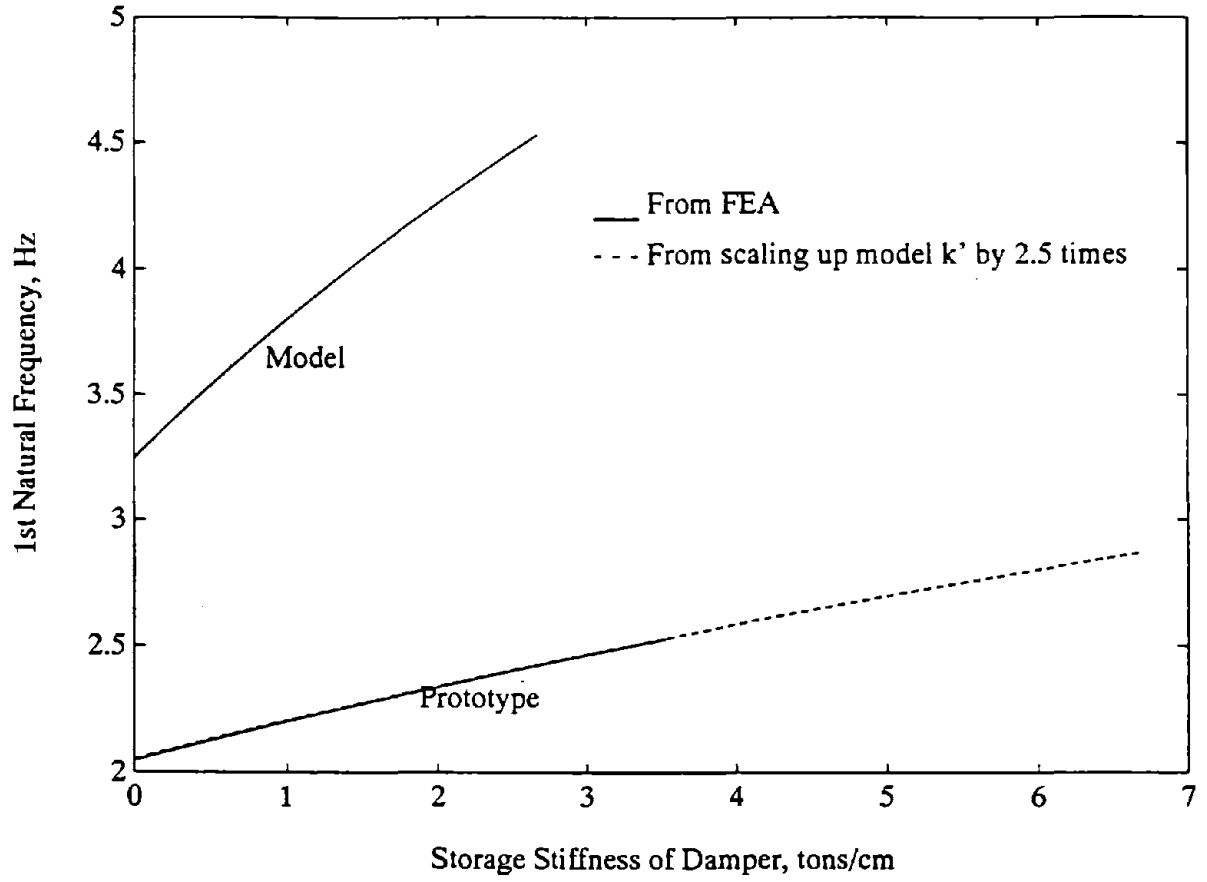
Fig. 6.4 First Natural Frequency vs. Damper Storage Stiffness for 2/5-scale Model and Full-scale Prototype

Centerplate

1.2 cm

V.E. Material

Steel Flange

8.9 cm

6.4 cm
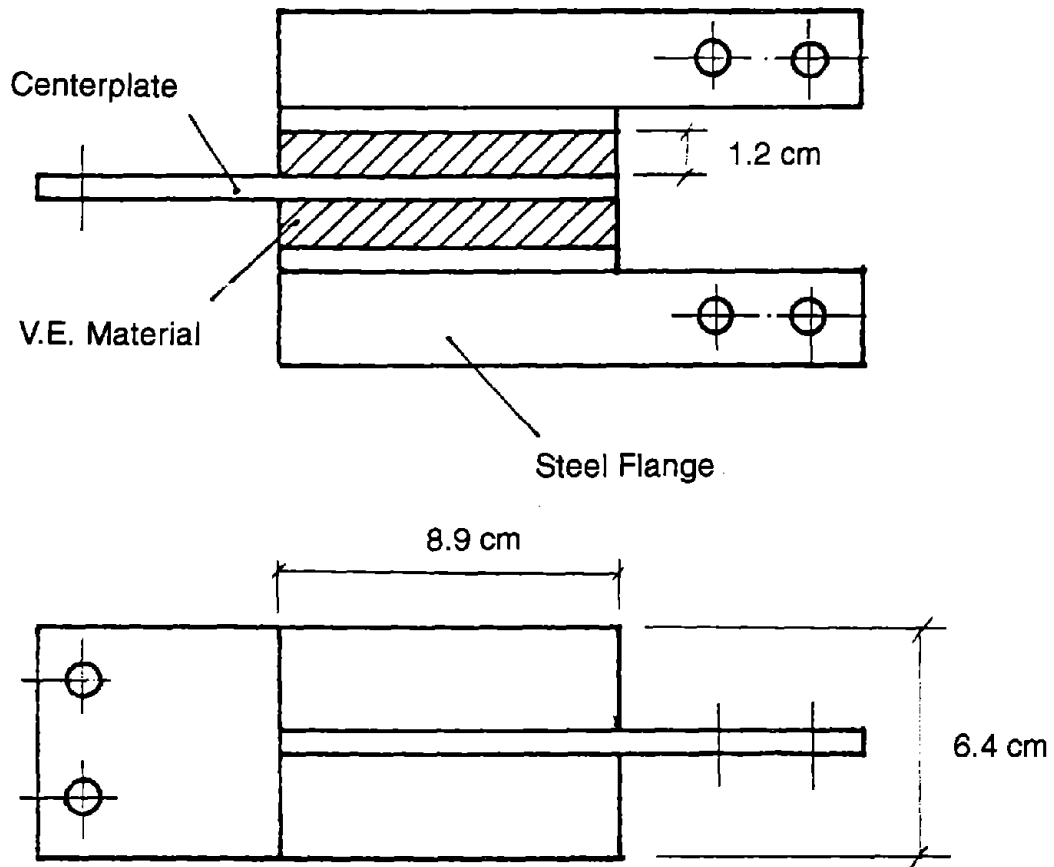
(A = 56.7 cm², Thickness = 1.2 cm)

Fig. 6.5   Viscoelastic Damper Used in Prototype Test
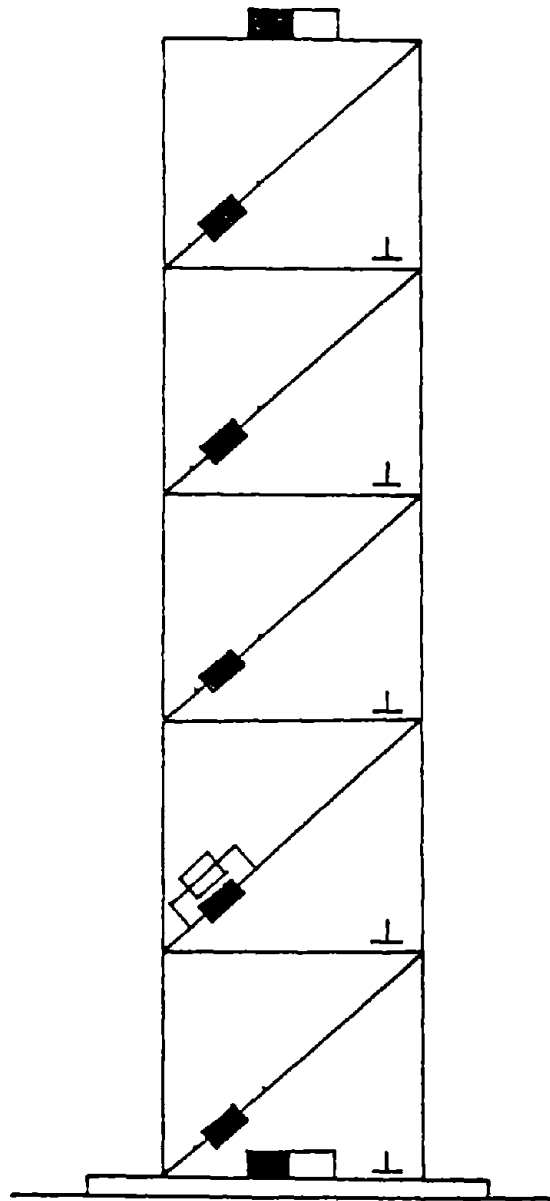
	Viscoelastic Damper
	WCY-2 Displacement Transducer
	Vibrator
⊥	W401R Accelerometer

Fig. 6.6   Test Set-up
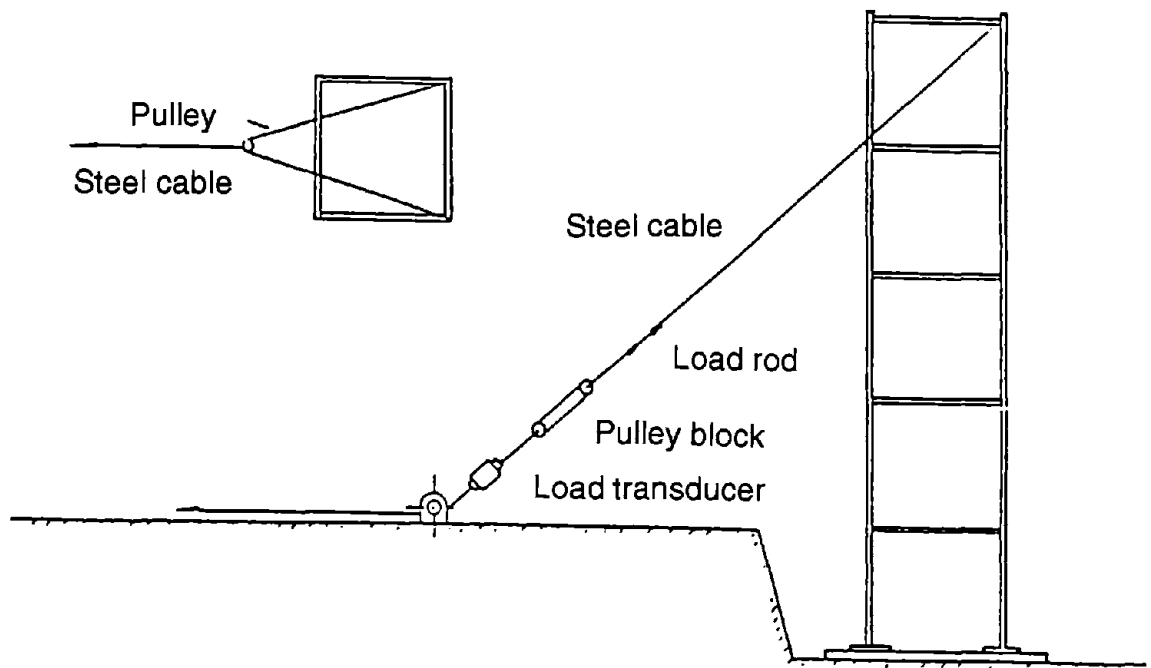
Fig. 6.7 Free Decay Test Set-up
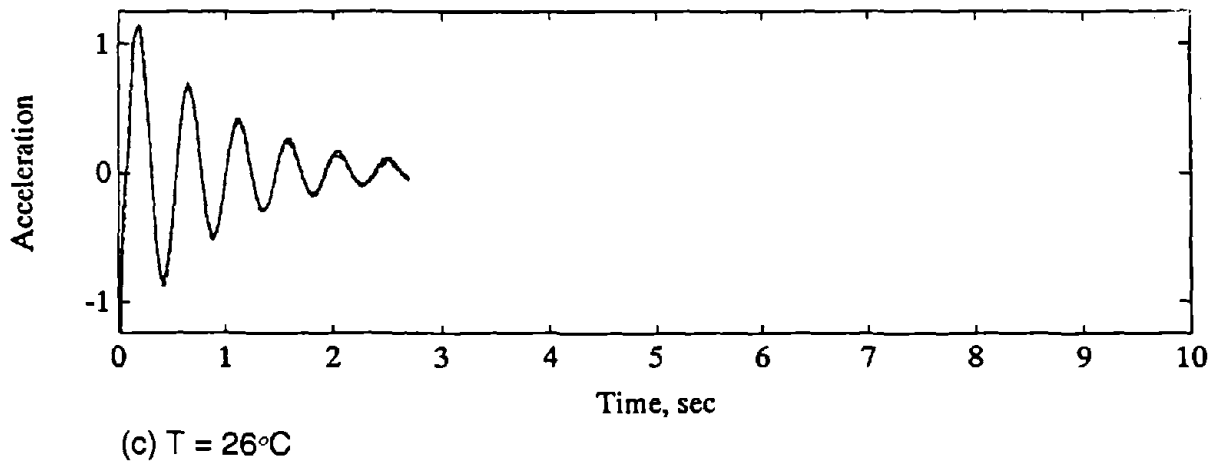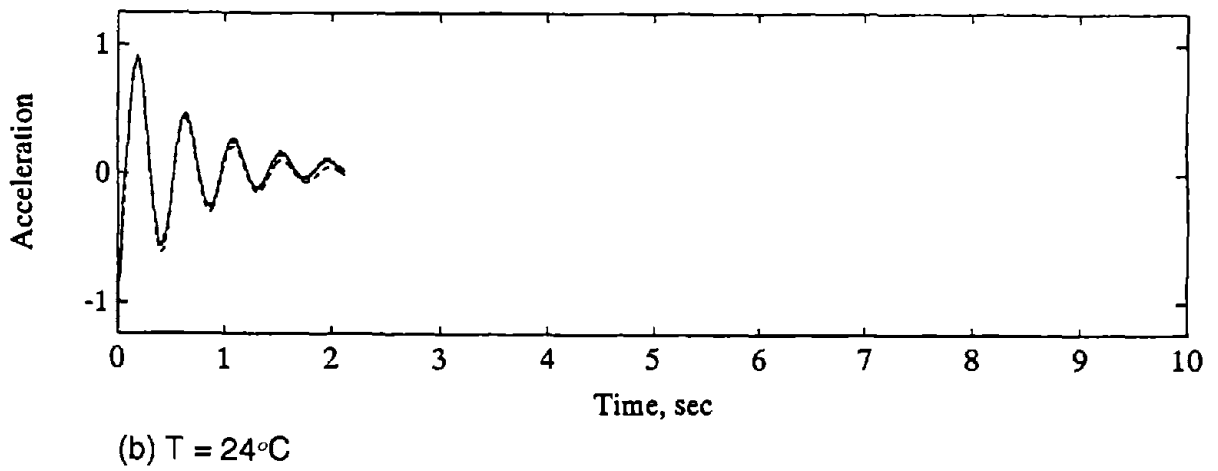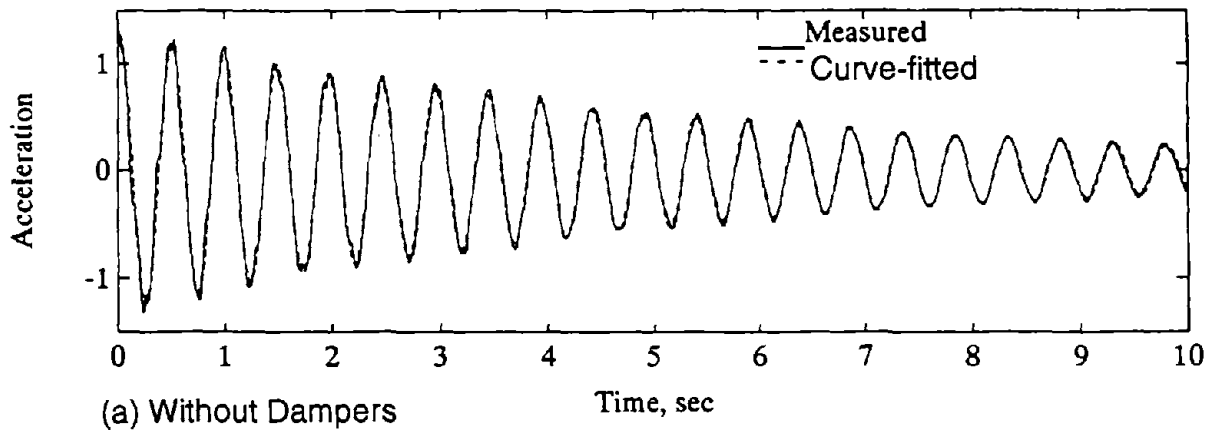
Fig. 6.8   Acceleration Responses at Different Temperatures

(d) T = 30°C

(e) T = 32°C

(f) T = 34°C
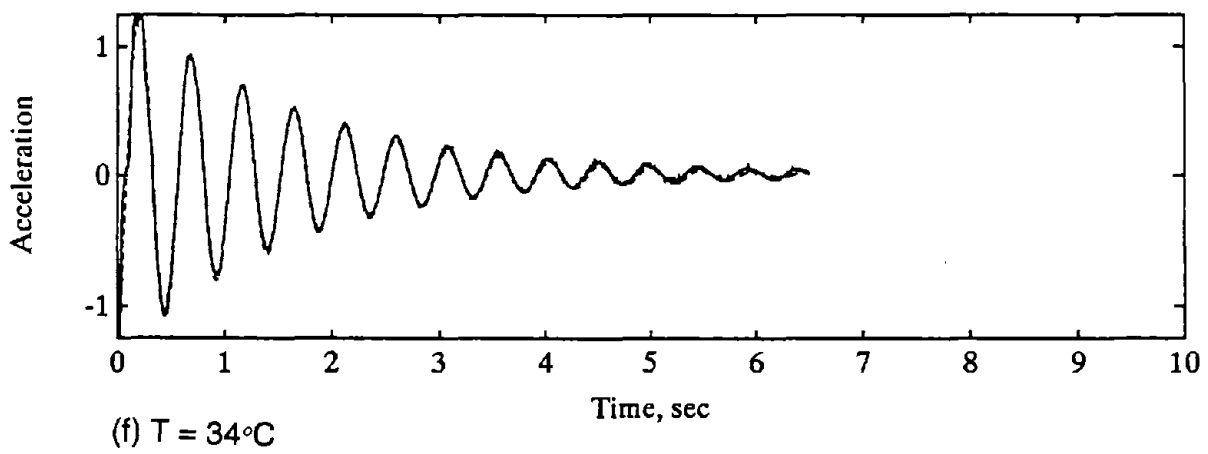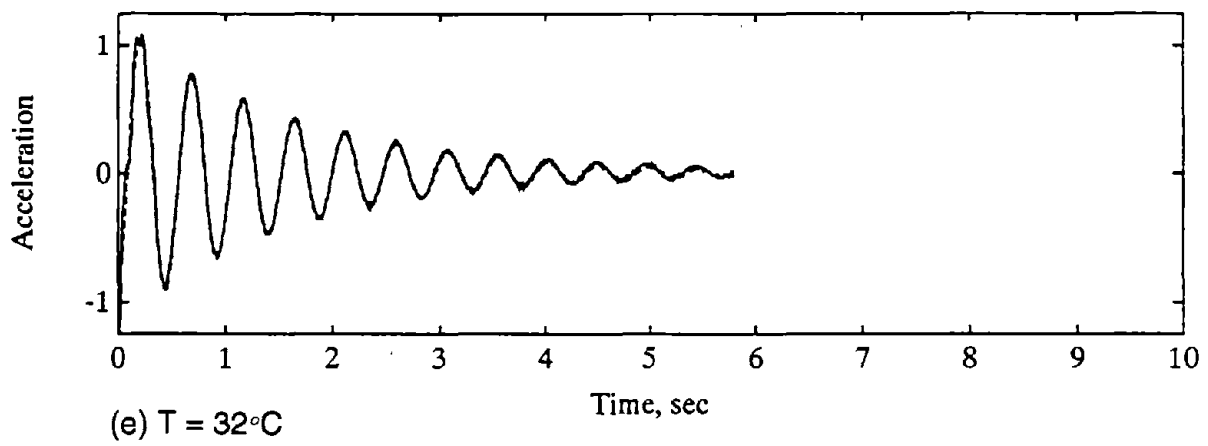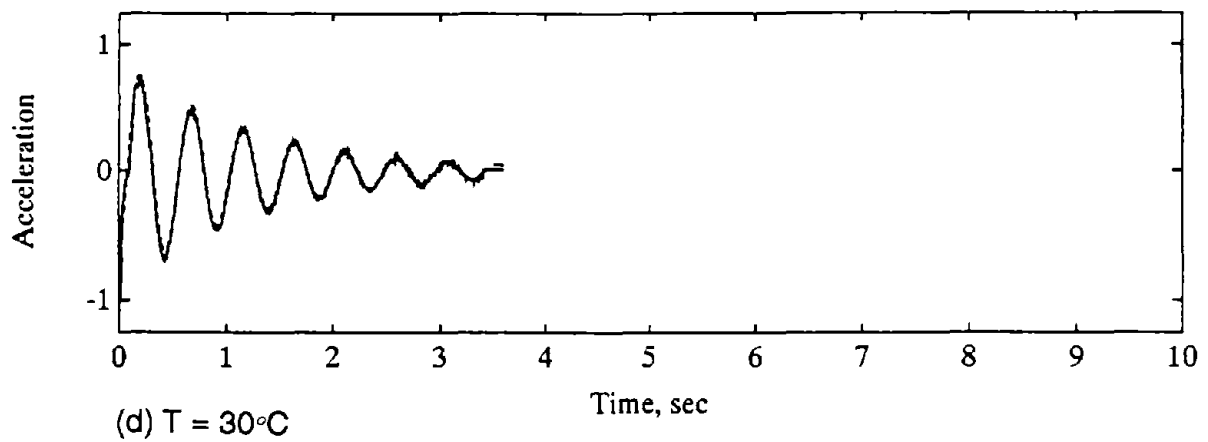
Fig. 6.8 (continued)
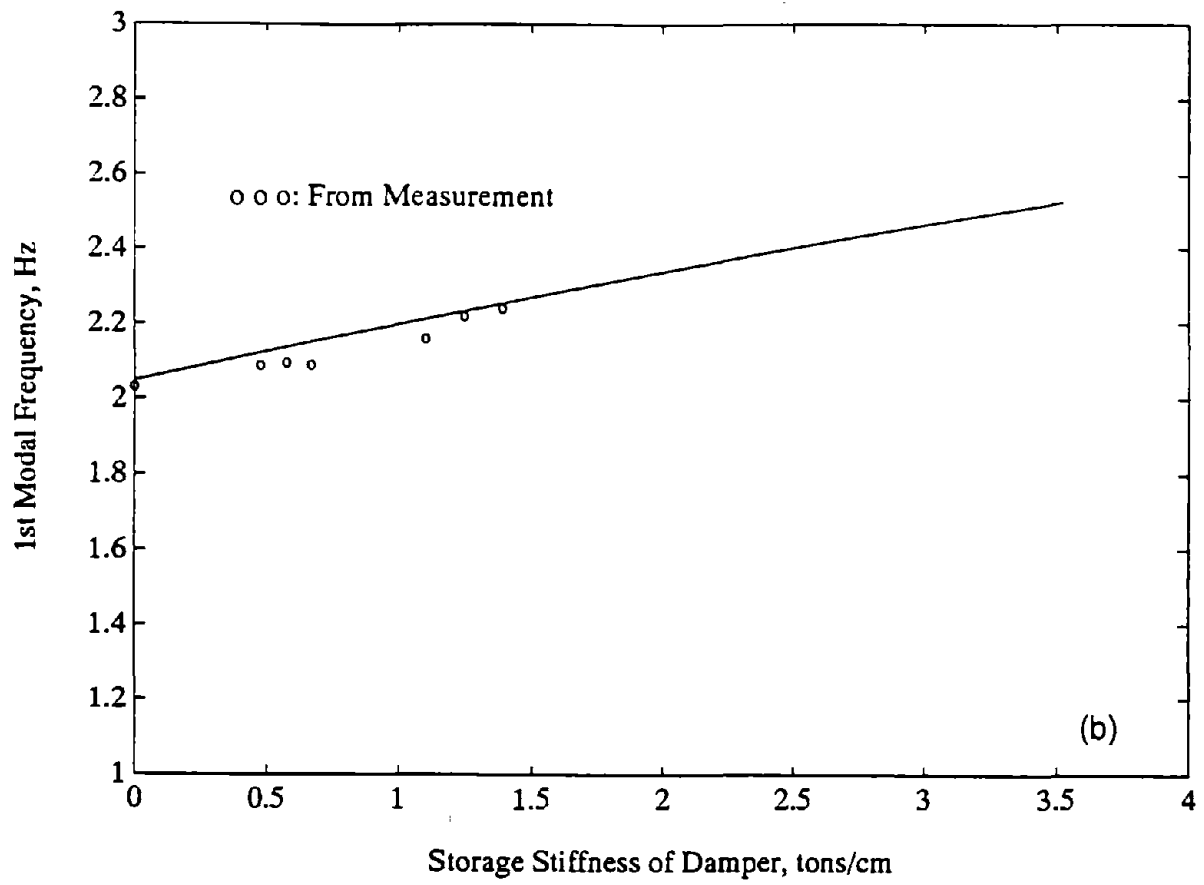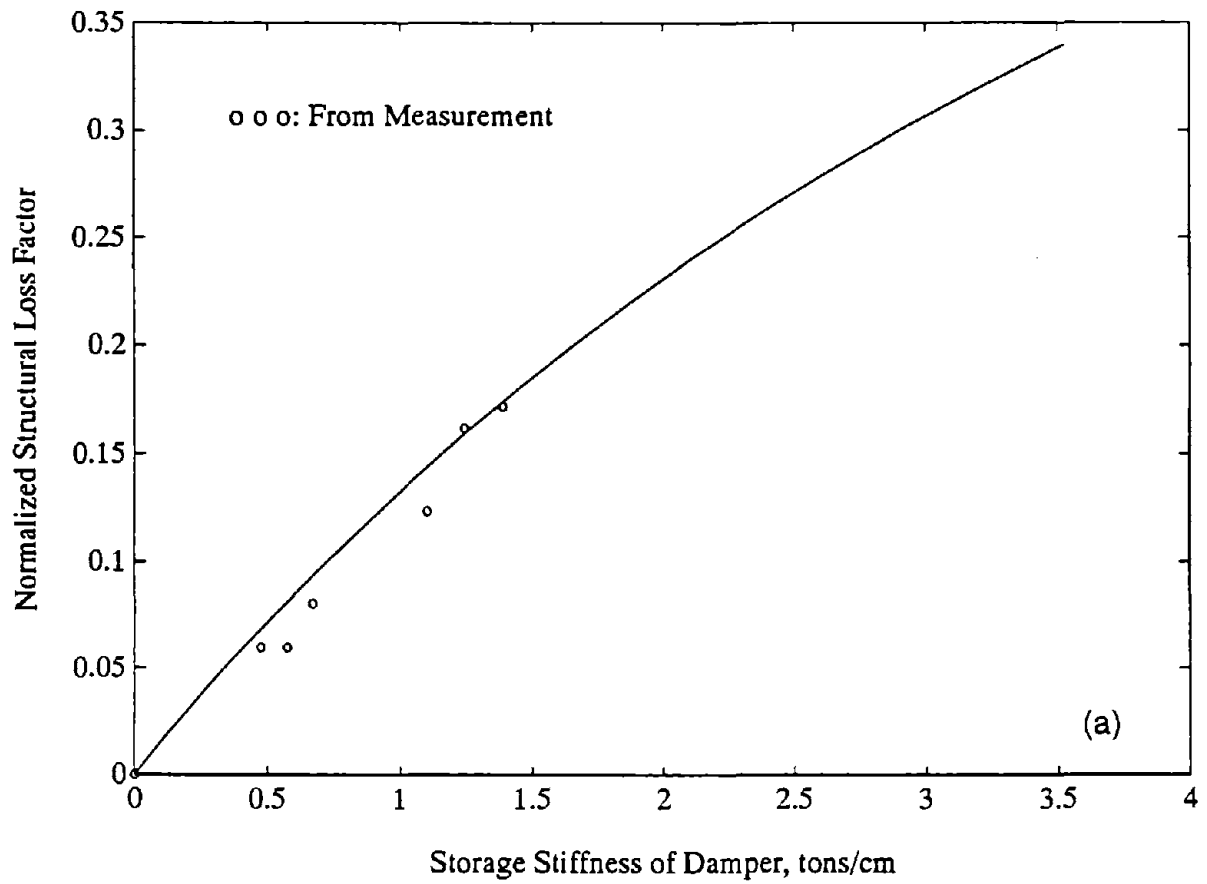
Fig. 6.9   Loss Factor and First Modal Frequency
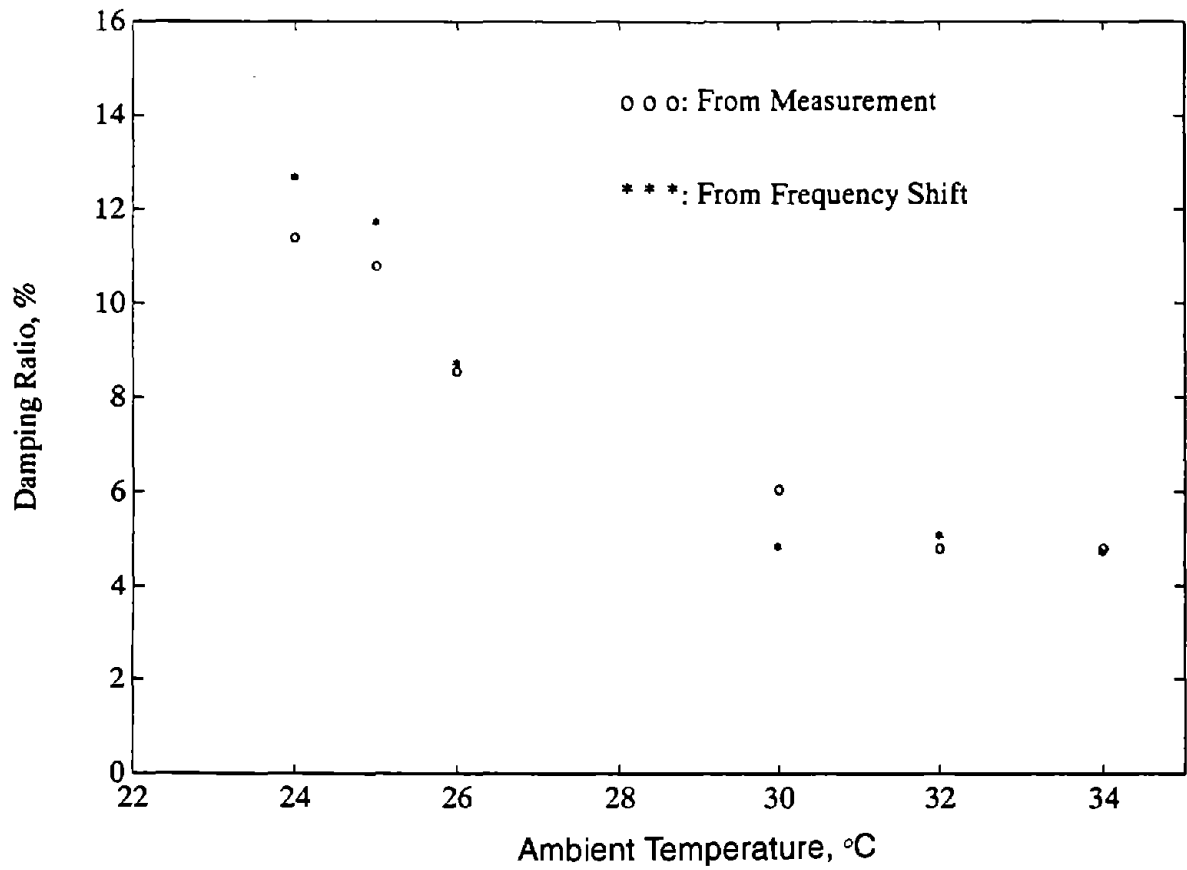
Fig. 6.10 Damping Ratios at Different Ambient Temperatures
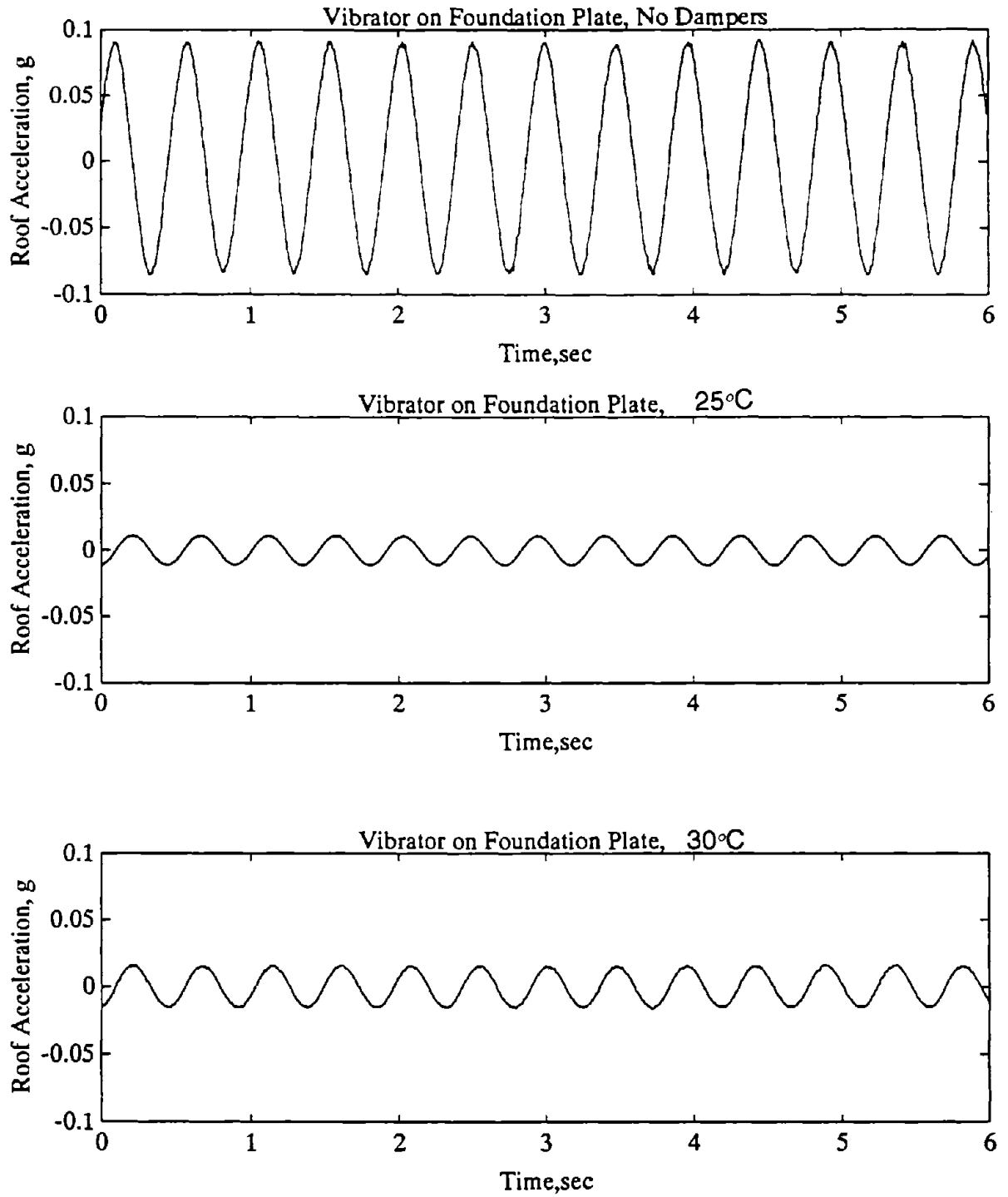
Fig. 6.11 Measured Roof Accelerations

Vibrator on Foundation
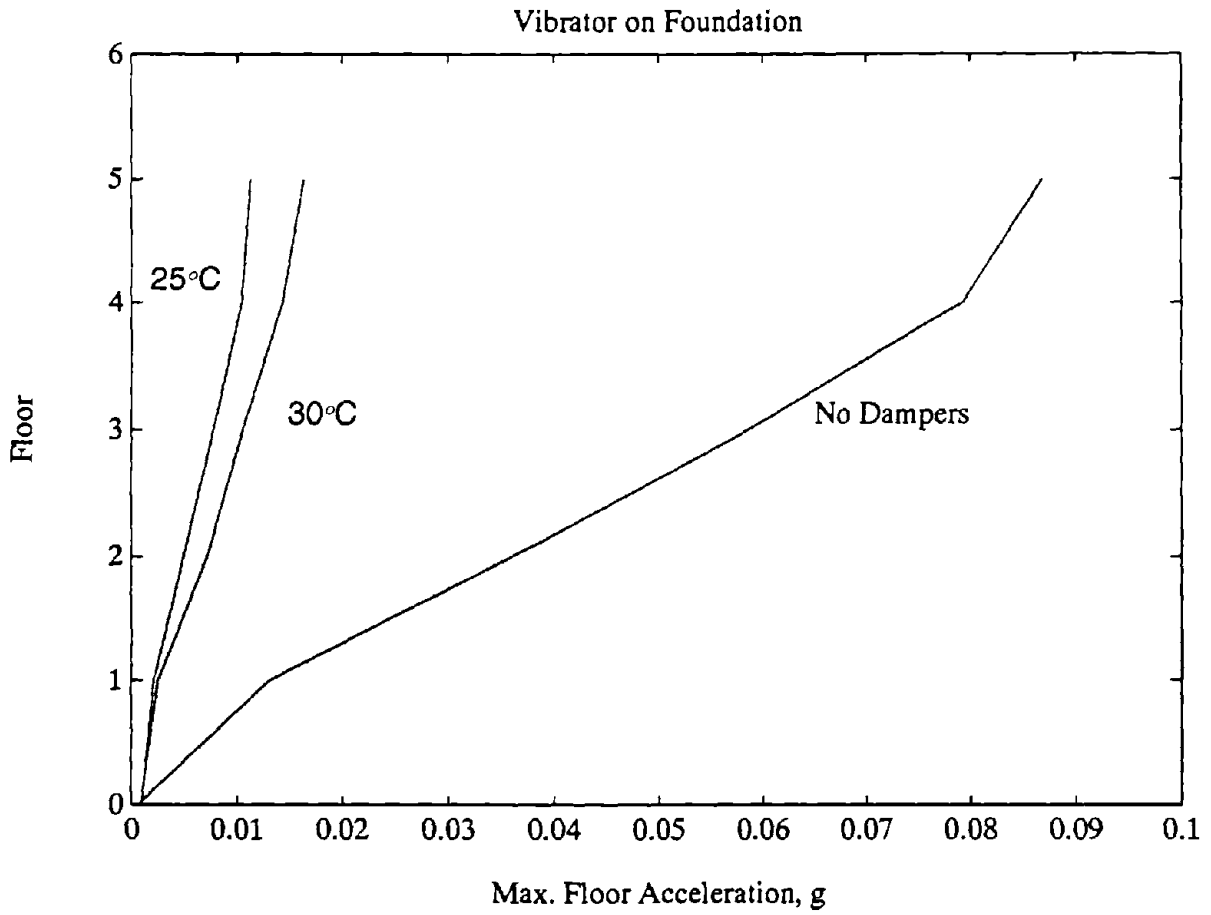
Fig. 6.12   Floor Acceleration Envelops, Vibrator on Foundation Plate
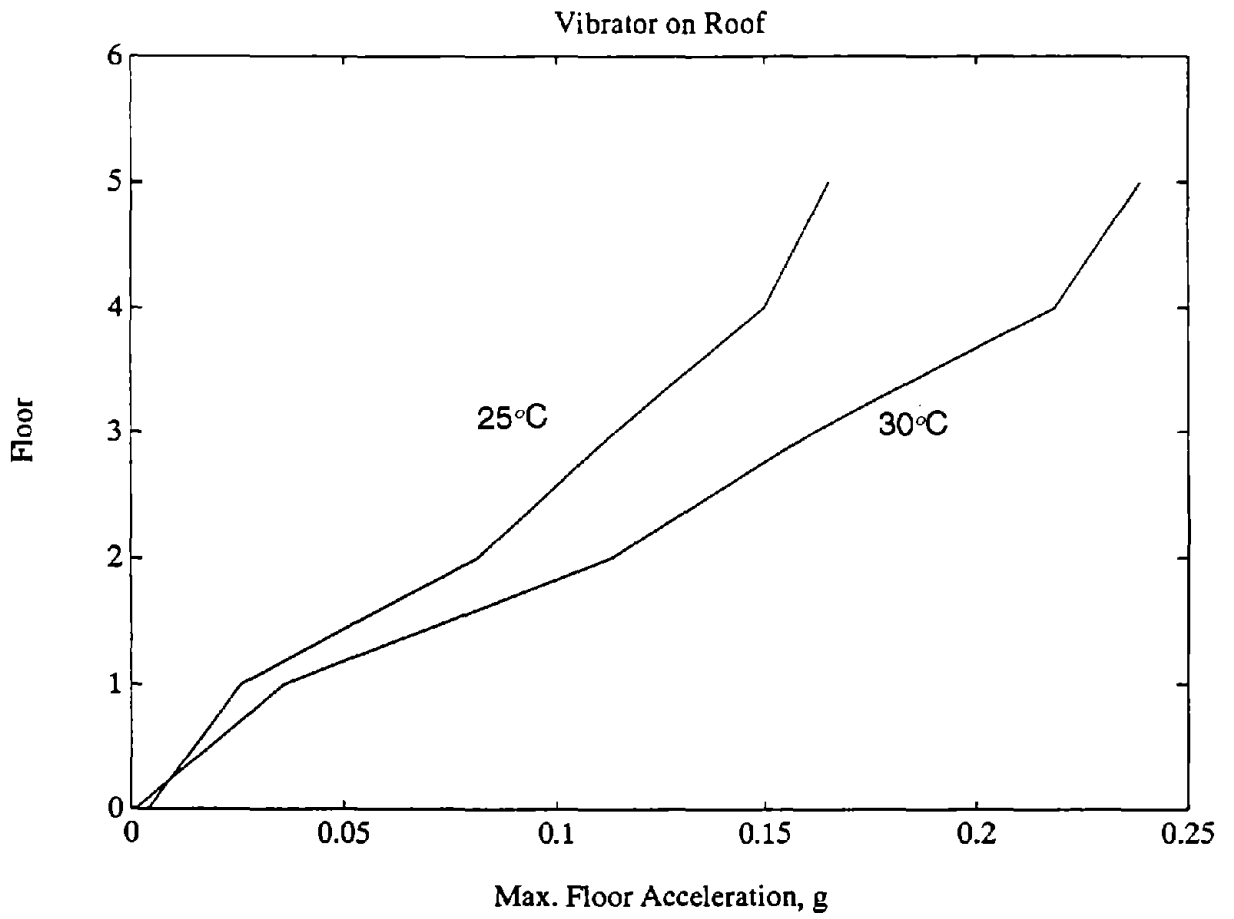
Fig. 6.13   Floor Acceleration Envelops, Vibrator on Roof
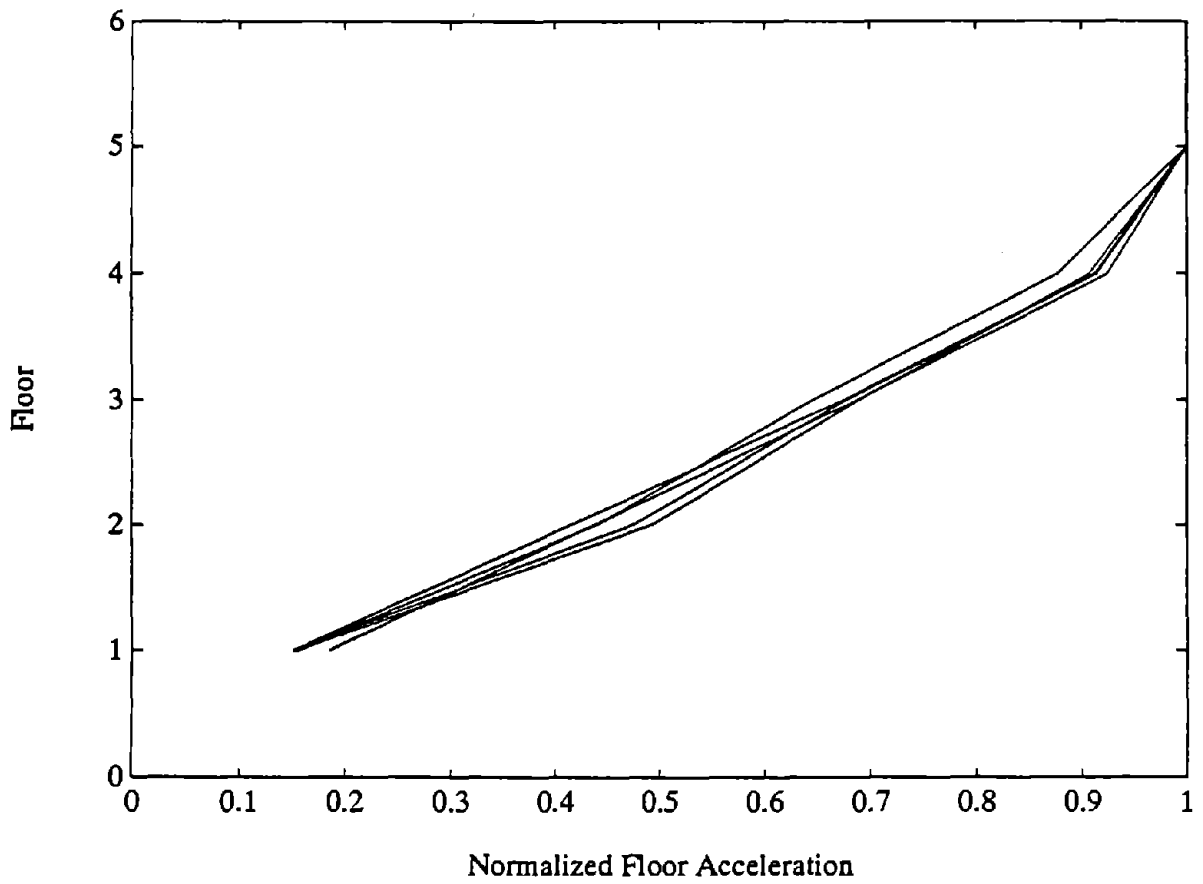
Fig. 6.14   Normalized Floor Acceleration Envelops

SECTION 7

SUMMARY

Experimental studies on the dynamic properties of viscoelastic dampers and on the seismic behavior of viscoelastically damped steel-frame structures have been carried out with three different types of dampers. The test structures are a full-scale test structure constructed in China as part of a US-China cooperative research program and a 2/5-scale model structure of this prototype fabricated at the State University of New York at Buffalo.

Test results on the effect of ambient temperature using the 2/5-scale model show that viscoelastic dampers are very effective in reducing excessive vibration of the test structure due to seismic excitations over a wide range of ambient temperatures. At 25°C, the dampers can achieve a reduction of about 80% of the maximum floor accelerations, maximum interstory drifts and maximum lateral displacements of the test structure without added dampers. At higher ambient temperatures, the viscoelastic material softens and the effectiveness of the dampers decreases. However, at temperatures as high as 42°C, the dampers could still achieve a response reduction by more than 40%. Of course, the viscoelastic dampers can be designed for higher efficiency with temperature depending on the specific temperature requirements of the application. In general, the viscoelastic dampers should be designed for the expected maximum ambient temperature to ensure adequate damping for the building.

The experimentally obtained responses of the 2/5-scale model structure with Type B dampers subjected to strong earthquakes were compared to those obtained from the inelastic analysis of the structure without added dampers. Both the analytical and experimental results clearly demonstrated the superior performance of the structure with added dampers. Under the El Centro earthquake scaled to 0.60g peak acceleration, reductions, in the lateral displacement and the interstory drift of the model structure of the order of 60% and 50%, respectively, resulted from the addition of the dampers. The reductions under the Hachinohe earthquake were slightly higher in both structural response quantities. Although the addition of dampers to the structure contributes to viscous damping as well as stiffness of the structure, it was concluded that the reduction of the seismic response resulted mostly from the increased damping effect. The amounts of temperature rise within the damper material recorded as 2.6°C and 4.5°C for the El Centro and Hachinohe earthquakes, respectively. These values are relatively high compared to

7-1

those obtained from the ambient temperature tests. However, this temperature rise has very little effect on the overall damper efficiency to dissipate seismic input energy due to strong earthquake ground motions.

Empirical equations for estimating the stiffness of each type of dampers used in this study were established based on regression analysis using data obtained from component tests of the dampers. These equations can adequately estimate the dynamic properties of the dampers under various ambient temperatures, excitation frequencies and deformations.

Numerical predictions of structural damping under various ambient temperatures, different damper locations and strong earthquake ground motions were conducted using the model strain energy method and the aforementioned empirical formulae. Numerical results show that structural damping with added dampers can be satisfactorily estimated by the modal strain energy method.

Numerical simulations were also carried out on the dynamic response of viscoelastically damped structures under seismic excitations. Comparisons between numerical simulation and test results show very good agreement.

A design procedure for structures with added viscoelastic dampers was proposed and a simple design example was provided. It is shown that this design procedure can be easily incorporated into conventional structural design procedures.

The test results obtained and the damper design procedure developed from the 2/5-scale model were verified by conducting full-scale structural tests using the prototype structure. Full-scale test results show that the measured damping ratios are in good agreement with the design values at all temperatures. It is also shown that the damper design procedure developed based on the 2/5-scale structure is applicable to the full-scale prototype. This full-scale test study provides an important link between the extensive test data obtained from the reduced scale structures and the implementation of viscoelastic dampers to full-scale structures.

SECTION 8

REFERENCES

1. Keel, C.J. and Mahmoodi. P. (1986), "Designing of Viscoelastic Dampers for Columbia Center Building," *Building Motion in Wind*, N. Isyumov and T. Tschanz (eds.)., ASCE, New York, NY.

2. Mahmoodi, P., Robertson, L.E., Yontar, M., Moy, C. and Feld, I. (1987), "Performance of Viscoelastic Dampers in World Trade Center Towers," *Dynamic of Structures, Structures Congress '87*, Orlando, FL.

3. Ashour, S.A. and Hanson, R.D. (1987), *Elastic Seismic Response of Buildings with Supplemental Damping*, Report No. UMCE 8701, The University of Michigan, Ann Arbor, MI.

4. Zhang, R.H., Soong, T.T. and Mahmoodi, P. (1989), "Seismic Response of Steel Frame Structures with Added Viscoelastic Dampers," *Earthquake Engineering and Structural Dynamics*, Vol. 18, 389-396.

5. Lin, R.C., Liang, Z., Soong, T.T. and Zhang, R.H. (1991), "An Experimental Study on Seismic Structural Response with Added Viscoelastic Dampers," *Engineering Structures,*, Vol. 13, 75-84.

6. Aiken, I.D., Kelly, J.M. and Mahmoodi, P. (1990), "The Application of Viscoelastic Dampers to Seismically Resistant Structures," *Proc. 4th US National Conference on Earthquake Engineering*, Vol. 3, 459-468.

7. Chang, K.C., Soong, T.T., Oh, S-T. and Lai, M.L. (1992), "Effect of Ambient Temperature on a Viscoelastically Damped Structure," *ASCE Journal of Structural Engineering*, Vol. 118(7), 1955-1973.

8. Oh, Soon-Taek (1992), *Seismic Behavior of a 2/5-Scale Steel Structure with Added Viscoelastic Dampers*, Ph.D. Dissertation, Department of Civil Engineering, State University of New York at Buffalo, Buffalo, NY.

9. Johnson, C.D. and Kienholz, D.A. (1982), "Finite Element Prediction of Damping in Structures with Constrained Viscoelastic Layers," *AIAA Journal*, Vol. 20(9), 1284-1290.

10. Soong, T.T. and Lai, M.L. (1991), "Correlation of Experimental Results with Predictions of Viscoelastic Damping for a Model Structure," *Proc. Damping '91*, San Diego, CA.

11. Oh, S-T., Chang, K.C., Lai, M.L. and Nielsen, E.J. (1992), "Seismic Behavior of Viscoelastically Damped Structure under Strong Earthquake Ground Motions," *Proc. 10WCEE*, Madrid, Spain.

12. Kasai, K., Munshi, J.A., Lai, M.L. and Maison, B.F. (1993), "Viscoelastic Damper Hysteretic Model: Theory, Experiment and Application," *Proc. ATC-17-1*, Vol. 2, 521-532.

13. Lee, H.H. and Tsai C-S., (1992), "Analytical Model for Viscoelastic Dampers to Jointed Structures for Seismic Mitigation," *Proc. 10WCEE*, Madrid, Spain.

14. Chang, K.C., Soong, T.T., Lai, M.L. and Nielsen, E.J. (1993), "Development of a Design Procedure for Structures with Added Viscoelastic Dampers," *Proc. ATC-17-1*, Vol. 2, 473-484.

15. Chang, K.C., Yao, G.C., Lee, G.C., Hao, D.S. and Yeh, Y.C. (1991), *Dynamic Characteristics of a Full Size Five Story Steel Structure and a 2/5 Scale Model*, Technical Report NCEER-91-0011, State University of New York at Buffalo, Buffalo, NY.

16. Hwang, J.S., Chang, K.C. and Lee, G.C. (1987), *The System Characteristics and Performance of a Shaking Table*, Technical Report NCEER-87-0004, State University of New York at Buffalo, Buffalo, NY.

17. Kanaan, A.E. and Powell, G.H. (1973), *Drain-2D - A General Purpose Computer Program for Dynamic Analysis of Inelastic Plane Structures*, Report No. UCB/EERC 73-06, University of California, Berkeley, CA.

18. Zhang, R.H. and Soong, T.T. (1992), "Seismic Design of Viscoelastic Dampers for Structural Applications," *ASCE Journal of Structural Engineering*, Vol. 118(5), 1375-1392.

19. Hao, D.S., Li, G.J. and Jin, Y.Q. (1980), "Development of QZJ-1 Synchronous Excitors," *Chinese Civil Engineering*, Vol. 9, 8-11.

20. China Academy of Building Research (1983), "Development of TQJ-4 Synchronous Excitors," *Report of Building Research*, 25.

21. Kasai, K. and Lai, M.L. (1994), "Finding of Temperature-Insensitive Viscoelastic Frames," *5th National Conference on Earthquake Engineering*, Chicago, July 10-14.

22. Chang, K.C., Shen, K.L., Soong, T.T. and Lai, M.L. (1994), "Seismic Retrofit of a Concrete Frame with Added Viscoelastic Dampers," *5th National Conference on Earthquake Engineering*, Chicago, July 10-14.

NATIONAL CENTER FOR EARTHQUAKE ENGINEERING RESEARCH
LIST OF TECHNICAL REPORTS

The National Center for Earthquake Engineering Research (NCEER) publishes technical reports on a variety of subjects related to earthquake engineering written by authors funded through NCEER. These reports are available from both NCEER's Publications Department and the National Technical Information Service (NTIS). Requests for reports should be directed to the Publications Department, National Center for Earthquake Engineering Research, State University of New York at Buffalo, Red Jacket Quadrangle, Buffalo, New York 14261. Reports can also be requested through NTIS, 5285 Port Royal Road, Springfield, Virginia 22161. NTIS accession numbers are shown in parenthesis, if available.

NCEER-87-0001　"First-Year Program in Research, Education and Technology Transfer," 3/5/87, (PB88-134275).

NCEER-87-0002　"Experimental Evaluation of Instantaneous Optimal Algorithms for Structural Control," by R.C. Lin, T.T. Soong and A.M. Reinhorn, 4/20/87, (PB88-134341).

NCEER-87-0003　"Experimentation Using the Earthquake Simulation Facilities at University at Buffalo," by A.M. Reinhorn and R.L. Ketter, to be published.

NCEER-87-0004　"The System Characteristics and Performance of a Shaking Table," by J.S. Hwang, K.C. Chang and G.C. Lee, 6/1/87, (PB88-134259). This report is available only through NTIS (see address given above).

NCEER-87-0005　"A Finite Element Formulation for Nonlinear Viscoplastic Material Using a Q Model," by O. Gyebi and G. Dasgupta, 11/2/87, (PB88-213764).

NCEER-87-0006　"Symbolic Manipulation Program (SMP) - Algebraic Codes for Two and Three Dimensional Finite Element Formulations," by X. Lee and G. Dasgupta, 11/9/87, (PB88-218522).

NCEER-87-0007　"Instantaneous Optimal Control Laws for Tall Buildings Under Seismic Excitations," by J.N. Yang, A. Akbarpour and P. Ghaemmaghami, 6/10/87, (PB88-134333). This report is only available through NTIS (see address given above).

NCEER-87-0008　"IDARC: Inelastic Damage Analysis of Reinforced Concrete Frame - Shear-Wall Structures," by Y.J. Park, A.M. Reinhorn and S.K. Kunnath, 7/20/87, (PB88-134325).

NCEER-87-0009　"Liquefaction Potential for New York State: A Preliminary Report on Sites in Manhattan and Buffalo," by M. Budhu, V. Vijayakumar, R.F. Giese and L. Baumgras, 8/31/87, (PB88-163704). This report is available only through NTIS (see address given above).

NCEER-87-0010　"Vertical and Torsional Vibration of Foundations in Inhomogeneous Media," by A.S. Veletsos and K.W. Dotson, 6/1/87, (PB88-134291).

NCEER-87-0011　"Seismic Probabilistic Risk Assessment and Seismic Margins Studies for Nuclear Power Plants," by Howard H.M. Hwang, 6/15/87, (PB88-134267).

NCEER-87-0012　"Parametric Studies of Frequency Response of Secondary Systems Under Ground-Acceleration Excitations," by Y. Yong and Y.K. Lin, 6/10/87, (PB88-134309).

NCEER-87-0013　"Frequency Response of Secondary Systems Under Seismic Excitation," by J.A. HoLung, J. Cai and Y.K. Lin, 7/31/87, (PB88-134317).

NCEER-87-0014　"Modelling Earthquake Ground Motions in Seismically Active Regions Using Parametric Time Series Methods," by G.W. Ellis and A.S. Cakmak, 8/25/87, (PB88-134283).

NCEER-87-0015　"Detection and Assessment of Seismic Structural Damage," by E. DiPasquale and A.S. Cakmak, 8/25/87, (PB88-163712).

A-1

Preceding page blank

NCEER-87-0016 "Pipeline Experiment at Parkfield, California," by J. Isenberg and E. Richardson, 9/15/87, (PB88-163720). This report is available only through NTIS (see address given above).

NCEER-87-0017 "Digital Simulation of Seismic Ground Motion," by M. Shinozuka, G. Deodatis and T. Harada, 8/31/87, (PB88-155197). This report is available only through NTIS (see address given above).

NCEER-87-0018 "Practical Considerations for Structural Control: System Uncertainty, System Time Delay and Truncation of Small Control Forces," J.N. Yang and A. Akbarpour, 8/10/87, (PB88-163738).

NCEER-87-0019 "Modal Analysis of Nonclassically Damped Structural Systems Using Canonical Transformation," by J.N. Yang, S. Sarkani and F.X. Long, 9/27/87, (PB88-187851).

NCEER-87-0020 "A Nonstationary Solution in Random Vibration Theory," by J.R. Red-Horse and P.D. Spanos, 11/3/87, (PB88-163746).

NCEER-87-0021 "Horizontal Impedances for Radially Inhomogeneous Viscoelastic Soil Layers," by A.S. Veletsos and K.W. Dotson, 10/15/87, (PB88-150859).

NCEER-87-0022 "Seismic Damage Assessment of Reinforced Concrete Members," by Y.S. Chung, C. Meyer and M. Shinozuka, 10/9/87, (PB88-150867). This report is available only through NTIS (see address given above).

NCEER-87-0023 "Active Structural Control in Civil Engineering," by T.T. Soong, 11/11/87, (PB88-187778).

NCEER-87-0024 "Vertical and Torsional Impedances for Radially Inhomogeneous Viscoelastic Soil Layers," by K.W. Dotson and A.S. Veletsos, 12/87, (PB88-187786).

NCEER-87-0025 "Proceedings from the Symposium on Seismic Hazards, Ground Motions, Soil-Liquefaction and Engineering Practice in Eastern North America," October 20-22, 1987, edited by K.H. Jacob, 12/87, (PB88-188115).

NCEER-87-0026 "Report on the Whittier-Narrows, California, Earthquake of October 1, 1987," by J. Pantelic and A. Reinhorn, 11/87, (PB88-187752). This report is available only through NTIS (see address given above).

NCEER-87-0027 "Design of a Modular Program for Transient Nonlinear Analysis of Large 3-D Building Structures," by S. Srivastav and J.F. Abel, 12/30/87, (PB88-187950).

NCEER-87-0028 "Second-Year Program in Research, Education and Technology Transfer," 3/8/88, (PB88-219480).

NCEER-88-0001 "Workshop on Seismic Computer Analysis and Design of Buildings With Interactive Graphics," by W. McGuire, J.F. Abel and C.H. Conley, 1/18/88, (PB88-187760).

NCEER-88-0002 "Optimal Control of Nonlinear Flexible Structures," by J.N. Yang, F.X. Long and D. Wong, 1/22/88, (PB88-213772).

NCEER-88-0003 "Substructuring Techniques in the Time Domain for Primary-Secondary Structural Systems," by G.D. Manolis and G. Juhn, 2/10/88, (PB88-213780).

NCEER-88-0004 "Iterative Seismic Analysis of Primary-Secondary Systems," by A. Singhal, L.D. Lutes and P.D. Spanos, 2/23/88, (PB88-213798).

NCEER-88-0005 "Stochastic Finite Element Expansion for Random Media," by P.D. Spanos and R. Ghanem, 3/14/88, (PB88-213806).

A-2

NCEER-88-0006   "Combining Structural Optimization and Structural Control," by F.Y. Cheng and C.P. Pantelides, 1/10/88, (PB88-213814).

NCEER-88-0007   "Seismic Performance Assessment of Code-Designed Structures," by H.H-M. Hwang, J-W. Jaw and H-J. Shau, 3/20/88, (PB88-219423).

NCEER-88-0008   "Reliability Analysis of Code-Designed Structures Under Natural Hazards," by H.H-M. Hwang, H. Ushiba and M. Shinozuka, 2/29/88, (PB88-229471).

NCEER-88-0009   "Seismic Fragility Analysis of Shear Wall Structures," by J-W Jaw and H.H-M. Hwang, 4/30/88, (PB89-102867).

NCEER-88-0010   "Base Isolation of a Multi-Story Building Under a Harmonic Ground Motion - A Comparison of Performances of Various Systems," by F-G Fan, G. Ahmadi and I.G. Tadjbakhsh, 5/18/88, (PB89-122238).

NCEER-88-0011   "Seismic Floor Response Spectra for a Combined System by Green's Functions," by F.M. Lavelle, L.A. Bergman and P.D. Spanos, 5/1/88, (PB89-102875).

NCEER-88-0012   "A New Solution Technique for Randomly Excited Hysteretic Structures," by G.Q. Cai and Y.K. Lin, 5/16/88, (PB89-102883).

NCEER-88-0013   "A Study of Radiation Damping and Soil-Structure Interaction Effects in the Centrifuge," by K. Weissman, supervised by J.H. Prevost, 5/24/88, (PB89-144703).

NCEER-88-0014   "Parameter Identification and Implementation of a Kinematic Plasticity Model for Frictional Soils," by J.H. Prevost and D.V. Griffiths, to be published.

NCEER-88-0015   "Two- and Three- Dimensional Dynamic Finite Element Analyses of the Long Valley Dam," by D.V. Griffiths and J.H. Prevost, 6/17/88, (PB89-144711).

NCEER-88-0016   "Damage Assessment of Reinforced Concrete Structures in Eastern United States," by A.M. Reinhorn, M.J. Seidel, S.K. Kunnath and Y.J. Park, 6/15/88, (PB89-122220).

NCEER-88-0017   "Dynamic Compliance of Vertically Loaded Strip Foundations in Multilayered Viscoelastic Soils," by S. Ahmad and A.S.M. Israil, 6/17/88, (PB89-102891).

NCEER-88-0018   "An Experimental Study of Seismic Structural Response With Added Viscoelastic Dampers," by R.C. Lin, Z. Liang, T.T. Soong and R.H. Zhang, 6/30/88, (PB89-122212). This report is available only through NTIS (see address given above).

NCEER-88-0019   "Experimental Investigation of Primary - Secondary System Interaction," by G.D. Manolis, G. Juhn and A.M. Reinhorn, 5/27/88, (PB89-122204).

NCEER-88-0020   "A Response Spectrum Approach For Analysis of Nonclassically Damped Structures," by J.N. Yang, S. Sarkani and F.X. Long, 4/22/88, (PB89-102909).

NCEER-88-0021   "Seismic Interaction of Structures and Soils: Stochastic Approach," by A.S. Veletsos and A.M. Prasad, 7/21/88, (PB89-122196).

NCEER-88-0022   "Identification of the Serviceability Limit State and Detection of Seismic Structural Damage," by E. DiPasquale and A.S. Cakmak, 6/15/88, (PB89-122188). This report is available only through NTIS (see address given above).

NCEER-88-0023   "Multi-Hazard Risk Analysis: Case of a Simple Offshore Structure," by B.K. Bhartia and E.H. Vanmarcke, 7/21/88, (PB89-145213).

A-3

NCEER-88-0024   "Automated Seismic Design of Reinforced Concrete Buildings," by Y.S. Chung, C. Meyer and M. Shinozuka, 7/5/88, (PB89-122170). This report is available only through NTIS (see address given above).

NCEER-88-0025   "Experimental Study of Active Control of MDOF Structures Under Seismic Excitations," by L.L. Chung, R.C. Lin, T.T. Soong and A.M. Reinhorn, 7/10/88, (PB89-122600).

NCEER-88-0026   "Earthquake Simulation Tests of a Low-Rise Metal Structure," by J.S. Hwang, K.C. Chang, G.C. Lee and R.L. Ketter, 8/1/88, (PB89-102917).

NCEER-88-0027   "Systems Study of Urban Response and Reconstruction Due to Catastrophic Earthquakes," by F. Kozin and H.K. Zhou, 9/22/88, (PB90-162348).

NCEER-88-0028   "Seismic Fragility Analysis of Plane Frame Structures," by H.H-M. Hwang and Y.K. Low, 7/31/88, (PB89-131445).

NCEER-88-0029   "Response Analysis of Stochastic Structures," by A. Kardara, C. Bucher and M. Shinozuka, 9/22/88, (PB89-174429).

NCEER-88-0030   "Nonnormal Accelerations Due to Yielding in a Primary Structure," by D.C.K. Chen and L.D. Lutes, 9/19/88, (PB89-131437).

NCEER-88-0031   "Design Approaches for Soil-Structure Interaction," by A.S. Veletsos, A.M. Prasad and Y. Tang, 12/30/88, (PB89-174437). This report is available only through NTIS (see address given above).

NCEER-88-0032   "A Re-evaluation of Design Spectra for Seismic Damage Control," by C.J. Turkstra and A.G. Tallin, 11/7/88, (PB89-145221).

NCEER-88-0033   "The Behavior and Design of Noncontact Lap Splices Subjected to Repeated Inelastic Tensile Loading," by V.E. Sagan, P. Gergely and R.N. White, 12/8/88, (PB89-163737).

NCEER-88-0034   "Seismic Response of Pile Foundations," by S.M. Mamoon, P.K. Banerjee and S. Ahmad, 11/1/88, (PB89-145239).

NCEER-88-0035   "Modeling of R/C Building Structures With Flexible Floor Diaphragms (IDARC2)," by A.M. Reinhorn, S.K. Kunnath and N. Panahshahi, 9/7/88, (PB89-207153).

NCEER-88-0036   "Solution of the Dam-Reservoir Interaction Problem Using a Combination of FEM, BEM with Particular Integrals, Modal Analysis, and Substructuring," by C-S. Tsai, G.C. Lee and R.L. Ketter, 12/31/88, (PB89-207146).

NCEER-88-0037   "Optimal Placement of Actuators for Structural Control," by F.Y. Cheng and C.P. Pantelides, 8/15/88, (PB89-162846).

NCEER-88-0038   "Teflon Bearings in Aseismic Base Isolation: Experimental Studies and Mathematical Modeling," by A. Mokha, M.C. Constantinou and A.M. Reinhorn, 12/5/88, (PB89-218457). This report is available only through NTIS (see address given above).

NCEER-88-0039   "Seismic Behavior of Flat Slab High-Rise Buildings in the New York City Area," by P. Weidlinger and M. Ettouney, 10/15/88, (PB90-145681).

NCEER-88-0040   "Evaluation of the Earthquake Resistance of Existing Buildings in New York City," by P. Weidlinger and M. Ettouney, 10/15/88, to be published.

NCEER-88-0041   "Small-Scale Modeling Techniques for Reinforced Concrete Structures Subjected to Seismic Loads," by W. Kim, A. El-Attar and R.N. White, 11/22/88, (PB89-189625).

NCEER-88-0042 "Modeling Strong Ground Motion from Multiple Event Earthquakes," by G.W. Ellis and A.S. Cakmak, 10/15/88, (PB89-174445).

NCEER-88-0043 "Nonstationary Models of Seismic Ground Acceleration," by M. Grigoriu, S.E. Ruiz and E. Rosenblueth, 7/15/88, (PB89-189617).

NCEER-88-0044 "SARCF User's Guide: Seismic Analysis of Reinforced Concrete Frames," by Y.S. Chung, C. Meyer and M. Shinozuka, 11/9/88, (PB89-174452).

NCEER-88-0045 "First Expert Panel Meeting on Disaster Research and Planning," edited by J. Pantelic and J. Stoyle, 9/15/88, (PB89-174460).

NCEER-88-0046 "Preliminary Studies of the Effect of Degrading Infill Walls on the Nonlinear Seismic Response of Steel Frames," by C.Z. Chrysostomou, P. Gergely and J.F. Abel, 12/19/88, (PB89-208383).

NCEER-88-0047 "Reinforced Concrete Frame Component Testing Facility - Design, Construction, Instrumentation and Operation," by S.P. Pessiki, C. Conley, T. Bond, P. Gergely and R.N. White, 12/16/88, (PB89-174478).

NCEER-89-0001 "Effects of Protective Cushion and Soil Compliancy on the Response of Equipment Within a Seismically Excited Building," by J.A. HoLung, 2/16/89, (PB89-207179).

NCEER-89-0002 "Statistical Evaluation of Response Modification Factors for Reinforced Concrete Structures," by H.H-M. Hwang and J-W. Jaw, 2/17/89, (PB89-207187).

NCEER-89-0003 "Hysteretic Columns Under Random Excitation," by G-Q. Cai and Y.K. Lin, 1/9/89, (PB89-196513).

NCEER-89-0004 "Experimental Study of 'Elephant Foot Bulge' Instability of Thin-Walled Metal Tanks," by Z-H. Jia and R.L. Ketter, 2/22/89, (PB89-207195).

NCEER-89-0005 "Experiment on Performance of Buried Pipelines Across San Andreas Fault," by J. Isenberg, E. Richardson and T.D. O'Rourke, 3/10/89, (PB89-218440). This report is available only through NTIS (see address given above).

NCEER-89-0006 "A Knowledge-Based Approach to Structural Design of Earthquake-Resistant Buildings," by M. Subramani, P. Gergely, C.H. Conley, J.F. Abel and A.H. Zaghw, 1/15/89, (PB89-218465).

NCEER-89-0007 "Liquefaction Hazards and Their Effects on Buried Pipelines," by T.D. O'Rourke and P.A. Lane, 2/1/89, (PB89-218481).

NCEER-89-0008 "Fundamentals of System Identification in Structural Dynamics," by H. Imai, C-B. Yun, O. Maruyama and M. Shinozuka, 1/26/89, (PB89-207211).

NCEER-89-0009 "Effects of the 1985 Michoacan Earthquake on Water Systems and Other Buried Lifelines in Mexico," by A.G. Ayala and M.J. O'Rourke, 3/8/89, (PB89-207229).

NCEER-89-R010 "NCEER Bibliography of Earthquake Education Materials," by K.E.K. Ross, Second Revision, 9/1/89, (PB90-125352).

NCEER-89-0011 "Inelastic Three-Dimensional Response Analysis of Reinforced Concrete Building Structures (IDARC-3D), Part I - Modeling," by S.K. Kunnath and A.M. Reinhorn, 4/17/89, (PB90-114612).

NCEER-89-0012 "Recommended Modifications to ATC-14," by C.D. Poland and J.O. Malley, 4/12/89, (PB90-108648).

NCEER-89-0013   "Repair and Strengthening of Beam-to-Column Connections Subjected to Earthquake Loading," by M. Corazao and A.J. Durrani, 2/28/89, (PB90-109885).

NCEER-89-0014   "Program EXKAL2 for Identification of Structural Dynamic Systems," by O. Maruyama, C-B. Yun, M. Hoshiya and M. Shinozuka, 5/19/89, (PB90-109877).

NCEER-89-0015   "Response of Frames With Bolted Semi-Rigid Connections, Part I - Experimental Study and Analytical Predictions," by P.J. DiCorso, A.M. Reinhorn, J.R. Dickerson, J.B. Radziminski and W.L. Harper, 6/1/89, to be published.

NCEER-89-0016   "ARMA Monte Carlo Simulation in Probabilistic Structural Analysis," by P.D. Spanos and M.P. Mignolet, 7/10/89, (PB90-109893).

NCEER-89-P017   "Preliminary Proceedings from the Conference on Disaster Preparedness - The Place of Earthquake Education in Our Schools," Edited by K.E.K. Ross, 6/23/89, (PB90-108606).

NCEER-89-0017   "Proceedings from the Conference on Disaster Preparedness - The Place of Earthquake Education in Our Schools," Edited by K.E.K. Ross, 12/31/89, (PB90-207895). This report is available only through NTIS (see address given above).

NCEER-89-0018   "Multidimensional Models of Hysteretic Material Behavior for Vibration Analysis of Shape Memory Energy Absorbing Devices, by E.J. Graesser and F.A. Cozzarelli, 6/7/89, (PB90-164146).

NCEER-89-0019   "Nonlinear Dynamic Analysis of Three-Dimensional Base Isolated Structures (3D-BASIS)," by S. Nagarajaiah, A.M. Reinhorn and M.C. Constantinou, 8/3/89, (PB90-161936). This report is available only through NTIS (see address given above).

NCEER-89-0020   "Structural Control Considering Time-Rate of Control Forces and Control Rate Constraints," by F.Y. Cheng and C.P. Pantelides, 8/3/89, (PB90-120445).

NCEER-89-0021   "Subsurface Conditions of Memphis and Shelby County," by K.W. Ng, T-S. Chang and H-H.M. Hwang, 7/26/89, (PB90-120437).

NCEER-89-0022   "Seismic Wave Propagation Effects on Straight Jointed Buried Pipelines," by K. Elhmadi and M.J. O'Rourke, 8/24/89, (PB90-162322).

NCEER-89-0023   "Workshop on Serviceability Analysis of Water Delivery Systems," edited by M. Grigoriu, 3/6/89, (PB90-127424).

NCEER-89-0024   "Shaking Table Study of a 1/5 Scale Steel Frame Composed of Tapered Members," by K.C. Chang, J.S. Hwang and G.C. Lee, 9/18/89, (PB90-160169).

NCEER-89-0025   "DYNA1D: A Computer Program for Nonlinear Seismic Site Response Analysis - Technical Documentation," by Jean H. Prevost, 9/14/89, (PB90-161944). This report is available only through NTIS (see address given above).

NCEER-89-0026   "1:4 Scale Model Studies of Active Tendon Systems and Active Mass Dampers for Aseismic Protection," by A.M. Reinhorn, T.T. Soong, R.C. Lin, Y.P. Yang, Y. Fukao, H. Abe and M. Nakai, 9/15/89, (PB90-173246).

NCEER-89-0027   "Scattering of Waves by Inclusions in a Nonhomogeneous Elastic Half Space Solved by Boundary Element Methods," by P.K. Hadley, A. Askar and A.S. Cakmak, 6/15/89, (PB90-145699).

NCEER-89-0028   "Statistical Evaluation of Deflection Amplification Factors for Reinforced Concrete Structures," by H.H.M. Hwang, J-W. Jaw and A.L. Ch'ng, 8/31/89, (PB90-164633).

NCEER-89-0029   "Bedrock Accelerations in Memphis Area Due to Large New Madrid Earthquakes," by H.H.M. Hwang, C.H.S. Chen and G. Yu, 11/7/89, (PB90-162330).

NCEER-89-0030   "Seismic Behavior and Response Sensitivity of Secondary Structural Systems," by Y.Q. Chen and T.T. Soong, 10/23/89, (PB90-164658).

NCEER-89-0031   "Random Vibration and Reliability Analysis of Primary-Secondary Structural Systems," by Y. Ibrahim, M. Grigoriu and T.T. Soong, 11/10/89, (PB90-161951).

NCEER-89-0032   "Proceedings from the Second U.S. - Japan Workshop on Liquefaction, Large Ground Deformation and Their Effects on Lifelines, September 26-29, 1989," Edited by T.D. O'Rourke and M. Hamada, 12/1/89, (PB90-209388).

NCEER-89-0033   "Deterministic Model for Seismic Damage Evaluation of Reinforced Concrete Structures," by J.M. Bracci, A.M. Reinhorn, J.B. Mander and S.K. Kunnath, 9/27/89.

NCEER-89-0034   "On the Relation Between Local and Global Damage Indices," by E. DiPasquale and A.S. Cakmak, 8/15/89, (PB90-173865).

NCEER-89-0035   "Cyclic Undrained Behavior of Nonplastic and Low Plasticity Silts," by A.J. Walker and H.E. Stewart, 7/26/89, (PB90-183518).

NCEER-89-0036   "Liquefaction Potential of Surficial Deposits in the City of Buffalo, New York," by M. Budhu, R. Giese and L. Baumgrass, 1/17/89, (PB90-208455).

NCEER-89-0037   "A Deterministic Assessment of Effects of Ground Motion Incoherence," by A.S. Veletsos and Y. Tang, 7/15/89, (PB90-164294).

NCEER-89-0038   "Workshop on Ground Motion Parameters for Seismic Hazard Mapping," July 17-18, 1989, edited by R.V. Whitman, 12/1/89, (PB90-173923).

NCEER-89-0039   "Seismic Effects on Elevated Transit Lines of the New York City Transit Authority," by C.J. Costantino, C.A. Miller and E. Heymsfield, 12/26/89, (PB90-207887).

NCEER-89-0040   "Centrifugal Modeling of Dynamic Soil-Structure Interaction," by K. Weissman, Supervised by J.H. Prevost, 5/10/89, (PB90-207879).

NCEER-89-0041   "Linearized Identification of Buildings With Cores for Seismic Vulnerability Assessment," by I-K. Ho and A.E. Aktan, 11/1/89, (PB90-251943).

NCEER-90-0001   "Geotechnical and Lifeline Aspects of the October 17, 1989 Loma Prieta Earthquake in San Francisco," by T.D. O'Rourke, H.E. Stewart, F.T. Blackburn and T.S. Dickerman, 1/90, (PB90-208596).

NCEER-90-0002   "Nonnormal Secondary Response Due to Yielding in a Primary Structure," by D.C.K. Chen and L.D. Lutes, 2/28/90, (PB90-251976).

NCEER-90-0003   "Earthquake Education Materials for Grades K-12," by K.E.K. Ross, 4/16/90, (PB91-251984).

NCEER-90-0004   "Catalog of Strong Motion Stations in Eastern North America," by R.W. Busby, 4/3/90, (PB90-251984).

NCEER-90-0005   "NCEER Strong-Motion Data Base: A User Manual for the GeoBase Release (Version 1.0 for the Sun3)," by P. Friberg and K. Jacob, 3/31/90 (PB90-258062).

NCEER-90-0006   "Seismic Hazard Along a Crude Oil Pipeline in the Event of an 1811-1812 Type New Madrid Earthquake," by H.H.M. Hwang and C-H.S. Chen, 4/16/90(PB90-258054).

NCEER-90-0007   "Site-Specific Response Spectra for Memphis Sheahan Pumping Station," by H.H.M. Hwang and C.S. Lee, 5/15/90, (PB91-108811).

NCEER-90-0008   "Pilot Study on Seismic Vulnerability of Crude Oil Transmission Systems," by T. Ariman, R. Dobry, M. Grigoriu, F. Kozin, M. O'Rourke, T. O'Rourke and M. Shinozuka, 5/25/90, (PB91-108837).

NCEER-90-0009   "A Program to Generate Site Dependent Time Histories: EQGEN," by G.W. Ellis, M. Srinivasan and A.S. Cakmak, 1/30/90, (PB91-108829).

NCEER-90-0010   "Active Isolation for Seismic Protection of Operating Rooms," by M.E. Talbott, Supervised by M. Shinozuka, 6/8/9, (PB91-110205).

NCEER-90-0011   "Program LINEARID for Identification of Linear Structural Dynamic Systems," by C-B. Yun and M. Shinozuka, 6/25/90, (PB91-110312).

NCEER-90-0012   "Two-Dimensional Two-Phase Elasto-Plastic Seismic Response of Earth Dams," by A.N. Yiagos, Supervised by J.H. Prevost, 6/20/90, (PB91-110197).

NCEER-90-0013   "Secondary Systems in Base-Isolated Structures: Experimental Investigation, Stochastic Response and Stochastic Sensitivity," by G.D. Manolis, G. Juhn, M.C. Constantinou and A.M. Reinhorn, 7/1/90, (PB91-110320).

NCEER-90-0014   "Seismic Behavior of Lightly-Reinforced Concrete Column and Beam-Column Joint Details," by S.P. Pessiki, C.H. Conley, P. Gergely and R.N. White, 8/22/90, (PB91-108795).

NCEER-90-0015   "Two Hybrid Control Systems for Building Structures Under Strong Earthquakes," by J.N. Yang and A. Danielians, 6/29/90, (PB91-125393).

NCEER-90-0016   "Instantaneous Optimal Control with Acceleration and Velocity Feedback," by J.N. Yang and Z. Li, 6/29/90, (PB91-125401).

NCEER-90-0017   "Reconnaissance Report on the Northern Iran Earthquake of June 21, 1990," by M. Mehrain, 10/4/90, (PB91-125377).

NCEER-90-0018   "Evaluation of Liquefaction Potential in Memphis and Shelby County," by T.S. Chang, P.S. Tang, C.S. Lee and H. Hwang, 8/10/90, (PB91-125427).

NCEER-90-0019   "Experimental and Analytical Study of a Combined Sliding Disc Bearing and Helical Steel Spring Isolation System," by M.C. Constantinou, A.S. Mokha and A.M. Reinhorn, 10/4/90, (PB91-125385).

NCEER-90-0020   "Experimental Study and Analytical Prediction of Earthquake Response of a Sliding Isolation System with a Spherical Surface," by A.S. Mokha, M.C. Constantinou and A.M. Reinhorn, 10/11/90, (PB91-125419).

NCEER-90-0021   "Dynamic Interaction Factors for Floating Pile Groups," by G. Gazetas, K. Fan, A. Kaynia and E. Kausel, 9/10/90, (PB91-170381).

NCEER-90-0022   "Evaluation of Seismic Damage Indices for Reinforced Concrete Structures," by S. Rodriguez-Gomez and A.S. Cakmak, 9/30/90, PB91-171322).

NCEER-90-0023   "Study of Site Response at a Selected Memphis Site," by H. Desai, S. Ahmad, E.S. Gazetas and M.R. Oh, 10/11/90, (PB91-196857).

NCEER-90-0024   "A User's Guide to Strongmo: Version 1.0 of NCEER's Strong-Motion Data Access Tool for PCs and Terminals," by P.A. Friberg and C.A.T. Susch, 11/15/90, (PB91-171272).

NCEER-90-0025 "A Three-Dimensional Analytical Study of Spatial Variability of Seismic Ground Motions," by L-L. Hong and A.H.-S. Ang, 10/30/90, (PB91-170399).

NCEER-90-0026 "MUMOID User's Guide - A Program for the Identification of Modal Parameters," by S. Rodriguez-Gomez and E. DiPasquale, 9/30/90, (PB91-171298).

NCEER-90-0027 "SARCF-II User's Guide - Seismic Analysis of Reinforced Concrete Frames," by S. Rodriguez-Gomez, Y.S. Chung and C. Meyer, 9/30/90, (PB91-171280).

NCEER-90-0028 "Viscous Dampers: Testing, Modeling and Application in Vibration and Seismic Isolation," by N. Makris and M.C. Constantinou, 12/20/90 (PB91-190561).

NCEER-90-0029 "Soil Effects on Earthquake Ground Motions in the Memphis Area," by H. Hwang, C.S. Lee, K.W. Ng and T.S. Chang, 8/2/90, (PB91-190751).

NCEER-91-0001 "Proceedings from the Third Japan-U.S. Workshop on Earthquake Resistant Design of Lifeline Facilities and Countermeasures for Soil Liquefaction, December 17-19, 1990," edited by T.D. O'Rourke and M. Hamada, 2/1/91, (PB91-179259).

NCEER-91-0002 "Physical Space Solutions of Non-Proportionally Damped Systems," by M. Tong, Z. Liang and G.C. Lee, 1/15/91, (PB91-179242).

NCEER-91-0003 "Seismic Response of Single Piles and Pile Groups," by K. Fan and G. Gazetas, 1/10/91, (PB92-174994).

NCEER-91-0004 "Damping of Structures: Part 1 - Theory of Complex Damping," by Z. Liang and G. Lee, 10/10/91, (PB92-197235).

NCEER-91-0005 "3D-BASIS - Nonlinear Dynamic Analysis of Three Dimensional Base Isolated Structures: Part II," by S. Nagarajaiah, A.M. Reinhorn and M.C. Constantinou, 2/28/91, (PB91-190553).

NCEER-91-0006 "A Multidimensional Hysteretic Model for Plasticity Deforming Metals in Energy Absorbing Devices," by E.J. Graesser and F.A. Cozzarelli, 4/9/91, (PB92-108364).

NCEER-91-0007 "A Framework for Customizable Knowledge-Based Expert Systems with an Application to a KBES for Evaluating the Seismic Resistance of Existing Buildings," by E.G. Ibarra-Anaya and S.J. Fenves, 4/9/91, (PB91-210930).

NCEER-91-0008 "Nonlinear Analysis of Steel Frames with Semi-Rigid Connections Using the Capacity Spectrum Method," by G.G. Deierlein, S-H. Hsieh, Y-J. Shen and J.F. Abel, 7/2/91, (PB92-113828).

NCEER-91-0009 "Earthquake Education Materials for Grades K-12," by K.E.K. Ross, 4/30/91, (PB91-212142).

NCEER-91-0010 "Phase Wave Velocities and Displacement Phase Differences in a Harmonically Oscillating Pile," by N. Makris and G. Gazetas, 7/8/91, (PB92-108356).

NCEER-91-0011 "Dynamic Characteristics of a Full-Size Five-Story Steel Structure and a 2/5 Scale Model," by K.C. Chang, G.C. Yao, G.C. Lee, D.S. Hao and Y.C. Yeh," 7/2/91, (PB93-116648).

NCEER-91-0012 "Seismic Response of a 2/5 Scale Steel Structure with Added Viscoelastic Dampers," by K.C. Chang, T.T. Soong, S-T. Oh and M.L. Lai, 5/17/91, (PB92-110816).

NCEER-91-0013 "Earthquake Response of Retaining Walls; Full-Scale Testing and Computational Modeling," by S. Alampalli and A-W.M. Elgamal, 6/20/91, to be published.

NCEER-91-0014   "3D-BASIS-M: Nonlinear Dynamic Analysis of Multiple Building Base Isolated Structures," by P.C. Tsopelas, S. Nagarajaiah, M.C. Constantinou and A.M. Reinhorn, 5/28/91, (PB92-113885).

NCEER-91-0015   "Evaluation of SEAOC Design Requirements for Sliding Isolated Structures," by D. Theodossiou and M.C. Constantinou, 6/10/91, (PB92-114602).

NCEER-91-0016   "Closed-Loop Modal Testing of a 27-Story Reinforced Concrete Flat Plate-Core Building," by H.R. Somaprasad, T. Toksoy, H. Yoshiyuki and A.E. Aktan, 7/15/91, (PB92-129980).

NCEER-91-0017   "Shake Table Test of a 1/6 Scale Two-Story Lightly Reinforced Concrete Building," by A.G. El-Attar, R.N. White and P. Gergely, 2/28/91, (PB92-222447).

NCEER-91-0018   "Shake Table Test of a 1/8 Scale Three-Story Lightly Reinforced Concrete Building," by A.G. El-Attar, R.N. White and P. Gergely, 2/28/91, (PB93-116630).

NCEER-91-0019   "Transfer Functions for Rigid Rectangular Foundations," by A.S. Veletsos, A.M. Prasad and W.H. Wu, 7/31/91.

NCEER-91-0020   "Hybrid Control of Seismic-Excited Nonlinear and Inelastic Structural Systems," by J.N. Yang, Z. Li and A. Danielians, 8/1/91, (PB92-143171).

NCEER-91-0021   "The NCEER-91 Earthquake Catalog: Improved Intensity-Based Magnitudes and Recurrence Relations for U.S. Earthquakes East of New Madrid," by L. Seeber and J.G. Armbruster, 8/28/91, (PB92-176742).

NCEER-91-0022   "Proceedings from the Implementation of Earthquake Planning and Education in Schools: The Need for Change - The Roles of the Changemakers," by K.E.K. Ross and F. Winslow, 7/23/91, (PB92-129998).

NCEER-91-0023   "A Study of Reliability-Based Criteria for Seismic Design of Reinforced Concrete Frame Buildings," by H.H.M. Hwang and H-M. Hsu, 8/10/91, (PB92-140235).

NCEER-91-0024   "Experimental Verification of a Number of Structural System Identification Algorithms," by R.G. Ghanem, H. Gavin and M. Shinozuka, 9/18/91, (PB92-176577).

NCEER-91-0025   "Probabilistic Evaluation of Liquefaction Potential," by H.H.M. Hwang and C.S. Lee," 11/25/91, (PB92-143429).

NCEER-91-0026   "Instantaneous Optimal Control for Linear, Nonlinear and Hysteretic Structures - Stable Controllers," by J.N. Yang and Z. Li, 11/15/91, (PB92-163807).

NCEER-91-0027   "Experimental and Theoretical Study of a Sliding Isolation System for Bridges," by M.C. Constantinou, A. Kartoum, A.M. Reinhorn and P. Bradford, 11/15/91, (PB92-176973).

NCEER-92-0001   "Case Studies of Liquefaction and Lifeline Performance During Past Earthquakes, Volume 1: Japanese Case Studies," Edited by M. Hamada and T. O'Rourke, 2/17/92, (PB92-197243).

NCEER-92-0002   "Case Studies of Liquefaction and Lifeline Performance During Past Earthquakes, Volume 2: United States Case Studies," Edited by T. O'Rourke and M. Hamada, 2/17/92, (PB92-197250).

NCEER-92-0003   "Issues in Earthquake Education," Edited by K. Ross, 2/3/92, (PB92-222389).

NCEER-92-0004   "Proceedings from the First U.S. - Japan Workshop on Earthquake Protective Systems for Bridges," Edited by I.G. Buckle, 2/4/92.

NCEER-92-0005   "Seismic Ground Motion from a Haskell-Type Source in a Multiple-Layered Half-Space," A.P. Theoharis, G. Deodatis and M. Shinozuka, 1/2/92, to be published.

NCEER-92-0006 "Proceedings from the Site Effects Workshop," Edited by R. Whitman, 2/29/92, (PB92-197201).

NCEER-92-0007 "Engineering Evaluation of Permanent Ground Deformations Due to Seismically-Induced Liquefaction," by M.H. Baziar, R. Dobry and A-W.M. Elgamal, 3/24/92, (PB92-222421).

NCEER-92-0008 "A Procedure for the Seismic Evaluation of Buildings in the Central and Eastern United States," by C.D. Poland and J.O. Malley, 4/2/92, (PB92-222439).

NCEER-92-0009 "Experimental and Analytical Study of a Hybrid Isolation System Using Friction Controllable Sliding Bearings," by M.Q. Feng, S. Fujii and M. Shinozuka, 5/15/92, (PB93-150282).

NCEER-92-0010 "Seismic Resistance of Slab-Column Connections in Existing Non-Ductile Flat-Plate Buildings," by A.J. Durrani and Y. Du, 5/18/92.

NCEER-92-0011 "The Hysteretic and Dynamic Behavior of Brick Masonry Walls Upgraded by Ferrocement Coatings Under Cyclic Loading and Strong Simulated Ground Motion," by H. Lee and S.P. Prawel, 5/11/92, to be published.

NCEER-92-0012 "Study of Wire Rope Systems for Seismic Protection of Equipment in Buildings," by G.F. Demetriades, M.C. Constantinou and A.M. Reinhorn, 5/20/92.

NCEER-92-0013 "Shape Memory Structural Dampers: Material Properties, Design and Seismic Testing," by P.R. Witting and F.A. Cozzarelli, 5/26/92.

NCEER-92-0014 "Longitudinal Permanent Ground Deformation Effects on Buried Continuous Pipelines," by M.J. O'Rourke, and C. Nordberg, 6/15/92.

NCEER-92-0015 "A Simulation Method for Stationary Gaussian Random Functions Based on the Sampling Theorem," by M. Grigoriu and S. Balopoulou, 6/11/92, (PB93-127496).

NCEER-92-0016 "Gravity-Load-Designed Reinforced Concrete Buildings: Seismic Evaluation of Existing Construction and Detailing Strategies for Improved Seismic Resistance," by G.W. Hoffmann, S.K. Kunnath, A.M. Reinhorn and J.B. Mander, 7/15/92.

NCEER-92-0017 "Observations on Water System and Pipeline Performance in the Limón Area of Costa Rica Due to the April 22, 1991 Earthquake," by M. O'Rourke and D. Ballantyne, 6/30/92, (PB93-126811).

NCEER-92-0018 "Fourth Edition of Earthquake Education Materials for Grades K-12," Edited by K.E.K. Ross, 8/10/92.

NCEER-92-0019 "Proceedings from the Fourth Japan-U.S. Workshop on Earthquake Resistant Design of Lifeline Facilities and Countermeasures for Soil Liquefaction," Edited by M. Hamada and T.D. O'Rourke, 8/12/92, (PB93-163939).

NCEER-92-0020 "Active Bracing System: A Full Scale Implementation of Active Control," by A.M. Reinhorn, T.T. Soong, R.C. Lin, M.A. Riley, Y.P. Wang, S. Aizawa and M. Higashino, 8/14/92, (PB93-127512).

NCEER-92-0021 "Empirical Analysis of Horizontal Ground Displacement Generated by Liquefaction-Induced Lateral Spreads," by S.F. Bartlett and T.L. Youd, 8/17/92, (PB93-188241).

NCEER-92-0022 "IDARC Version 3.0: Inelastic Damage Analysis of Reinforced Concrete Structures," by S.K. Kunnath, A.M. Reinhorn and R.F. Lobo, 8/31/92, (PB93-227502, A07, MF-A02).

NCEER-92-0023 "A Semi-Empirical Analysis of Strong-Motion Peaks in Terms of Seismic Source, Propagation Path and Local Site Conditions, by M. Kamiyama, M.J. O'Rourke and R. Flores-Berrones, 9/9/92, (PB93-150266).

NCEER-92-0024 "Seismic Behavior of Reinforced Concrete Frame Structures with Nonductile Details, Part I: Summary of Experimental Findings of Full Scale Beam-Column Joint Tests," by A. Beres, R.N. White and P. Gergely, 9/30/92, (PB93-227783, A05, MF-A01).

NCEER-92-0025 "Experimental Results of Repaired and Retrofitted Beam-Column Joint Tests in Lightly Reinforced Concrete Frame Buildings," by A. Beres, S. El-Borgi, R.N. White and P. Gergely, 10/29/92, (PB93-227791, A05, MF-A01).

NCEER-92-0026 "A Generalization of Optimal Control Theory: Linear and Nonlinear Structures," by J.N. Yang, Z. Li and S. Vongchavalitkul, 11/2/92, (PB93-188621).

NCEER-92-0027 "Seismic Resistance of Reinforced Concrete Frame Structures Designed Only for Gravity Loads: Part I - Design and Properties of a One-Third Scale Model Structure," by J.M. Bracci, A.M. Reinhorn and J.B. Mander, 12/1/92, (PB94-104502, A08, MF-A02).

NCEER-92-0028 "Seismic Resistance of Reinforced Concrete Frame Structures Designed Only for Gravity Loads: Part II - Experimental Performance of Subassemblages," by L.E. Aycardi, J.B. Mander and A.M. Reinhorn, 12/1/92, (PB94-104510, A08, MF-A02).

NCEER-92-0029 "Seismic Resistance of Reinforced Concrete Frame Structures Designed Only for Gravity Loads: Part III - Experimental Performance and Analytical Study of a Structural Model," by J.M. Bracci, A.M. Reinhorn and J.B. Mander, 12/1/92, (PB93-227528, A09, MF-A01).

NCEER-92-0030 "Evaluation of Seismic Retrofit of Reinforced Concrete Frame Structures: Part I - Experimental Performance of Retrofitted Subassemblages," by D. Choudhuri, J.B. Mander and A.M. Reinhorn, 12/8/92.

NCEER-92-0031 "Evaluation of Seismic Retrofit of Reinforced Concrete Frame Structures: Part II - Experimental Performance and Analytical Study of a Retrofitted Structural Model," by J.M. Bracci, A.M. Reinhorn and J.B. Mander, 12/8/92.

NCEER-92-0032 "Experimental and Analytical Investigation of Seismic Response of Structures with Supplemental Fluid Viscous Dampers," by M.C. Constantinou and M.D. Symans, 12/21/92, (PB93-191435).

NCEER-92-0033 "Reconnaissance Report on the Cairo, Egypt Earthquake of October 12, 1992," by M. Khater, 12/23/92, (PB93-188621).

NCEER-92-0034 "Low-Level Dynamic Characteristics of Four Tall Flat-Plate Buildings in New York City," by H. Gavin, S. Yuan, J. Grossman, E. Pekelis and K. Jacob, 12/28/92, (PB93-188217).

NCEER-93-0001 "An Experimental Study on the Seismic Performance of Brick-Infilled Steel Frames With and Without Retrofit," by J.B. Mander, B. Nair, K. Wojtkowski and J. Ma, 1/29/93, (PB93-227510, A07, MF-A02).

NCEER-93-0002 "Social Accounting for Disaster Preparedness and Recovery Planning," by S. Cole, E. Pantoja and V. Razak, 2/22/93, to be published.

NCEER-93-0003 "Assessment of 1991 NEHRP Provisions for Nonstructural Components and Recommended Revisions," by T.T. Soong, G. Chen, Z. Wu, R-H. Zhang and M. Grigoriu, 3/1/93, (PB93-188639).

NCEER-93-0004 "Evaluation of Static and Response Spectrum Analysis Procedures of SEAOC/UBC for Seismic Isolated Structures," by C.W. Winters and M.C. Constantinou, 3/23/93, (PB93-198299).

NCEER-93-0005 "Earthquakes in the Northeast - Are We Ignoring the Hazard? A Workshop on Earthquake Science and Safety for Educators," edited by K.E.K. Ross, 4/2/93, (PB94-103066, A09, MF-A02).

NCEER-93-0006 "Inelastic Response of Reinforced Concrete Structures with Viscoelastic Braces," by R.F. Lobo, J.M. Bracci, K.L. Shen, A.M. Reinhorn and T.T. Soong, 4/5/93, (PB93-227486, A05, MF-A02).

NCEER-93-0007 "Seismic Testing of Installation Methods for Computers and Data Processing Equipment," by K. Kosar, T.T. Soong, K.L. Shen, J.A. HoLung and Y.K. Lin, 4/12/93, (PB93-198299).

NCEER-93-0008   "Retrofit of Reinforced Concrete Frames Using Added Dampers," by A. Reinhorn, M. Constantinou and C. Li, to be published.

NCEER-93-0009   "Seismic Behavior and Design Guidelines for Steel Frame Structures with Added Viscoelastic Dampers," by K.C. Chang, M.L. Lai, T.T. Soong, D.S. Hao and Y.C. Yeh, 5/1/93.

50272-101

REPORT DOCUMENTATION PAGE	1. REPORT NO. NCEER-93-0009	2.	3. PB94-141959

4. Title and Subtitle	5. Report Date
Seismic Behavior and Design Guidelines for Steel Frame Structures with Added Viscoelastic Dampers	May 1, 1993
	6.

7. Author(s)	8. Performing Organization Rept. No.
K.C. Chang, M.L. Lai, T.T. Soong, D.S. Hao and Y.C. Yeh	

9. Performing Organization Name and Address	10. Project/Task/Work Unit No.
State University of New York at Buffalo Department of Civil Engineering Buffalo, New York 14260	
	11. Contract(C) or Grant(G) No.
	(C) BCS 90-25010
	(G) NEC-91029

12. Sponsoring Organization Name and Address	13. Type of Report & Period Covered
National Center for Earthquake Engineering Research State University of New York at Buffalo Red Jacket Quadrangle Buffalo, New York 14261	Technical Report
	14.

16. Abstract (Limit: 200 words)
In order to determine the effectiveness of adding viscoelastic dampers to structures on the reduction of their seismic response, a comprehensive analytical and experimental program was carried out. The experimental program was first conducted on a 2/5-scale five-story steel frame under precisely controlled ambient temperatures and subject to simulated ground motions with peak accelerations ranging from 0.12g to 0.60g. Results show that viscoelastic dampers are very effective in attenuating seismic structural response at all levels of earthquake ground motions, and that their energy dissipation capacity decreases as ambient temperature increases. However, they are effective at all temperatures tested in the research program. A rational seismic design procedure for viscoelastically damped structure is developed based on these results. Further tests using a full-scale prototype structure confirm that damping in the full-scale structure can be significantly increased by adding relatively small viscoelastic dampers. The damper design procedure developed based on the scaled model can also be applied to the full-scale structure. This full-scale analytical and experimental study provides an important base for applying the extensive data generated from the scaled model testing to the full-scale structures.

17. Document Analysis   a. Descriptors

b. Identifiers/Open-Ended Terms

Steel frames.   Added damping devices.   Viscoelastic damping devices.   Design methods
Design guidelines.   Linear response analysis.   Modal strain energy method.
Scale models   Shaking table tests.   Full scale tests.   Forced vibration tests.
Earthquake engineering.

c. COSATI Field/Group

18. Availability Statement	19. Security Class (This Report)	21. No. of Pages
Release Unlimited *Preceding page blank*	Unclassified	136
	20. Security Class (This Page)	22. Price
	Unclassified	

(See ANSI–Z39.18)   See Instructions on Reverse   OPTIONAL FORM 272 (4–77)
(Formerly NTIS–35)